UNIVERSITY OF SOUTHAMPTON

DEPARTMENT OF AERONAUTICS AND ASTRONAUTICS

UNSTEADY MOTION OF SAILING CRAFT

(ROLLING)

by

CZESLAW ANTONY MARCHAJ

A Thesis Presented for the Degree of M.Phil of the University of Southampton in the Faculty of Engineering and Applied Science.

April 1976

CONTENTS

ABSTRACT

A series of tests on a rolling rig was performed in the wind tunnel in order to establish the relative influence of basic parameters such as:

angle of heading β_A

angle of trim of the sail δ_m

wind velocity V_A

Strouhal Number S_t

twist of the sail

damping due to hull action

on the dynamic behaviour of the rig.

During these tests it was proven beyond any doubt that wild rolling may be induced for an aerodynamic reason. A main-sail, when running down wind, may extract energy from the wind in a self-excited manner in such a way that the sail can be regarded as a rolling engine.

A theory has been developed which relates the model response to the stationary and non-stationary aerodynamic characteristics of the rig, and also predicts the condition in which the model will be dynamically stable or unstable. Attention was given to the problem of how to minimise or reverse the energy transfer to the system in order to prevent dynamic instability. A modification to the conventional rig, in the form of an anti-rolling sail, has been devised and this effectively eliminates the instability which might otherwise be induced by aerodynamic forces.

This work is dedicated to the memory of the late Thomas Tanner, founder of the Southampton University Yacht Research Group, in appreciation of His unfailing help and encouragement in this and many other projects.

Acknowledgements ,

This work on instability of sailing craft was sponsored by the Science and Research Council.

I am greatly indebted to Professors G.M. Lilley and G.J. Goodrich for the excellent facilities given to me while conducting the experimental work at Southampton University.

My warmest thanks go also to the late Thomas Tanner who helped me on many occasions to clarify my thoughts on some aspects of unstable motion of sailing yachts. In addition, I should like to record my appreciation of the suggestions made by Dr. J.Wellicome who read the first draft of this thesis.

When developing the apparatus for the Wind Tunnel Testing I was splendidly supported by Messrs. A.Allcock, J.Graham and T.Kelly, members of the University Staff.

Finally, I should express thanks to my colleagues Mr. E.Kamman and Dr. M.Yendell for their practical assistance in the Wind Tunnel.

1. DEFINITIONS AND NOMENCLATURE

The following four sets of reference axes and nomenclature are adopted for a study of the aerodynamic aspects of the unsteady motion of a yacht. (1,2,3,4,5)*

1.1 The body or ship axes x,y,z, - right hand orthogonal system of axes fixed in the body at the origin O located on the line of intersection of the yacht centre-line plane and the designed water-plane at the point where the centre of the mast intersects the designed water-line plane.

x - the longitudinal or principal axis, positive towards the bow, is the line of intersection of the centre-line plane and the designed water-plane.

y - the transverse axis, positive to starboard is perpendicular to the centre-line plane y-z.

z - the normal axis, positive downwards is perpendicular to the designed water-line plane.

It is assumed that the yacht is sailing on the port tack so that the sail force in the + oy direction (leeward side) is positive, Fig.1.

1.2 The wind axes reference system

The aerodynamic forces developed by the sails are related to the apparent wind direction and its velocity V_A. The apparent wind axis serves as a means of deriving the lift L and drag D acting on a yacht when under motion (see Fig.2). Referring to the wind tunnel experiments, the principal wind axis V_A coincides with the centre-line of the wind tunnel or the direction of air flow ahead of the rig.

---

*See list of references

1.3 The track axes reference system

The actual track of a yacht sailing through the water and oscillating along three axes - surging, swaying and heaving, the rotation about three axes - rolling, pitching and yawing, may frequently not lie along the x-axis. It is therefore convenient to set up a second rectangular system (see Fig.2) of co-ordinates in which the principal axis of the three coincides with the velocity vector representing the instantaneous direction of motion of the yacht. Referring to the towing tank experiments, the principal track axis V_S coincides with the centre line of the tank or the direction of tow.

The track of a boat is defined as a trace of her motion (point of origin of the co-ordinate system) in the horizontal plane.

1.4 The fixed axes

It is convenient to have a reference or fixed system of co-ordinates to which the body axes can be related. This reference system is fixed with respect to a tangent plane at any point on the flat sea surface (or space) and the relevant axes x_o, y_o, z_o called fixed axes, are designed as follows:

x_o - the fixed longitudinal axis lying in the horizontal plane, considered as positive in the heading direction (see Fig.2),

y_o - the fixed transverse axis, lying in the horizontal plane perpendicular to x_o, positive to starboard,

z_o - the vertical axis perpendicular to the other two, directed downward.

In the case of a yacht which is floating to her DWL in a flat sea the body axes x, y, z coincide with fixed axes x_o, y_o, z_o. Both systems of co-ordinates have the same point of origin O.

The fixed co-ordinate system x_o, y_o, z_o, moves with the mean forward speed of the boat and the boat oscillates in various ways with respect to this system.

Velocities, forces and moments relative to the fixed axes x_o, y_o, z_o are designated as:

u, v, w - components of velocity of origin O of the co-ordinate system along the fixed axes x_o, y_o, z_o respectively.

p, q, r - components of angular velocity about the fixed axes x_o, y_o, z_o - rolling, pitching and yawing respectively.

X_A, Y_A, Z_A - aerodynamic force components referred to as longitudinal, lateral (or transverse) and vertical (or keelward) forces along fixed axes x_o, y_o, z_o.

K_A, M_A, N_A - aerodynamic moment components referred to as rolling, pitching and yawing moments about the x_o, y_o, z_o axes respectively (see sign convention in Fig.1).

A boat sailing obliquely relative to the direction of wave crests may exercise six possible degrees of freedom involving three translational and three rotational oscillations. The translational motions are surging along the x_o-axis, side-swaying along the lateral or y_o-axis and heaving along the vertical z_o-axis. The rotations about x_o, y_o, z_o axes are rolling, pitching and yawing. The table 1 and Figs.1 and 3 give further details concerning these motions.

1.5 General terms used

Angle of heel ϕ is measured about the longitudinal fixed (space) axis x_o, between a steady-state or mean inclined position of the centre-line plane x-y and the vertical fixed axis z_o.

TABLE 1

Axes	Displacement		Velocities	
	Translational (Linear)	Rotational (Angular)	Translational* (Linear)	Rotational (Angular)
O_{x_o} Longitudinal	x surging	ϕ rolling	U, u	p
O_{y_o} Transverse	y swaying	θ pitching	V, v	q
O_{z_o} Vertical	z heaving	ψ yawing	W, w	r

Axes	Forces	Moments	Moments of Inertia
O_{x_o} Longitudinal	X_A	K_A rolling	I_x
O_{y_o} Transverse	Y_A	M_A pitching	I_y
O_{z_o} Vertical	Z_A	N_A yawing	I_z

Angle of roll $\pm \phi$ is measured about the longitudinal fixed axis x_o, between the instantaneous position of the centre-line plane x-y when the boat is rolling and the vertical fixed (space) axis z_o. A multitude of starboard and port rolling angles usually average out to zero.

Rolling is the angular component of the oscillatory motion of a boat about her longitudinal or principal fixed axis x_o. In the case of small angle of yaw ψ the angle of roll ϕ can, with reasonable degree of accuracy, be measured relative to either system of axes, i.e. the body axes or fixed (space) axes. As a matter of fact the investigation of rolling

---

*Upper case symbols are used for steady velocities and lower case symbols for varying velocities or for perturbation velocities.

motion presented in this thesis is restricted to one degree of freedom, i.e. the effects of coupling with yawing and pitching motion are not considered.

Angle of pitch $\pm \theta$ is the angle measured about the horizontal or fixed axis y_o, between the instantaneous position of the longitudinal body axis x when pitching and the horizontal fixed (space) axis x_o.

Pitching is the angular component of the oscillatory motion of a boat about her transverse fixed axis y_o.

Trim, the steady-state longitudinal angular position of a boat to be distinguished from pitching, which is an oscillatory motion. The sense of the trim angle is defined as bow up (trim by stern) - positive.

Angle of leeway β_H is defined as the angle between the principal track axis which coincides with instantaneous velocity vector V_s and the horizontal axis x_o. The direction of this horizontal line is termed the yacht heading. The arrangement and adequate nomenclature are illustrated in Figs.2 and 3.

Angle of yaw ψ is measured about a vertical axis z_o, between the instantaneous longitudinal fixed axis x_o of the boat and her mean heading (see Fig.3a).

Yawing is the angular component of the oscillatory motion of a boat relative to the mean heading. Change of heading is a change in the forward direction of the longitudinal axis or the bow of a boat in the horizontal plane.

Heading refers to the direction of the longitudinal axis of a boat with respect to the apparent wind direction, V_A.

Course of a boat refers to the direction of the path of her centre of gravity G reckoned by its direction of motion. The difference in an angle between the course and heading is the leeway angle.

The path (or track) of a boat, is defined as a trace of its moving centre of gravity G in the horizontal plane.

Controllability as distinguished from manoeuvrability, is that quality of a boat and her appendages, both fixed and moveable, which demonstrates the effectiveness of the controls in producing any desired uniformity or any change, at a specified rate, in the attitude, position or motion of a moving boat. For these operations, the equilibrium of a boat may be stable, unstable or neutral, and it may or may not possess dynamic stability.

Manoeuvrability as distinguished from controllability is an expression of the degree or rate at which a boat can change her course or attitude.

The motion of a boat can be regarded as steady with respect to a given axes if all aspects of her motion remain constant with time, otherwise it is unsteady.

1.6 The definitions concerning static and dynamic stability[2,6]

Equilibrium is a state of balance between opposing forces or moments. The equilibrium of a boat is said to be stable if, after being displaced, the new orientation of forces or moments is such that they tend to bring the boat to her original equilibrium (or trimmed) attitude. It is unstable if the forces and moments act to increase the initial displacement from this attitude.

Stability is a boat property which causes her, when equilibrium is disturbed, to develop forces or moments acting to restore her to the original condition of equilibrium. If the boat possesses instability, she deviates further from her original condition when disturbed.

Static stability is that property of a boat which causes her to maintain her steadiness or stability by reason of her angular displacement. In a static stability discussion it follows that the complete motion is not considered at all and when a boat is said to be statically stable it means only that, after being disturbed, the static forces and moments tend to restore the boat to her equilibrium (or

trimmed) state. It is assumed that the accelerations set up are small and inertia forces introduced by oscillatory acceleration or deceleration are negligible.

Dynamic stability is that property of a boat which causes her to maintain her steadiness or stability only by reason of her motion. This general term is not to be confused with what is known in some quarters as dynamic metacentric stability, involving the righting energy available to bring a heeled boat back to her initial upright or trimmed position. In dynamic stability we consider the motion of a boat (system) following a disturbance from the equilibrium state, taking into account inertia forces and damping forces, as well as static forces or moments.

A statically stable system may oscillate about the equilibrium condition without ever remaining in it. In such a case the system although statically stable may be dynamically unstable.

Metacentric stability is that property of a boat by which the action of the buoyancy and weight forces cause her to return to her original position if her equilibrium about a given axis is disturbed. This occurs when the metacentre M lies above the centre of gravity G.

If a ship is stable against a disturbance in heel she has transverse metacentric stability; if against a disturbance in trim, she has longitudinal metacentric stability. If the centre of buoyancy B and metacentre M are above the centre of gravity G, the boat is said to have pendulum stability.

1.7 Symbols

A Subscript for aerodynamic symbols

A_L Lateral area (underwater part of the hull)

AR Aspect ratio = p^2/S_A

b Coefficient of damping term in diff. eq. of motion

B	Centre of buoyancy
B_{MAX}	Maximum beam
c	Chord length of the sail
C	Coefficient = Force/$q.S_A$
C_D	Drag coefficient
C_L	Lift coefficient
C_{TA}	Total force coefficient (aerodynamic)
C_{XA}	Coefficient of force in direction of x-axis
C_{YA}	Coefficient of force in direction of y-axis
CE	Aerodynamic centre of effort
CLR	Centre of lateral resistance
D	Rated depth of the hull
D	Aerodynamic drag, component of T_A in direction of V_A
DM	Maximum depth of the hull
DWL	Design water line
E	Energy in general
E	Length of the foot of the main sail (Intern. Formula)
f	Frequency in general (f = 1/T)
F	Force in general
g	Acceleration due to gravity (9.806 65 ≈ 9.81m/s^2)
G	Centre of gravity
GM	Metacentric height = distance from the centre of gravity G to the transverse metacentre M
GM_L	Longitudinal metacentric height
GZ	Righting arm
H	Horizontal lateral water force component of T_H
H	Subscript for hydrodynamic symbols
I	Moment of inertia in general

I	Height of the foretriangle
I_x, I_y, I_z	Moments of inertia relative to x, y, z axes
J	Base of the foretriangle
K	Coefficient of restoring term in differential equation of motion, also reduced frequency $\frac{\omega c}{2U}$
K	Radius of gyration
K_A	Aerodynamic heeling or rolling moment
L	Lift, aerodynamic component of T_A in direction normal to V_A
La	Actual lift
Lo	Stationary lift
LOA	Length over-all
LWL	Load water line
m	Mass in kg
M	Metacentre
M	Moment in general
M_A	Aerodynamic pitching moment
MH	Mast height i.e. distance from x-axis to top of sail plan
n	Scale factor (full size/model size)
N_A	Aerodynamic yawing moment
O	Origin of co-ordinate systems
p	Static pressure, force per unit area
P	Length of the mainsail hoist
p,q,r	Components of angular velocity relative to x_o, y_o, z_c
q	Dynamic pressure = $\frac{\rho V^2}{2g}$
Q	Torque
R	Hydrodynamic resistance i.e. component of T_H in direction of V_S

r	Radius in general, also the ratio $^{La}/_{Lo}$ = actual lift/quasi-static lift
Re	Reynolds number = $\frac{Vc}{\nu}$
S_A	Sail area
S_H	Wetted area
S_t	Strouhal Number = $\frac{\omega c}{V_A}$
t	Time in seconds
$T_{\phi,\theta,\psi}$	Period of time for complete cycle (roll, pitch, yaw)
T_A	Total aerodynamic force measured in horizontal plane
T_H	Total hydrodynamic force measured in horizontal plane
V	Velocity in general
V_A	Apparent wind velocity
V_{MG}	Speed made good to windward
V_S	Boat velocity
V_T	True wind velocity
w	Weight density = $\rho.g$
W	Weight in general in N
x	Body axis through O in design water plane and hull symmetry plane
X_A	Aerodynamic force component along x-axis
y	Body axis through O in design water plane, normal to x-axis
Y_A	Aerodynamic force component along y
z	Body axis through O in perpendicular direction to the design water plane
Z_A	Aerodynamic force component along z
α	Angle of incidence i.e. angle between V_A and the boom
β	Relative wind angle, between V_A and V_S; $\beta = \beta_A + \beta_H$

β_A	Apparent wind angle, between V_A and x-axis
β_H	Leeway angle, between V_S and x-axis
γ	True wind angle, between V_T and V_S
Γ	Circulation
δ	Damping coefficient, logarithmic decrement
δ_f	Foresail trim angle, between a line joining the tack and the clew and boat symmetry plane
δ_m	Mainsail trim angle, between the boom and symmetry plane of the boat
δ_r	Trim angle of the anti-rolling sail
ε_A	Aerodynamic drag angle, arc tan D/L
ε_H	Hydrodynamic drag angle, arc tan R/H
ξ	Damping ratio b/bc
η	Phase angle (forcing function)
Δ	Displacement weight (N)
∇	Displacement volume (m^3)
ν	Kinematic viscosity air - $1{,}45.10^{-5}$ m^2/s (0,145 cm^2/s) water - $1{,}01.10^{-6}$ m^2/s (0,0101 cm^2/s)
θ	Pitch angle or longitudinal trim angle
ϕ	Heel angle or rolling angle
ϕ_o	Maximum or initial angle of heel
ρ	Mass density of water or air per unit volume $\rho_w = 1030$ kg/m^3(sea), $\rho_A = 1.22$ kg/m^3
ψ	Yaw angle
ω	Natural circular frequency in general
ω_ϕ	Natural circular frequency for rolling $2\pi/T_\phi$
ω_θ	Natural circular frequency for pitching $2\pi/T_\theta$
ω_ψ	Natural circular frequency for yawing $2\pi/T_\psi$

ω_o	Natural circular frequency of undamped motion
ω_d	Natural circular frequency of damped motion
ω_f	Frequency of forcing function
$\Omega = \frac{\omega_f}{\omega_o}$	Tuning ratio

TABLE 2

The following basic International System of Units (SI) was adopted. The primary units are boxed.

Quantity	Unit	Symbol	Remarks
Time	second	s	
Length	metre	m	1m = 100 centimetres
Mass	kilogramme	kg	
Force	newton	N(kg m/s^2)	
Velocity	metre per second	m/s	
Acceleration	metre per second squared	m/s^2	Acceleration due to gravity = 9.807 $^m/_{s2}$
Angular displacement	dimensionless	rad.	
Angular velocity	radian per second	rad./s	
Angular acceleration	radian per second squared	$rad./s^2$	
Moment of force	newton metre	N m	
Moment of inertia	kilogramme metre squared	kg m^2	May be expressed in N m sec^2
Work, energy	joule	J(Nm)	
Power rate of doing work	watt	W(J/s)	
Tortional damping constant (b)	newton metre seconds per radian	Nm/(rad/sec) Nms/rad	
Restoring moment coefficient /constant/ - k	newton metre per radian	Nm/rad	$k = \frac{K_A}{\phi}$ for rolling

2. INTRODUCTION

In contrast with "normal" weather conditions when moderate winds and relatively flat seas facilitate a steady character of yacht motion along a straight line, heavy weather sailing is associated to a large extent with unsteadiness. Then stability and controllability, or steering problems, become pre-eminent factors.

For example, when running before a fresh wind, the rhythmic rolling and broaching tendency becomes an almost inevitable characteristic of all sailing crafts, not just of small racing dinghies. It is not uncommon nowadays to see heavy keelboats involved in a spectacular and very unpleasant rolling.

Another example of unsteady motion which is coupled with rolling, and which appears to be exagerated in some modern yacht designs, is a directional instability which leads occasionally to vicious broaching. In particular, it seems to affect those boats which have a short heel (of high aspect ratio) and reduced wetted area of the hull.

It was reported from the U.S.A. that a yacht with a shorter keel, of about 29 ft. DWL, which had been tank tested and performed well to windward, proved unmanageable down wind. In one race, on the leeward leg, she could not be kept on course and broached thirty-three times in three hours.*

When sailing close-hauled in a head sea, the performance of any water-borne craft is more or less affected by a sustained oscillation in pitch. In some circumstances the pitching amplitude builds up to such an extent that it may effectively stop all head-way.

---

*SNAME No.3 1967, P.Spens, P.De Saix, P. Brown. Some Further Experimental Studies of the Sailing Yacht.

These three different types of oscillatory or unsteady motion, rolling, broaching and pitching, to which some yachts are prone, apart from affecting overall performance, may also become potentially dangerous.

Sailing yachts are normally designed in such a way that they are statically stable and yacht designers are usually content when the boat has a degree of transverse static stability, which is measured by the restoring moment, determined by the amount of leeward shift of the centre of buoyancy B relative to the centre of gravity G, or the equivalent metacentric height GM. This in turn limits the boat's "power to carry sail" and also her performance.

The Dellenbaugh Angle Method or the Wind Pressure Coefficient Method[7] might be used to check whether a sailboat will be 'tender' in response or 'stiff'. This rather empirical criterion of yacht stability may be justifiable, since the presence of some degree of static stability usually ensures that the sailing craft, after being disturbed, will return towards the equilibrium position in some oscillatory manner. The word "usually" is used because as will be seen it is not always so; a yacht which is statically stable is not necessarily dynamically stable. There are both aerodynamic as well as hydrodynamic reasons for dynamic instabilities in yacht behaviour.

The object of this work is to determine and investigate the aerodynamic parameters on which the dynamic character of yacht motion depends. The complementary hydrodynamic aspects of boat motion are purposely discussed here in broad terms only, since they are objects of separate investigations.

On the assumption that safety at sea is of primary importance relative to performance considerations, priority was given to rolling, when planning the experiments in the wind tunnel.

3. PLAUSIBLE EQUATION OF ROLLING MOTION OF THE BOAT IN SMOOTH WATER

As a result of the combined action of the aerodynamic, hydrodynamic, gravitational, inertial and buoyancy forces the attitude of a sailing boat, while under way, can vary simultaneously relative to all three reference axes x_o, y_o, z_o. For example, when a boat sails in rough water the rolling, pitching, heaving, swaying and yawing are almost invariably all imposed on the boat in addition to the forward motion.

In order to avoid unnecessary mathematical complications inseparable when dealing with a system of many degrees of freedom, it became advisable to reject the rigorous consideration of coupling effects and mutual interaction between various kinds of motion.

In the case of rolling the theoretical and experimental methods of studying this type of unsteady motion were reduced to one degree of freedom.

This first assumption is justifiable since from the experience of many investigators in the past it appears to be legitimate to treat each component of boat motion separately, in so far as for each component motion the circumstances in which maximum effects are developed are not substantially affected by the simultaneous existence of other component motions.[8]

The second assumption, which largely simplified the design of the physical model of a yacht for wind tunnel testing and also facilitated the analysis of the results, was that the hydrodynamic action of the hull, when executing rolling, can be represented by a linear differential equation.

Bearing in mind that the primary purpose of this work was an investigation of aerodynamic aspects of unsteady motion

of sailing craft, the linearization of hydrodynamic response of a boat seemed to be highly desirable since it helps to trace nonlinear effects which might be imposed on the rolling boat by the aerodynamic action of the rig.

An example of resisted rolling in smooth water given below and an examination of basic factors involved in hull motion should indicate to what extent the second assumption may be acceptable.

A yacht without sails hoisted may be given a rolling motion by the action of external moments or forces which are periodic in character. It could be accomplished by rocking the hull by means of a halyard when a boat is moored in harbour, by the crew sallying back and forth across the deck.

Let us assume that the disturbing force or moment is suddenly removed when the mast has reached an angle of heel - θ_o to port, Fig.4a. The boat will tend to return towards the upright equilibrium position due to the action of the righting moment ΔGZ. The gravitational potential energy stored in the heeled position

$$Ep = \Delta GM(1 - \cos\phi)^{*} = \int_{\phi=o}^{\phi_o} \Delta GZ d\phi \qquad 1$$

where $\Delta = \rho g \nabla$ is displacement weight, is converted into the kinetic energy of rotary motion. When the mast reaches the upright position and the angular velocity p is at maximum, the kinetic energy accumulated is also at maximum.

$$E_k = \tfrac{1}{2} I \cdot p^2 \qquad 2$$

where I is the moment of inertia about a longitudinal axis through the centre of gravity.

---

*Approximate expression valid for centroid hull with fixed GM. Round-bottomed hull of wine glass section is very close in shape to centroid.

The hull and the mast, therefore, continue their rotation to starboard. However, not all of this kinetic energy is converted into potential energy as the yacht heels to starboard; a portion is drained away by the work done against the resistance offered by the water. The yacht is therefore brought to rest at a smaller angle of heel $+\phi_1$ than that $-\phi_o$, from which the rolling was started. The cycle of rotary motion begins again and the yacht will perform a series of successive rolls to port and back to starboard, each being less than the previous one until, due to the damping action of the water, until it finally comes to rest in the upright position.

The energy dissipation ΔE in one roll is given by

$$\Delta E = \tfrac{1}{2}\Delta GM(\phi_o^2 - \phi_1^2) \qquad 3$$

$$= \Delta GM\left(\frac{\phi_o + \phi_1}{2}\right)(\phi_o - \phi_1)$$

$$= \Delta GM\phi\delta\phi \qquad 3A$$

where $\frac{\phi_o + \phi_1}{2}$ is mean amplitude of roll

$\delta\phi$ is angular decrement/oscillation

The reduction in amplitude $\delta\phi$ can be called decrement per roll. In the limit it equals the slope of roll decrement curve plotted against number of swings $(\frac{d\phi}{dn})$ shown in Fig.4b.

As the rate of energy dissipation due to damping is a measure of the actual forces resisting the roll, the comparison of damping efficiency can conveniently be made on a basis of energy transfer.

Such damped oscillations are graphically represented in Fig.4b. Since the amplitude of roll decays with time,

the hull in rolling motion is dynamically stable. The rate ($\delta\phi$) at which the initial perturbation dies with time is a measure of the dynamic stability of the hull, which in contrast with static stability is a time dependent quality.

Once a metacentric height GM and a moment of inertia or radius of gyration K are known, the natural rolling period

$$T_R = 2\pi\sqrt{\frac{K^2}{gGM}} = 2{\cdot}006\sqrt{\frac{K^2}{GM}} = 2\pi\sqrt{\frac{I}{\Delta GM}} \qquad 4$$

(where K - radius of gyration about a longitudinal axis through the centre of gravity) of this so-called natural oscillation can be shown to be a characteristic which is fairly constant for each boat. It might be about 2-3 seconds for a small dinghy and about 6-8 seconds for a heavy keelboat.

If within the angles of roll the slope of the statical stability curve (expressed by $GM\phi$ as a function of ϕ) is constant, the periodic time T_R is the same whatever be the initial angle of roll. In that case the rolling is said to be <u>isochronous</u>.[8,9,10]

Pure rolling without swaying is possible only if the inclinations of the hull are equivolumetric and the axis of equivolumetric inclinations passes through the centroid of the water line area and the centre of gravity G lies in the plane of the flotation water line.

If the centre of gravity G is located above or below the area bounded by the load water line then the inclinations will obviously be not equivolumetric. It can be shown[10], however, that the departure from equivolumetric inclination, in the case when G is not located in the plane of flotation line, is negligible and may be ignored under the admitted accuracy of this study.

Ignoring sail action, the character of the damped rolling of the hull, its period and the rate of decay depend on three fundamental factors:

1. Moment of inertia of the boat; a large amount of inertia serves to increase the periodic time T_R.

2. Stability of the hull (GM), which affects the oscillation so that a stiff hull, of high stability, performs faster oscillations than a tender one.

3. Damping forces, which are responsible for the gradual extinguishing of rolling motion. They arise as a result of:

   a) the presence of frictional forces between the wetted surface of the hull and the surrounding water,

   b) the expenditure of energy in the generation of water waves,

   c) the dissipation of energy due to the hydrodynamic action of the swinging appendages: fin-keel and rudder.

These components of hydrodynamic damping are not equally significant. In the case of the keel-boat, the predominant role may be played by the action of appendages - the fin proper or centreboard and rudder, and also their configuration. Of course, high damping efficiency is desirable, since rolling, apart from bringing discomfort to the crew, is also potentially dangerous.

At the moment there is little known about fin-keel or centreboard efficiency as damping or antirolling devices. However, there is at least a certain theoretical foundation for believing that the modern tendency to reduce the length of the keel and cutting down the wetted area in order to improve the windward performance of the boat may lead to a reduction in the hydrodynamic damping in rolling.

Due to a lack of information correlating the geometry of the appendages and the damping characteristics, it was assumed that hydrodynamic damping is linear and proportional to angular velocity $\frac{d\phi}{dt}$.

Assuming further, according to Eq.2, 3 (Appendix), that within an amplitude of roll of the order of 30 degrees rolling motion can be regarded as isochronous, the equation of motion, for the hull rolling in still water, can be derived by writing equilibrium relation between the moments applied (taking the centre of gravity G as the origin of the co-ordinate system Fig.4a).

$$I\frac{d^2\phi}{dt^2} + b\frac{d\phi}{dt} + \Delta GM\phi = 0 \qquad 5$$

Designating $\Delta GM = K$ the Eq.5 can be written in the form:

$$I\cdot\ddot{\phi} + b\dot{\phi} + K\phi = 0 \qquad 6$$

where b - damping coefficient (in Nms/rad)

K - stability or stiffness coefficient (in Nm/rad).

The motion of the rolling hull therefore can be analysed as a dynamic non-conservative system (see Appendix Eq.16) having two different forms of energy storage, the kinetic energy and the potential energy, and also a form of energy dissipation. With reservations already listed the Eq.6 may be recognised as a linear, second order equation with time invariant or constant coefficients.

Natural motion of such a system will always be made up of some combination of two elementary motion patterns:-

a) sinusoidal motion which, in a way, represents the variation of kinetic and potential energy, and

b) exponential decay which gives a rate of energy dissipation with time as represented in Fig.4b.

When such a system is disturbed by some forcing function (it can be aerodynamic moment due to sail action) the resultant motion will be the sum of the two distinct components:[11]

a) natural motion whose character depends entirely on the physical parameters of the system itself (inertia, stability, damping) and not upon the forcing function,

b) excited motion which resembles in character the forcing or exciting function.

Thus with a single degree of freedom the plausible equation of motion for a complete yacht including the driving function due to aerodynamic action of the rig can be written:

$$I_x\ddot{\phi} + b\dot{\phi} + K\phi = K_A \qquad 7$$

where K_A is the disturbing aerodynamic heeling or rolling moment, and is not constant.

The object of direct wind tunnel testing was twofold, firstly to determine the fundamental parameters which affect the exciting or driving moment K_A, and secondly to establish the influence of K_A as a function of some parameters (course sailed, trim, wind velocity, etc.) on the stability of the rolling yacht.

4. PHYSICAL MODEL OF THE ROLLING BOAT

4.1 Test Apparatus and Similarity Problem

The diagrammatic sketch in Fig.5 together with Photographs 1 and 2 show the apparatus used during preliminary tests before it was put into the special tank recessed below the wind tunnel floor in order to reduce possible blockage effect. Photo 2 depicts the apparatus situated in the wind tunnel and also some details of the arrangement inside the tank. The apparatus, based on pendulum stability, incorporates:

- an airbearing support, permitting almost friction free oscillations about horizontal axis.
- variable and controllable magnetic damping (viscous in character) produced by an aluminium disc swinging between the poles of an electro-magnet.
- a flexure combined with a differential transformer to measure the variation in the drag component D due to rolling.
- a rotary pick-off to measure the amplitude of rolling ϕ versus time, with linear response up to $\pm$ 30°.
- recording facilities, linear recording of angular displacement ϕ, and drag D versus time by means of an ultraviolet galvanometer recorder.

A semi-rigid una-rig model of a 1/5th scale 'Finn' type sail made of "Melinex" was used for a series of initial tests. The 'Finn' rig was chosen bearing in mind its apparent simplicity; there is only a single sail which is rigged on a mast unsupported by any shroud. Further the 'Finn' is well known as a very bad and dangerous "roller" and therefore worthy of investigation.

When designing the oscillating part of the apparatus, including mast and sail, special attention was given to the problem of dynamic similarity. From a mechanical point of view, the two systems, model and full-scale, must not only be geometrically similar in shape (form) but also in mass distribution (moment of inertia) and stiffness (stability).

Assuming that the total mass of the full scale 'Finn' is 250 kg and taking the geometric scale factor n = 5, the mass of the model should be $\frac{250}{n^3}$ = 2 kg. It was not possible to satisfy this condition without reducing the strength of the structure below a practical limit, in fact the actual mass of the model was 3.49 kg. There was also another factor of primary importance which interfered to a certain extent with mechanical similarity demand, this was the Strouhal number - S_t or the so called 'reduced frequency'. In order to satisfy this condition it would require a relatively short period of oscillation which for some practical reasons could only be achieved by increasing the mass of the pendulum.

The Strouhal number, which can be expressed nondimensionally in the form:

$$S_t = \frac{\omega \cdot c}{V} \qquad 8$$

was regarded as the most natural and fundamental parameter in considering unsteady aerodynamic forces. An interesting interpretation of the Strouhal number was given by Karman. Consider that a disturbance occurs at a point on an airfoil and oscillates together with the airfoil. The air (fluid) influenced by the disturbance moves downstream with mean velocity $\bar{V}$. If the frequency of the oscillation of the airfoil and the disturbance is ω, then the spacing, or wave length of the disturbance, defined as a state of disturbance which is propagated from one place to another at finite speed is $2\pi V/\omega$. Therefore, the ratio

$$\frac{c}{\frac{2\pi V}{\omega}} = \frac{\omega \cdot c}{2\pi V}$$

which is proportional to the Strouhal number - S_t shows that S_t represents a ratio of the characteristic length of the airfoil (in our case the mean chord c of the sail) to the wave length of the disturbance. In other words, the Strouhal number characterizes the way a disturbance (it can be a vortex shed by the airfoil) is felt at other points of the airfoil. Since every point of an oscillating airfoil disturbs the flow, one may say that the Strouhal number characterizes the mutual influence between the motion at various points of the oscillating airfoil.[16].

Observation indicates that rolling instability, in the case of the full scale 'Finn', clearly occurs at a wind velocity of the order of V_A = 10 m/sec which corresponds to a fresh breeze, or force 5 on the Beaufort scale and that the period of oscillation T is approximately 2.5 sec. The mean chord of the sail is c = 1.95 m so that one can calculate the appropriate Strouhal number:—

$$S_t = \frac{\omega \cdot c}{V} = \frac{2.5 \times 1.95}{10} = 0.49$$

where $\omega \simeq \frac{2\pi}{T} = \frac{2\pi}{2.5} \simeq 2.5$ radians/sec.

Since the period of model oscillation selected for some practical reason is of the order T_m = 1.45 sec., the wind tunnel velocity which will satisfy the Strouhal number condition should be of the order:

$$V_m = \frac{\omega_m \cdot c_m}{S_t} = \frac{4.35 \times 0.39}{0.49} = 3.46^{m}/_{s} \simeq 11.3^{ft}/_{s}$$

where $\omega_m = \frac{2\pi}{1.45} \simeq 4.33$ (radians per sec)

c_m = 0.39m - mean chord of the model sail.

When planning the experiments in the wind tunnel it was decided to cover a range of Strouhal numbers corresponding to wind tunnel velocities V_m = 10, 12, 14 ft/s (3.05, 3.66, 4.27$^m/_s$). The corresponding full-scale wind velocities $V_{f.s.}$ would then be $V_{f.s.} = 2.9\ V_m$ = 8.85, 10.6, 12.4$^m/_s$ or 17.2, 20.6, 24.0 knots respectively. The appropriate values of the Strouhal number are:

$$S_t = 0.55,\ 0.46,\ 0.39 \text{ respectively.}$$

Reynolds number was regarded as a factor of secondary importance relative to the Strouhal number, and within the range of used wind tunnel velocities, 3.06 - 4.27$^m/_s$, covered the region:-

$$R_e = \frac{V_m \cdot c_m}{\nu} = \frac{3.06 \times 0.39 \times 10^5}{1.45} \text{ to } \frac{4.27 \times 0.39 \times 10^5}{1.45} \approx 0.8 \cdot 10^5 \text{ to } 1.15 \cdot 10^5$$

The corresponding values of Re for the full scale rig would be

$$R_e = \frac{V_{f.s.} \cdot 1.95 \cdot 10^5}{1.45} \approx 1.2 \times 10^6 - 1.7 \times 10^6$$

4.2 The Quasi-static approach to unsteady motion and static tests on the 'Finn' sail

Attempting to answer the question of "why and when" the rolling oscillations might be aerodynamically excited, a classical quasi-static approach seemed to be justified and promising as a preliminary approximation. This was based on the assumption that forces acting on the oscillating sail are the same as if the sail was in steady motion under the given conditions, i.e. that the flow about the oscillating sail and corresponding forces were determined

by the instantaneous incidence and velocity which are the controlling factors in uniform motion.

All we need when applying a quasi-static approximation is the static Lift and Drag characteristics of the rig. These two forces were measured using the balance system in the large wind tunnel section.

The model of a 1/5th scale 'Finn' type sail, made of "Melinex" and designed for the dynamic experiments, was tested over a range of static incidence from 15^{o} to 180^{o}. These angles cover all possible sailing courses. Since the twist of a sail is a function of wind velocity and this was quite high in relation to the rigidity of the model ($V = 7.63^{m}/s$ = 25 ft/sec), the actual twist of the sail model was rather large. A series of similar tests was therefore carried out on 2/5th scale Finn sail in order to establish the influence of the twist on the aerodynamic properties of the rig.

Figs.6, 7, 8 and Tables III, IV, V represent the geometry of the sail and some results. As would be expected for the twisted sail sections with a mast along the leading edge, both the L and the D curves are unsymmetrical relative to a line drawn through 90 degrees of incidence(α)measured between the boom of the sail and the wind direction. When the twist was reduced, both the L and the D curves were bodily shifted to the left (see Fig.8) towards the lower values of incidence α. It is worth noting that this shift is associated with increased negative slope of the L curve.

These facts, as will be seen later, are of importance as far as the stability in rolling is concerned. The results presented in Figs.7, 8 have not been corrected for blockage effects; in fact the test on the 2/5 scale model of the 'Finn' sail gave unusually high values of the drag coefficient, of the order 2.2. The test on the 1/5 scale model gave quite realistic values of drag coefficient close to the expected $C_{D_{max}} \simeq 1.2$.

4.2.1 Down wind rolling

Using the information provided by these tests, we may now examine the conditions in which rolling instability due to aerodynamic action of a sail may occur. If a una-rigged yacht is running down wind (Fig.9a) the course sailed relative to the apparent wind β_A is 180 degrees and the angle of incidence α of the sail to the wind direction is about 90^o. The total aerodynamic force T_A generated by the sail is more or less steady and acts very nearly along the course sailed.

If now by some means (it might be wave action) a small rolling motion is induced in the boat's hull, and the sail swings to say port, acquiring an angular velocity p, then the resultant wind, its incidence and aerodynamic force vectors L and D change both in magnitude and direction. This is shown in Fig.9b which refers to a narrow, horizontal strip of sail cut at some distance, z, from the axis of rotation.

As the sail swings to port the apparent wind V_A is modified by the velocity v induced by the swing. The resultant wind V_R which is, at any instant, the sum of the two wind vectors V_A and v will increase in magnitude and the instantaneous angle of incidence relative to the sail chord will be less than 90 degrees by an amount $\frac{pz}{V_A}$. When the sail swings to starboard the whole situation is reversed and as a result, the instantaneous angle of incidence α will be greater than 90^o, see Fig.10a,b. Under these conditions, the force component Y_A may act in the same direction as the rolling velocity (see Fig.9b) and can be expressed as

$$-Y_A = -L \cos\alpha_1 + D \sin\alpha_1$$

Since $\alpha_1 = 90-\alpha$;

Then

$$Y_A = L \cos(90 - \alpha) - D \sin(90 - \alpha)$$

$$Y_A = L \sin\alpha - D \cos\alpha \qquad 9$$

The actual magnitude and direction of action of the Y_A component will depend on the relative magnitudes of the L and D components at given instantaneous incidence α which is modified by the velocity induced by rolling.

Differentiating Y_A with respect to α gives the rate of change of Y_A due to rolling in qualitative sense. Thus

$$\frac{\partial Y_A}{\partial \alpha} = \sin\alpha\left(\frac{\partial L}{\partial \alpha} + D\right) + \cos\alpha\left(L - \frac{\partial D}{\partial \alpha}\right) \qquad 10$$

when $\alpha \simeq 90^{\circ}$ and the amplitude of oscillation is small then $\sin\alpha \to 1$ and $\cos\alpha \to 0$, therefore the second term of Eq.10 is negligible, and

$$\frac{\partial Y_A}{\partial \alpha} = \frac{\partial L}{\partial \alpha} + D \qquad 11$$

Since the drag D is always positive there are three possibilities to consider, namely:-

I	$\frac{\partial Y_A}{\partial \alpha} = 0;\ \left\lvert -\frac{\partial L}{\partial \alpha}\right\rvert = D$	11a	rolling motion is therefore not affected by the aerodynamic forces
II	$\frac{\partial Y_A}{\partial \alpha} < 0;\ \left\lvert -\frac{\partial L}{\partial \alpha}\right\rvert > D$	11b	instability may be induced by the aerodynamic forces
III	$\frac{\partial Y_A}{\partial \alpha} > 0;\ \left\lvert -\frac{\partial L}{\partial \alpha}\right\rvert < D$	11c	a stabilizing effect of aerodynamic forces can be expected.

Note | | means numerical value.

Thus positive $\frac{\partial L}{\partial \alpha}$ means a stabilizing effect in any case.

Let us analyse in some detail the physical meaning of case II when $\frac{\partial L}{\partial \alpha}$ is negative and its numerical value is greater than D. In Fig.7, which presents the static aerodynamic characteristics of the 1/5th scale Finn sail, a graph of $\frac{\partial L}{\partial \alpha}$ is plotted together with L and D curves against incidence α. One can see two regions of potential instability where $\frac{\partial L}{\partial \alpha}$ is negative and, at the same time, its numerical value is greater than the D component, which can be regarded as being a positive damping factor. In order to facilitate immediate comparison of $\frac{\partial L}{\partial \alpha}$ and D values the graph of $\frac{\partial L}{\partial \alpha}$ is plotted with the negative values above the abscissa.

These results are modified in Fig.11. It can be seen that besides the original L, D and $\frac{\partial L}{\partial \alpha}$ curves, there is drawn a hypothetical shift of the above mentioned curves which could be expected due to the reducing the twist in the sail. This prediction is based on results of experiments presented in Fig.8 on the 2/5th scale model of the same type of rig; the set of curves shown clearly indicate such a tendency.

It is evident that sail twist may exert a significant effect on dynamic stability by shifting the region of instability (marked in Fig.7 and 11 by the shaded areas) relative to the angle of incidence α of the sail.

A modification of the original results as presented in Fig.11 was made bearing in mind the fact that it was anticipated that the subsequent dynamic tests would be performed at a lower wind speed (3.05 - 4.27 m/sec) to satisfy the appropriate Strouhal number. Therefore the effect of the twist of the sail had to be taken into consideration. In further discussion reference will be made to the modified set of curves.

Fig.10a,b depicts configurations of wind and force vectors for the case when the initial incidence α is 90 degrees and the yacht is running down wind; as before the two drawings refer to a narrow horizontal strip of sail some

distance from the axis of roll. When the sail, being disturbed for some reason, acquires an angular velocity swinging to port so that α decreases, the flow pattern round the sail changes quite drastically from that when there is no rolling. A circulation appears (marked by the dotted line) which in turn affects the instantaneous lift and drag in such a way that the total aerodynamic force T_A is inclined towards the direction of the sail motion. This total force T_A can be resolved into two components as shown in Fig.9a.

1) X_A component acting along the axis of rolling X_O

2) Y_A component acting perpendicular to X_O.

The boat is now rolling to port under the action of a sail force component Y_A induced by the velocity of roll. As the heel angle increases the righting moment due to the lateral stability of the hull, and the damping due to the combined action of the hull and appendages increasingly oppose the rolling and finally start to return the boat to the upright position. The sail now swings to starboard and the flow pattern is reversed. This is shown in Fig.9b. The circulation is opposite to that in the previous swing and the aerodynamic force component Y_A is again directed towards the motion pushing the sail to starboard. Because of the action of these alternating forces operating in phase with roll velocity, the amplitude of rolling may be magnified progressively. Fig.11 represents, in a way, a potential ability of the system to develop <u>divergent oscillations</u> in which amplitude of roll grows progressively. The initial experiments in the wind tunnel have shown that the model responded dynamically according to the prediction based on an analysis of Eq.10. Fig.12 depicts a typical behaviour of the model when the rig way set at $\beta_A = 180^\circ$ and the angle of trim of the sail $\delta_m = 85^\circ$ ($\alpha = 95^\circ$). The rolling

amplitude ϕ builds up even in the absence of any obvious external disturbances, i.e. even in a completely flat sea.

This type of yacht behaviour clearly manifests dynamic instability. Refering to Fig.4b and 12 we can say that in both cases the boat is statically stable, since a certain tendency to return to an upright position is maintained; however in the second case there is a divergence superimposed on the oscillation. This is due to the lack of energy balance - energy lost due to damping and energy taken from the wind.

This test proved beyond any doubt that wild rolling may be induced by a sail for an aerodynamic reason. When running down wind, a sail can extract energy from the wind in a self-exciting manner by its own periodic motion in such a way that the sail can be regarded as a rolling engine. When studying the self-excited rolling of a yacht, one should focus one's attention on two opposing elements of the rolling motion: namely, the excitation element and the dissipation element. The character and magnitude of these two factors determine whether or not, and to what extent, the boat will be able to roll. The process of magnification of rolling amplitude will continue until the rate of wind energy input due to the sail action is matched by the rate of dissipation of energy in damping due to the action of the underwater part of the hull.

4.2.2 Rolling when sailing close hauled

The quasi-static approach, which proves to be most helpful in grasping the principles of down wind rolling conditions of stability, seems to be equally suitable for investigating rolling stability when sailing to windward. Fig.13 which refers to a narrow, horizontal strip of sail cut at a certain distance, z, from the axis of rolling, depicts force and wind vectors as well as some geometrical relations between them. When, for example, due to wave

action, the sail swings to port, the apparent wind V_A is being modified by the wind $v = p.z$ induced by the swing. The instantaneous angle of incidence of the sail α will be affected by the variation in direction of the resultant wind V_R, which is the sum of the two wind vectors V_A and v. Assuming that v is small relative to V_A, the aerodynamic force component Y_A which affects rolling can be expressed at any instant as:

$$Y_A = L \cos(\beta_A \pm \Delta\beta) + D \sin(\beta_A \pm \Delta\beta) \qquad 12$$

$$Y_A = L \cos\beta'_A + D \sin\beta'_A \qquad 12a$$

A differentiation of Eq.12a with respect to β_A will give us a rate of change of Y_A due to rolling which might be imposed on the system by the action of an external moment.

$$\frac{\partial Y_A}{\partial \beta_A} = \frac{\partial L}{\partial \beta_A} \cos\beta_A - L \sin\beta_A + \frac{\partial D}{\partial \beta_A} + D \cos\beta_A$$

$$= \cos\beta_A \left(\frac{\partial L}{\partial \beta_A} + D\right) - \sin\beta_A \left(L - \frac{\partial D}{\partial \beta_A}\right) \qquad 13$$

Since the variation in L and D with β_A are equivalent to variations due to changes in α (see Fig.13), the Eq.13 can be rewritten in the form:

$$\frac{\partial C_{YA}}{\partial \alpha} = \cos\beta_A \left(\frac{\partial C_L}{\partial \alpha} + C_D\right) - \sin\beta_A \left(C_L - \frac{\partial C_D}{\partial \alpha}\right) \qquad 14$$

which is more convenient to analyse, having already at hand the characteristics of the rig expressed in standard form

of C_L and C_D coefficients plotted against α. They are shown in Fig.14 which presents the variation of C_L and C_D of the Finn rig with incidence angle α of the sail. The boom was pulled vertically downward to four different positions with the mainsheet (17). The various sail shapes, with their associated twist and camber changes resulting from the four boom positions, produced different aerodynamic characteristics. They can be used to assess Eq.14 numerically.

Let us assume that $\beta_A = 30^\circ$. The slope of all C_L curves , i.e. the value of $\frac{\partial C_L}{\partial \alpha}$ is more or less constant within the practical limits of incidence $\alpha = 10\text{-}20^\circ$ (typical for close hauled sailing). The value of $\frac{\partial C_L}{\partial \alpha}$ (α being expressed in radians) equals approximately 2.86. The relevant average value of $\frac{\partial C_D}{\partial \alpha}$, for the drag curve VIII is approximately 0.98. Assuming further that $\alpha = 15^\circ$ we can estimate $\frac{\partial C_{YA}}{\partial \alpha}$ substituting relevant numerical data from Fig.14 (run VIII). Thus

$$\frac{\partial C_{YA}}{\partial \alpha} = \cos\beta_A \left(\frac{\partial C_L}{\partial \alpha} + C_D\right) - \sin\beta_A \left(C_L - \frac{\partial C_D}{\partial \alpha}\right)$$

$$= 0.866(2,86 + 0.2) - 0,5(0,95 - 0,98) \qquad 14a$$

One can see that the first term in the equation is positive and much greater than the second one, which for other values of α might be negative but still negligible in comparison with the first one. Substituting appropriate values of $\frac{\partial C_L}{\partial \alpha}$, $\frac{\partial C_D}{\partial \alpha}$, L and D in Eq.14 for other values of β_A and α we find that in a close hauled condition $\frac{\partial C_{YA}}{\partial \alpha}$ is always positive. Referring back to Eq.11c it would mean that when sailing to windward, one should expect a stabilizing or damping effect from the aerodynamic forces on the rolling motion of the boat in the case when rolling occurs for hydrodynamic reasons.

Experiments in the wind tunnel on the model shown in Fig.15 and observations of the full scale boat behaviour

clearly indicate that the theoretical conclusion drawn from Eq.13 are correct. During tests in the wind tunnel the Finn type rig was set at $\beta_A = 30^o$ and the angle of trim of the sail δ_m was about 15^o. At the wind speed V_A = 3m/s an average angle of heel was about 8 degrees to starboard and the model oscillated about this mean angle in a random way $\pm 2^o$ due to unsteadiness in the air stream. After a certain time the model was displaced to 20^o of heel, and kept there for a while, then left free. The return to the mean angle of heel $\phi = 8^o$ was immediate without overshot. The model responded in the same way when the heel was reduced to 0^o, and then released. In both cases the magnetic damping was zero. The results recorded in Fig.15 indicate that the positive damping generated by the sail is very great indeed. In fact the system is over damped (see Appendix Eqs.20-21). When watching a large fleet of racing yachts on a windward leg, one is easily struck by the steadiness of all the yachts in maintaining a constant angle of heel even in strong, gusty winds. This fact was surely discovered through trials and errors by fishermen who hoisted a sail on motor driven vessels when sailing to windward, not as a driving device but as a rolling stabilizer.

Referring to Fig.11 one can conclude that the same aerodynamic forces and process which may translate energy taken from the air into incipient rolling can also act as a suppressor. All is dependent upon whether the aerodynamic forces generated by the system after disturbance are related to the negative or positive slope of the $C_L \sim \alpha$ curve. The system, after being disturbed, may develop instability in rolling when the aerodynamic forces and the arising moments are related to the negative slope of the L (or C_L) curve. The steeper the negative slope, the greater will be the energy transfer from the air to the system and the instability response in rolling motion will be more conspicuous. Vice-versa, the aerodynamic forces related to the positive slope of the L (or C_L) curve should certainly stabilize or damp any rolling motion induced by hydrodynamic forces.

There is, however, a certain degree of uncertainty left in the conclusions just derived. This is because the quasi-static method does not take into account the time factor required for the build-up of circulation around an oscillating airfoil, and subsequently there is a time lag between the forces actually generated and the forces expected on the quasi-static basis. This might yield an inaccuracy in the prediction of the degree of stability or instability. Therefore a certain correction to the quasi-static approach should be introduced to check whether and to what extent conclusions already derived are correct in a quantitative sense.

The accepted theories of non-uniform or oscillatory motion developed by H. Wagner (19), Th. Theodorsen (20), Th. Karman (18,21,22), Glauert (23), and others takes into consideration two effects which are absent from uniform or quasi-stationary motion. One arises from non-uniform acceleration and deceleration of the mass of fluid taking part in circulation round the oscillating airfoil,ie. in the direction normal to that of the translatory motion. The other originates in the velocities induced in the vicinity of the airfoil (or hydrofoil) by the wake of transverse vortices discharged when the variation in circulation takes place. The actual flow about an oscillating airfoil thus depends not only upon the angle of incidence and local velocity, which are controlling factors in uniform motion, but also upon the instantaneous acceleration or deceleration and past history of the motion.

4.3 The non-stationary forces developed on an oscillating airfoil

In order to define the basic difference between the stationary and non-stationary aspects of the flow around the airfoil a short review of the circulatory theory for the simple case of two-dimensional foil operating in the range

of incidence angles related to the rising slope of the C_L curve i.e. below the stall angle, is essential.

When a symmetrical airfoil shown in Fig.16a set at incidence $\alpha = 0^o$ moves steadily with a velocity U relative to the air at rest only the drag could be measured. This would consist mainly of skin friction plus a small contribution of profile drag. The wake left behind is relatively small and insignificant. When the airfoil is suddenly set at an angle of incidence α (Fig.16b) a circulation is being developed of sufficient strength to shift and hold the rear stagnation point at the trailing edge, T.E. At the same time, according to the theorem of conservation of the moment of momentum, a counter-circulation develops, called the "starting vortex". At the initial stages of the transition period, before the circulation round the airfoil is fully developed, the "starting" or cast-off vortex-sheet begins to operate in a form of concentrated vortex between the trailing edge T.E. and the rear stagnation points situated on the upper surface upstream at a small distance from the trailing edge. When, during this transition period, the starting vortex has developed to a certain strength, it breaks away from the airfoil and passes down stream in the wake followed by a sheet of small vortices. In the course of time the starting vortex travels further and further downstream where it can finally no longer influence the flow round the airfoil, and the airfoil is then in steady motion with a fairly fixed magnitude of circulation and associated steady lift. One can say that a physical role of the starting vortex is to shift the rear stagnation point S towards the trailing edge. In a way the starting vortex serves as a kind of "prolonged ignition" or stimulus for circulation. In this way the elegant and famous Kutta-Joukowski theorem and condition are fulfilled. Fulfilment of this condition is necessary in order to exclude the possibility of an infinite velocity around the sharp trailing edge of the airfoil.

An assumption that the starting vortex is so far behind the airfoil that it does not influence the flow in the vicinity of the airfoil and α and U are constant, leads to the so-called stationary flow theory of airfoils according to which the circulation is given by:

$$\Gamma = \tfrac{1}{2}c\ U\alpha\ \frac{\partial C_L}{\partial \alpha} \qquad 15$$

and is constant (incidence angle α is measured from the no lift angle). The lift, L, per unit span can be expressed as

$$L = \rho \cdot U \cdot \Gamma \qquad 16$$

and

$$C_L = \frac{2\Gamma}{c \cdot U} \qquad 17$$

In fact the magnitude of the fully developed circulation is subject to a small fluctuation (24). When the vorticity of the boundary layer passes downstream in a vortex wake it develops into a Karman vortex street and, to maintain this system, vortices of opposite sign are shed alternately from the upper and lower surfaces of the airfoil. Since the sum of the circulation round the airfoil and of the strengths of all the vortices of the wake must be zero, it follows that the circulation round the airfoil will oscillate between the limits $\Gamma \pm \tfrac{1}{2}\gamma$, where Γ is the mean circulation and γ is the strength of the vortex street. For a good aerofoil section at a small incidence the vortex wake is narrow and weak, and the circulation round the airfoil is sensibly constant. However, when the angle of incidence increases, approaching stall angle, the oscillation in the magnitude of the circulation and associated lift may become

an important fraction of the mean values. Tests performed by Fage and Johansen (25) below and above the stalling angle proved beyond any doubt that the velocity fluctuations in the wake due to the presence of vorticity shed from the airfoil are function of the Strouhal Number.

Referring back to an early stage of circulation being developed when the angle of incidence was suddenly changed from 0 to α one should realise that the circulation pattern around an airfoil does not spring into being without a certain time lag. Therefore the lift normally associated with the changed angle of incidence α does not reach its nominal value immediately but only a fraction is reached, the remaining value being developed in the time taken to travel a certain number of chords. This is shown in the graph on the right side of Fig.16, which presents the rate of growth of lift and circulation with time. For example, about 0.9 of the steady state value of the lift L_α is reached after a time $t = \frac{6c}{U}$. A half of the L_α value is reached almost immediately. This fact was first discussed by Wagner (19), who gave the theoretical reason for this behaviour of the lift, and the phenomenon on this account is usually referred to as the "Wagner effect". His theory was experimentally verified by Walker (19), who found that the actual measured circulation at any stage in the early motion of the airfoil was approximately the same fraction of its final value as that deduced from Wagner's theory. Wagner's theory may, therefore, be considered to account for the initial motion to the same extent that the classical theory accounts for steady motion.

Studies of unsteady aerodynamics indicate that the lift build-up has the nature, but not the exact shape of an exponential as indicated by the graph in Fig.16. A reasonable approximation of actual lift L_a at a given time is:

$$L_a = L_o(1 - e^{-t/\sigma}) \qquad 18$$

where L_o = stationary lift at incidence α

$\sigma = f(c/U)$

c = average surface chord

U = forward velocity

When an airfoil performs translatory oscillations within an amplitude $\pm y$, as shown in Fig.16c, the instantaneous angle of incidence $\alpha = \tan^{-1} v/U$, (where v is the instantaneous velocity in y direction), will vary and, according to Eq.15, every change of the state of motion must be accompanied by a change of the circulation Γ around the airfoil.

It appears that for every change of Γ, and likewise for every change in the angle of incidence, a vortex must leave the trailing edge of the airfoil. The strength of this vortex is equal to the change of the circulation and the rate at which vorticity is deposited in the wake in the vicinity of the T.E. is given by

$$\frac{\partial \Gamma}{\partial t} = \tfrac{1}{2} c\, U \frac{\partial \alpha}{\partial t} \frac{\partial C_L}{\partial \alpha} \qquad 19$$

Hence the vorticity shed per unit movement forward is:

$$\frac{\partial \Gamma}{\partial x} = \frac{1}{U} \cdot \frac{\partial \Gamma}{\partial t} = \tfrac{1}{2} c \frac{\partial \alpha}{\partial t} \frac{\partial C_L}{\partial \alpha} \qquad 20$$

In the case of a continuously changing circulation a band of vortices develops behind the airfoil. Physically, the generation and shedding of each vortex, as shown in Fig.16c, is somewhat similar to the process described earlier when discussing the "starting vortex" mechanism depicted in Fig.16b. Continuous shedding of the vortices into the wake is accompanied by simultaneously occuring shifts of forward and rear stagnation points and therefore subsequent

oscillations in local pressure. The vortices being shed affect also the downward velocity at the airfoil and hence alter the flow pattern and circulation.

When analysing Eqs.19 and 20, one can say that if the changes of circulation are very slow, the vortex intensity in the wake is very small. The flow around the airfoil is then almost the same as in the steady state, and a quasi-static approach is therefore justifiable. However, in general, the forces on the airfoil will depend upon the vortex intensity in the wake and the influence of this wake must be taken into account.

On the assumptions of an infinite aspect ratio airfoil, a small amplitude of motion and some other restrictions, Karman and Sears (22,26) presented a theory of non-uniform motion which very much aids the prediction of lift characteristics for the case of sinusoidal motion. This is applicable both for oscillating sail and hydrofoil as a fin-keel.

According to this theory the actual lift L_a developed by the oscillating airfoil is the sum of three components:

L_o - the "quasi-static" lift

L_1 - the "apparent mass" lift

and L_2 - the "wake effect" i.e. modification to the actual lift due to velocity induced by vorticity within the wake.

Hence

$$L_a = L_o + L_1 + L_2 \qquad 21$$

If we take, for example, the case of an aerofoil set at some angle of incidence and oscillating in translatory motion perpendicular to the undisturbed stream, the lift

characteristics predicted by the theory include:

a) the actual lift which varies in a sinusoidal manner,

b) a variation in lift which may be either greater or less than that which would occur if the oscillations were infinitely slow, i.e. if at each angle of incidence the lift were that corresponding to the steady motion,

c) a variation of lift which may either lead or lag that angle of incidence,

d) a phase angle and amplitude of the variation of lift which will depend on the so-called "reduced frequency", or in other words the Strouhal number divided by two.

These predictions are illustrated diagramatically in Fig.17. The broken line sine curve shows the hypothetical variation of lift which would occur if at each instantaneous angle of incidence α the lift value was that corresponding to steady state motion. The solid-line represents the actual variation of lift L_a. The physical significance of Eq.21 may be clarified by means of a "vector diagram" as shown in Fig.18, which presents the phase relationships of the quantities involved L_o, L_1, and L_2 as well as their magnitudes (22), plotted in complex plane.

Unsteady lift function can be defined as:

$$L_a(t) = Fe^{i\omega t}\{f_1(^{\omega}/_{U}) + if_2(^{\omega}/_{U})\} \qquad 22$$

where $L_a(t)$ represents lift as a function of time; F is a constant involving only the dynamic pressure $\rho\frac{U^2}{2}$ and the amplitude of the oscillation y; and f_1 and f_2 are real

functions. The real part of this expression which is the actual lift L_a may be written as

$$Re|L_a(t)| = F(f_1 \cos\omega t + f_2 \sin\omega t)$$

$$= F\sqrt{f_1^2 + f_2^2}\cos(\omega t + \lambda) \qquad 23$$

where $\lambda = \tan^{-1}(f_2/f_1)$.

Thus, in vector representation, the lift vector has the magnitude $F\sqrt{f_1^2 + f_2^2}$ and leads the vector of the velocity of oscillation, v, by a phase angle λ as shown in Fig.18, which depicts how the total lift vector is composed for a certain value of ω/U. The quasi-steady part, L_o, being in phase with the velocity of oscillation, v, appears as a horizontal vector, while the vector L_2 tends to diminish the lift and cause it to lag behind the velocity. The apparent-mass lift, L_1, being proportional to the acceleration, is directed vertically i.e. leads the velocity by 90°. The total actual lift, L_a, is the sum of these three vectors and has the phase angle λ.

A curve plotted in Fig.19 gives the magnitudes of the lift together with their phase angles λ for various values of the Strouhal number (or reduced frequency). The length r of the vector drawn from the origin to the appropriate value of the reduced frequency $\frac{\omega \cdot c}{2U}$ on the curve gives the ratio of the total actual lift L_a, to the corresponding quasi-steady lift, L_o. The λ angle between r and the horizontal axis gives the phase angle relative to the velocity of oscillation v. It is seen that within the limits of the Strouhal number investigated in the wind tunnel tests on Finn sail model i.e. 0.39-0.55, the maximum value of the lift, L_a, slightly decreases and the lift vector lags slightly behind the velocity v.

4.3.1 Aerodynamic damping when sailing to windward

Yacht oscillation can be called aerodynamically unstable if the effect of an initial transient rolling disturbance imposed on the sail, say, by wave action is magnified as time increases. In such a case the sail extracts the energy from the wind in completing a swing (cycle). If the reverse is true, i.e. the effect of an initial transient disturbance dies out as time increases, it means that the sail dissipates energy in a full cycle of oscillatory motion. One may say that such oscillation is aerodynamically stable, or, in other words, aerodynamic damping is positive. In this case the work done by a sail is negative, i.e. energy is given or lost to the airstream.

On the basis of the theory of non-uniform motion presented in (4.3) let us consider work done Δw by the unsteady lift produced by a strip element of the sail area ΔS_A at some distance Z from the axis of roll X_o. For that unit area which is horizontal strip of the sail, we can regard its oscillatory motion in close-hauled conditions as the translatory one when considering amplitude:

$$y = y_o e^{i\omega t} \qquad 24$$

If oscillations are small, a certain difference in magnitude between velocity vectors V_A and V_R can be ignored (see Fig.13). Hence $V_A \simeq V_R = U$. We shall concentrate attention on the lift only, since, according to Eqs.14 and 14a, the contribution of this component of Y_A force will be dominating as far as damping moment due to Y_A action is concerned.

The velocity induced by a swing of the sail to windward can be expressed as:

$$v = \frac{dy}{dt} = i\omega y_o e^{i\omega t} \qquad 25$$

If $\frac{dy}{dt}$ were a constant, the windward swing will induce a lift force L_o on the sail

$$L_o = \tfrac{1}{2}\rho U^2 \Delta S_A \frac{\partial C_L}{\partial \alpha} \frac{\frac{dy}{dt}}{U} \qquad 26$$

The actual instantaneous lift would be

$$L_a = L_o \, r \, e^{i\lambda} \qquad 27$$

where r, according to Fig.19 represents the ratio of the actual value of the instantaneous lift L_a to that of the quasi-steady lift L_o, and λ is the phase angle by which the actual lift leads or lags the quasi-steady value.

When a sail moves through a distance dy the work done by the lift is

$$dW = -L_a dy = -L_a \frac{dy}{dt} dt \qquad 28$$

since, by definition, work can be expressed as

$$W = L \cdot y \cos\lambda$$

where λ is an angle between the force and displacement, if $\lambda = 180^o$ $\cos\lambda = -1$.

It must be recognized that when L_a and $\frac{dy}{dt}$ are given in the complex form as in Eqs.25 and 27, the physical quantities of L_a and $\frac{dy}{dt}$ are represented only by the real parts.

Therefore Eq.28 can be rewritten as

$$dW = -\mathrm{Re}\left[L_a\right] \cdot \mathrm{Re}\left[\frac{dy}{dt}\right] dt \qquad 29$$

Substituting Eqs.25 and 27 into 29 yields

$$dW = -\mathrm{Re}\left[\tfrac{1}{2}\rho U^2 \Delta S_A \frac{\partial C_L}{\partial \alpha} \frac{i\omega y_o e^{i\omega t}}{U} r \cdot e^{i\lambda}\right] \mathrm{Re}\left[i\omega y_o e^{i\omega t}\right] dt$$

$$= -\rho/2 \; U\Delta S_A \frac{\partial C_L}{\partial \alpha} \mathrm{Re}\left[i\omega y_o r e^{i(\omega t + \lambda)}\right] \mathrm{Re}\left[i\omega y_o e^{i\omega t}\right] dt \qquad 30$$

Taking only the real parts of Eq.30 and integrating over the complete cycle of oscillation 2π (whole period T), we obtain the total work done ΔW by the wind on the unit area of the sail, ΔS_A.

$$\Delta W = -\int_o^{2\pi/\omega} \left[\rho/2 \; U^2 \Delta S_A \frac{\partial C_L}{\partial \alpha} \cdot \frac{\omega y_o r}{U} \cos(\omega t + \lambda) \cdot \omega y_o \cos\omega t\right] dt$$

$$\Delta W = -\frac{\rho}{2\omega} U\Delta S_A \frac{\partial C_L}{\partial \alpha} (\omega y_o)^2 r \int_o^{2\pi} \cos(\omega t + \lambda)\cos\omega t \, d(\omega t)$$

$$\Delta W = -\frac{\pi}{2} \rho U \Delta S_A \frac{\partial C_L}{\partial \alpha} \omega y_o^2 r \cos\lambda \qquad 31$$

We can see that the tapping of energy ΔW by the sail from the wind is proportional to $(-\cos\lambda)$ therefore if $-\frac{\pi}{2} < \lambda < \frac{\pi}{2}$ work is negative i.e. the oscillating sail will lose energy to the airstream. The system will be stable or, in other words, aerodynamic damping will be positive.

Referring to actual tests and Fig.19, it is seen that the condition of stability $-\frac{\pi}{2} < \lambda < \frac{\pi}{2}$ in close hauled conditions is satisfied. Within the limits of the Strouhal

number investigated in the wind tunnel and met in practice, the phase angle λ is not very far from O. So, the expected stabilizing effect of the sail on the rolling motion should be strong; this was confirmed by experiments. Analysing Eq.31 one may anticipate that the higher AR, shorter period of oscillation, greater sail area, stronger wind, the more effective will be the sail as a damping device.

This conclusion, as deduced from Eq.31, is in agreement with the previous one based on the static tests incorporated in Figs.11, 14 and also with Eqs.11 and 14. The work done by an oscillating rig will be negative if the forces developed by the sail are related to the rising slope of the $C_L \sim \alpha$ curve i.e. $\frac{\partial C_L}{\partial \alpha}$ is positive.

4.3.2 Some remarks about damping efficiency of the fin-keel and rudder

In down-wind sailing conditions, when a large amplitude of rolling can be induced for aerodynamic reasons, the hydrodynamic damping efficiency of the hull becomes an important factor limiting the degree of instability. High damping efficiency is desirable. It is justified to assume that the predominant role in producing positive damping is played by the action of appendages, the fin-keel proper or centreboard and rudder and also their configuration.

At the moment there are no experimental data facilitating an estimation of damping efficiency of the appendages. However, Eq.31 may provide some clue to the problem.

The total work done on an oscillating aerofoil or hydrofoil by the stream, as expressed in Eq.31 can be estimated by integration of the unit work done by the lift on a strip element (ΔW) over the total area of the hydrofoil. The area of the appendages is therefore an important factor affecting damping and one can say that the modern tendency to reduce the wetted area of the fin in

order to improve the boat's performance might lead to a drastic reduction of damping efficiency of the hull. This tendency is illustrated in Fig.20, which shows a typical modern One Ton Cup contender. The traditional shape of the underwater part of the hull is illustrated by a broken line.

Since the aspect ratio of the 'shark's fin' is bigger than the traditional one, the value of $\frac{\partial C_L}{\partial \alpha}$, which enters Eq.31, should be affected advantageously. So losses in damping efficiency due to reduced wetted area may be compensated to a certain extent by the effect of increased slope of the C_L - α curve. However, the higher the aspect ratio of the fin-keel, the more probable it is that the tip will reach a stalling condition at the extreme angle of rolling thus giving rise to a large hysteresis effect.

Hysteresis may be defined as a lagging or retardation of an effect (in this case lift) behind a change in the influencing mechanism which causes the effect. In general the hysteresis phenomenon is exhibited by a system whose state (i.e. the forces developed) depends on its previous history. This is clearly shown by Photo 3, in which it can be seen that fully separated flow persists even when the angle of incidence is being reduced to zero.

Assuming that the total lift generated by the oscillating hydrofoil is related to the rising slope of the L curve, so $\frac{\partial C_L}{\partial \alpha}$ is positive, one can expect that the work done on the system will be negative, as shown in Fig.21. This negative work, -W, would correspond to positive damping or positive stability. If an oscillating hydrofoil or a part of it approaches or exceeds the stalling angle and $\frac{\partial C_L}{\partial \alpha}$ becomes negative, one should expect a hysteresis loop with positive work, +W (shown in Fig.21). This corresponds to negative damping. In such circumstances one may expect that the total damping efficiency of the hydrofoil will be reduced, depending on the area of the hydrofoil affected by the stalling conditions.

Assuming that for the yacht shown in Fig.20a the maximum depth of the fin-keel is 6.2 feet, the period of rolling oscillation T = 3,5 sec., the boat speed $V_s = 1.2\sqrt{LWL} = 1.2\sqrt{26,7} = 6,2$ knots = 10,5 ft/sec, one can calculate the approximate instantaneous maximum angle of incidence at the tip of the fin-keel for the angle of roll $\phi = 30^{o}$.

The maximum angular velocity induced by the roll will be

$$p = \frac{2\pi}{T} \cdot \frac{30 \cdot \pi}{180} = 0,94 \text{ rad/sec}$$

The maximum linear velocity v at the tip will be

$$v = p \times 6.2 = 5,8 \text{ ft/sec}$$

so that the instantaneous maximum angle of incidence would be in the order of

$$\alpha = \tan^{-1} \frac{v}{V_s} = \frac{5.8}{10.5} \approx 29 \text{ degrees.}$$

Whether or not the tip of the oscillating fin-keel reaches stalling conditions at so large angle of incidence cannot be answered without tests. The experiments described in (27, 28) suggest that the hydrodynamic forces developed on a hydrofoil oscillating sinusoidally at or near the stall vary in a periodic but nonsinusoidal manner. The form of the periodic variations of the fundamental lift component and the subsequent damping efficiency depends on the Strouhal number, the amplitude of oscillation, the shape of the hydrofoil, and the Reynolds number.

Apart from damping efficiency considerations of the fin-keel proper, there is also another aspect of the same problem, namely the interaction effect between the fin-keel and the separated rudder. When the fin-keel is swinging continuously from port to starboard as shown schematically in Figs.16c and 20b, relevant eddies are being detached alternately from the trailing edge of the fin at a practically constant rate for a given velocity of the flow V_s (U). The double row of vortices and the velocity fluctuation induced by them within the wake will affect the oncoming flow relative to the rudder and subsequently the forces generated by the rudder. In some critical conditions, depending on vortex spacing and vortex intensity, the effectiveness of the rudder may be reduced, both as a steering device and as a roll damper. One might even anticipate a possibility that the oscillating velocity within the wake may set up a component of rudder force in phase with the rolling velocity. In this extreme but quite probable case the rudder may work as a roll magnifier.

Due to the very peculiar and complicated character of unsteady aerodynamic and hydrodynamic reactions being generated on a rolling boat, and their mutual interactions and setback effects, in some sailing conditions, an energy gap or energy deficit may occur. In other words, the energy input to the system cannot be matched by the energy dissipation; the amplitude of rolling will then build up rapidly.

4.3.3 Flow behind a stationary and an oscillating cambered plate. Water-channel experiments

When a flat or cambered plate or a cylinder, moves through a fluid with its length normal to the flow direction, vortices are shed into the wake periodically forming the well-known Karman vortex trail. This phenomenon, which has been observed by various investigators through centuries:-

Leonardo da Vinci (see Fig.22), Strouhal, Bernard, Karman and many others, is still far from being completely understood. However, the basic mechanism explained in a way by Karman (1911), who made a stability analysis of the vortices being formed in a certain geometrical pattern, is fairly well known, at least for a stationary or non-oscillating body. Each time a vortex is released into the wake, an unbalanced transverse force Y acts on the body (see Fig.23), apart from the normal force component X. Whether the surrounding fluid is air or water does not change the basic physical principles nor the mathematical relations involved in the theory. The generation of vortices alternately on either side of the cambered plate, as shown in Fig.23, proceeds in accordance with a basic theorem of aerodynamics which states that the circulation around any closed curve within a fluid must remain constant with time (21, 24, 30).

With a vortex swirling in the direction shown in Fig.23, close behind an edge of the cambered plate, there is instantaneous circulation developed round the plate. An enlarged picture of this edge vortex being formed is presented in Photo 4, (32) which depicts the process of growth of the vortex:- small scale undulations which form a kind of vortex sheet are rolled up and superimposed upon a big-scale circular vortex. The presence of this vortex and the induced circulation produces a differential static pressure component resulting in a transverse force Y pushing the plate in the direction Y perpendicular to the basic flow direction X. The circulation around the unit span of the plate varies continuously from $+\Gamma$ to $-\Gamma$.

An oscillating transverse force $\pm Y$ in a direction away from the last vortex has a frequency equal to the eddy formation rate. For two-dimensional flow and a stationary plate, it was found (25,29) that the frequency, f, with which the vortices are shed from one side, is determined by the Strouhal number expressed as:

$$S_t = \frac{f \cdot c}{U} = 0.15 - 0.18$$

where f - vortex shedding frequency is given in cycles/sec.
c - width of the body in (m)
U - undisturbed flow in (m/sec) - or any consistent units.

Recent experiments (33,34) revealed that the vortex shedding behaviour is not uniform in the spanwise direction and the complete correlation based on the Strouhal number can be assumed only over a small portion of a blunt body in two dimensional flow. It was found that the velocity fluctuations within the wake recorded simultaneously at two different points z_1, z_2 along the span P resembled each other in character and period but were out of phase at a large separation $(z_2 - z_1)$.

Records of velocity fluctuation (measured by hot-wire anemometers) presented in Fig.24, taken from Fage, Johansen work (25), show that even for the same point in the wake the velocity fluctuations do not appear to be harmonic, although they are periodic in character.

The random velocity fluctuations at various points z_1 and z_2 along the plate, being a function of spanwise position and time, will of course affect the total transverse force Y as well as the moment acting on the entire plate.

Letting Y be a total instantaneous force acting on a plate of length P and ΔY be a local instantaneous force acting on a segment dz, the total force Y can be expressed

$$Y(t) = \int_0^P \Delta Y(z,t)dz$$

The integration cannot, however, be performed easily since $\Delta Y_1(z_1 t)$ and $\Delta Y_2(z_2 t)$ at two different points along the

span, apart from being complicated functions due to fully separated flow conditions, do not depend on z_1 and z_2 only, but also on the difference $\Delta z = z_2 - z_1$. This in turn is a function of many variables the significance of which will become clear later, on the basis of experiments.

The mechanism affecting the magnitude of the force and also the spanwise phase lag in vortex development within the three-dimensional wake becomes more complicated when the plate, being free to oscillate with its own frequency, begins to oscillate under the influence of the periodic transverse force Y (Fig.23). Once set in motion, the plate appreciably modifies its wake of vorticies, their intensity and distribution.

With the hope of gaining a better understanding of the factors which determine the influence of the wake on the aerodynamic (or hydrodynamic) reaction of the oscillating plate (airfoil), two dimensional, water-channel experiments were carried out. In a way the experiments and the idea of the apparatus shown in Photo 5 were inspired by the drawing shown in Fig.22. A cambered plate of 2" chord was given a controlled oscillatory motion across 12" width water channel by means of a slider-crank mechanism. The movement of the plate being 1" either side of the centreline of the water channel. In order to make visible the vortex pattern being formed behind the plate, aluminium powder was scattered upstream on the water surface. Photo 5 and 6 show several pictures taken by the camera situated above the oscillating plate, at two different velocities of water flow 4,0 inch/sec and 8,0 inch/sec. The amplitude of oscillation was constant = 2 inches, and the period T = 2.5 sec. The angle of incidence of the plate relative to the flow was 90° which corresponds to $\beta_A = 180$ in the case of a boat sailing downwind.

From photographs and direct observation of the wake pattern it appears that the oscillating plate imposes its

own frequency on the vortex shedding and modifies the phase relationship relative to its own oscillation. The wake consists of a more or less orderly series of vortices, as shown in Fig.23, which alternate in position about the X axis. Between the two rows of vortices there is a velocity induced in the negative X direction indicated in Fig.23 by the arrows and a broken line. The part of the wake affected by this velocity oscillates from one side of the X axis to the other as the vortices alternately form and detach from the plate edges. As the plate swings from one side to the other it passes close to the vortex left in the previous swing, and this vortex can have considerable effect on the circulation round the plate and also on the phase relations.

The higher the velocity of the flow, the more vigorous is the circulation and induced velocity within the wake and the more pronounced should be the modifying influence of the wake on the circulation round the plate and subsequently on the forces and moments arising from the motion.

A similar situation, but a much more complicated one, might be observed in the case of a rolling sail, when the amplitude of oscillation is not constant but increases continuously. The sail, being a three-dimensional, tapered airfoil oscillating in a rotary manner, is bound to develop a nonuniform wake. The wind tunnel investigation of the wake behind the rolling sail by means of a grid tufted at 2 inch intervals revealed that the vortex wake in a plane parallel to the sail plan is spiral or helical in character and circulates clock-wise or anti-clock-wise, depending on the direction of sail swing.

The wind tunnel and water channel experiments suggest that the oscillations identified with vortex shedding at the beginning of the motion of the sail can be classified as forced oscillations. In this case the alternating forces associated with vortex frequency ω, that initiate the oscillation can be related to the Strouhal number and the

wake itself may be regarded as a "fluid oscillator" which in a way is responsible for "ignition" of the oscillatory motion. Once the system is set in motion, the alternating forces that amplify and sustain the oscillation are created and controlled by the oscillating system itself. Since the periodic aerodynamic force is automatically resonant with the natural frequency of the system, ω_o we can distinguish this kind of oscillation from a forced one as 'self-excited! Unstable oscillation occuring in the case of a rolling boat may therefore be defined as self-excitation.

Fig.12, which presents a record of behaviour of a 1/5 scale Finn rig, illustrates this point; the system, initially in equilibrium begins to oscillate, being forced to do so by the "fluid oscillator" i.e. wake, which produces an unbalanced transverse force independently of the motion of the system.

Referring to the rolling instability of sailing boats, one should realise that the basic characteristic of self-excited systems, which make them difficult to handle mathematically, is that the forcing function K_A in Eq.7 :-

$$I_x\ddot{\phi} + b\dot{\phi} + K\phi = K_A$$

is of a very complex nature, being affected by a number of parameters such as the course sailed β_A, the angle of trim δ_m, the twist of the sail, the aspect ratio, and so on. Therefore at this stage it does not seem to be practical to search for the direct, purely analytical solution to the Eq.7. It can be done experimentally using the apparatus as designed and shown in Fig.5, which incorporates the essential features of the real system and allows systematic investigation of the most important factors which can be held under close control, measured and compared.

5. THE WIND TUNNEL EXPERIMENTS

The crucial questions to be answered by the wind tunnel experiments were:

1. in which conditions is the "Finn" type rig, as shown in Photo 1 and Fig.6, stable in rolling; in which does it become unstable and to what extent is the theory incorporated in Eqs.11, 14 and 31 in agreement with the model behaviour.

2. what is the relative influence of basic parameters such as:

angle of heading β_A

angle of trim of the sail δ_m

wind velocity V_A (Strouhal number S_t)

twist of the sail

damping

on the rolling behaviour of the rig.

Since most of the parameters listed above (β_A, δ_m, twist and damping) are in fact controlled to some extent by the helmsman, it is believed that a better understanding of the essential factors and phenomenae involved in rolling instability should be of some practical value.

5.1 The test procedure and results

5.1.1 Calibration and magnetic damping tests

The angle of roll or angle of heel ϕ measured by means of a rotary pick-off (see Photo 2) was recorded by an ultraviolet galvanometer recorder. Fig.25 gives the results of calibration tests, angular displacement ϕ against the response of the recorder. Linearity error or departure from the ideal straight line expressed as a percentage of the output for a given angle of heel ϕ was of the order $\pm 4\%$.

Figs.26, 26a and 26b present the records of damped oscillations for various degrees of magnetic damping, with the rig attached to the apparatus and no wind. The magnetic damping is based on the effect of eddy-currents which are generated when the aluminium plate swings back and forth between the poles of an electromagnet (see Fig.5). As the aluminium disc moves through the gap of the electromagnet a current is induced in the disc producing a force which opposes the motion in such a way that the retardation is proportional to the angular velocity, or in other words, is viscous in character. By changing the current or the width of the gap between the poles, one can change the intensity of damping. The period of oscillation T = 1,45 sec. was not noticably affected by the changes in damping introduced in the course of the experiments. This is in agreement with Eq.33 discussed in the Appendix.

Fig.26c shows the relation between the amount of magnetic damping (m.d.) expressed in arbitrary units 1, 2, 3 and the logarithmic decrement δ calculated on the basis of Eqs.28 and 30a (Appendix) used to analyse records in Figs.26, 26a and 26b. Zero magnetic damping (m.d. = 0) means that the recorded damping (Fig.26) was due to air friction generated on the sail and the mast only. As expected, the damping actually recorded was basically viscous in character, however a certain departure from linearity was observed due to the fact that the oscillating sail (without wind) manifests a fluttering tendency. This was, of course, absent during "normal" experiments with the wind on.

5.1.2 The influence of the heading angle β_A on rolling

Figs.27a,b,c,d,e, give examples of rolling oscillations for various angles β_A from 145^o - 200^o. The tests were performed at constant wind velocity V_A = 3,05m/sec, constant angle of trim of the sail $\delta_m = 85^o$ and constant

magnetic damping m.d. = 1,0 which corresponds to the logarithmic decrement δ = 0.078 i.e. the system was only slightly damped. At the beginning of each run for the selected β_A the rig was given an initial displacement $\phi = -5^o$ and then released.

Within the scope of β_A = 145 - 180 degrees the recorded oscillations are divergent and the model clearly manifests instability in rolling due to the action of aerodynamic forces. It is apparent that the energy input to the system is not matched by the energy dissipation (limited in a way by the amount of available positive damping), therefore the amplitude of rolling grows continuously.

In Figs.27 and 27a the exponential envelopes are plotted so that they fit the linear equation:

$$\phi = \phi_o e^{-(\delta/2\pi)\omega t} \cos\omega t$$

(see Appendix Eqs.24 and 31) in the best possible way.

The oscillation represented by this equation is made up of the product of two terms or curves, the cosine curve defined by ωt and the exponential curve defined by the logarithmic decrement δ. One can notice that the actual behaviour of the system, which is basically non-linear, differs from the linearised one by less than 10 per cent.

It was regarded, for practical reasons, that such a linear approximation of the system response as shown by the exponential envelopes can be accepted in order that the linearised logarithmic decrement δ may be used as a convenient index of system instability. This is shown in Fig.27f. The negative value of δ is associated with instability, and when substituted into the equation given above produces divergent oscillation.

The degree of instability being a maximum at $\beta_A \approx 165^o$, decreases when β_A increases. By setting the sail model in the position of a boat sailed slightly "by the lee" ($\beta_A = 200^o$), the rig becomes dynamically stable and rolling has a definite tendency to die out with time. This behaviour is recorded in Fig.27e which shows the rate of rolling decay when the initial displacement was 5 degrees and 20 degrees. When β_A is greater than 180^o the excitation element predominates only until a certain amplitude is reached and then an energy balance occurs between the self-excitation and the dissipation elements. In a condition when damping is capable of balancing the energy input due to the sail action, the system reaches a limit cycle steady-state motion of finite amplitude. This type of behaviour shown in Figs.27b, c, might be regarded as a transition from negative to positive stability. The system is unstable at small amplitudes but becomes stable at larger ones. The magnitude of amplitude ϕ at which the limit cycle is reached decreases when β_A increases. Fig.27f depicts the relationship between β_A and the logarithmic decrement δ used as an index of stability.

5.3.1 The influence of trim angle δ_m on rolling

Figs.28a and b show records of oscillations for various angles of the sail δ_m measured between the boom and the axis of rotation. The tests were performed at constant wind velocity $V_A = 3{,}05$ m/s, constant $\beta_A = 180^o$ and constant magnetic damping m.d. = 1.0.

The rolling instability was most spectacular at a large angle of trim $\delta_m = 85^o$. By gradually hauling in the mainsheet and decreasing δ_m, the degree of instability was drastically reduced. At $\delta_m = 70^o$ the rig reaches a kind of neutral stability in rolling. Further pulling in the boom encouraged a positive stability, i.e. the aerodynamic force developed on the sail acted as a suppressor of rolling,

producing positive damping. The curve plotted in Fig.28c shows that the damping efficiency of the rig increases very rapidly when the sail setting δ_m is reduced below 70 degrees.

The aerodynamic positive damping is quite profound, particularly when the initial amplitude of rolling ϕ_o is large (see Fig.28b, $\delta_m = 65^o$). The recorded response indicates clearly the existence of a certain randomness in the rolling motion. The rate of amplitude decay, which is a measure of positive damping, is not uniform or linear but passes through cycles during which damping efficiency increases and decreases periodically.

Fig.28d shows the rolling oscillation for $\delta_m = 85^o$ recorded in the same conditions as before (i.e. $\beta_A = 180^o$, $V_A = 3.05$ m/s and m.d. = 1.0), but the twist of the sail was increased by easing the tension in the kicking strap. One can see that the initial instability at the beginning of the rolling motion is much higher than in the case when the twist was relatively small (see Fig.28a) and the rig behaves differently. After several swings, during which the amplitude increases rapidly, the rig reaches a limit cycle with steady-state motion of finite amplitude of about 22 degrees.

5.1.4 The influence of wind velocity V_A on rolling

Figs.29a, b and c represent the records of divergent oscillations for three different wind velocities, $V_A = 3.05$, 3.66 and 4.27 m/sec, which correspond to the Strouhal numbers 0.55, 0.46 and 0.39 respectively. During the tests $\beta_A = 180^o$, $\delta_m = 85^o$ and m.d. = 1.0 were kept constant.

Applying the same method of linearization of the system response as before (§5.1.2), one can find that the instability expressed by the logarithmic decrement δ is greater at lower wind velocity. This rather surprising result shown by the curve plotted in Fig.29c indicates that the Strouhal number is an important parameter indeed.

5.1.5 The influence of damping on rolling

Figs.30a, b, c represent the records of rolling instability affected by damping of various intensity, 1.0-3.0 (see Fig.26c). During the tests V_A = 3.05 m/sec, $\beta_A = 180^o$ and $\delta = 80^o$ were kept constant. As expected, the combination of resisted rolling due to the action of viscous damping and self-excitation due to sail action must produce different response, depending on the amount of positive damping introduced to the system. The higher the degree of magnetic damping, the less rapidly the amplitude of rolling builds up and the lower is the final amplitude reached in limit cycle steady state motion. There is a certain critical damping which makes the system dynamically stable. This is shown in Fig.30d.

5.2 Anti-rolling sail

An attempt was also made to devise an anti-rolling rig which could produce a positive aerodynamic damping. Fig.31 and Photo 7 show some details concerning the anti-rolling sail. It is a tall and narrow sail, much shorter in the foot than any head sail would be, and its area is about 20 per cent of that of the mainsail. The tack can be taken to a point on the gunwale or a spreader (strut) on the opposite side to the mainsail. It seems to be essential for the damping efficiency of the anti-rolling sail that there should be no excessive gap between the mast and the "leach" of the sail, which is attached to the foreside of the mast. The damping characteristics of the rig depend on the angle of trim of the anti-rolling sail δ_r relative to the centre-line of the hull (or axis of rotation X_o). This is shown in Figs.32a, b, c, d. When δ_r is greater than 45 degrees and less than 110 degrees, the rig becomes dynamically stable even in the absence of magnetic damping. The tests were performed at V_A = 3.05 m/sec, $\beta_A = 180^o$ and $\delta_m = 85^o$. The damping efficiency of the rig represented in Fig.32d is

greatest when the angle of trim of the anti-rolling sail δ_r = 65 - 70 degrees. The effectiveness of the anti-rolling sail is greater at a large amplitude and this tendency is shown in Fig.32b (upper records) by the two linearized exponential envelopes plotted in the sine curves representing actual response of the system to the initial displacement $\phi_o = -20^o$. Experiments with the anti-rolling sail attached to the "Dragon" type rig plus spinnaker (see Photo 7) show the same pattern of behaviour. When the wind was switched on, the whole rig stood firm and upright, with scarcely any tendency to oscillate.

6. DISCUSSION OF RESULTS

An inspection of the recorded behaviour of the rolling rig presented in Fig.27a, b, c, d and e clearly suggests that the nature of the forcing function K_A in Eq.7:

$$I_x \cdot \ddot{\phi} + b\dot{\phi} + K\phi = K_A \qquad 7$$

plays a key role in determining the type of stability of the physical model of a sailing boat. In fact one can distinguish three basic types of model behaviour. They are shown in Fig.33. The curve A depicts dynamic instability, the oscillations being self-excited. The curve B shows typical damped oscillations when the system becomes dynamically stable, so the rolling has a definite tendency to die out with time. The third, a boundary case between the two A and B, occurs when the rolling oscillations initiated by the external moment neither grow nor decay with time, being of constant amplitude. Such a type of model behaviour, which we will call C, is very close to the marginal case shown in Fig.27d. A certain modification to this type of stability, a combination between A and C patterns, very interesting from the mathematical point of view, is shown in Fig.27b, where after a certain period of time during which the system manifests dynamic instability, a limit cycle steady state motion of constant amplitude is reached.

All the other recorded oscillations described in §5.1 and shown in subsequent Figs.28-32 can be classified as belonging to one of the basic types, A, B, C, so that the discussion of all experimental results can be reduced to these fundamental patterns of model response.

The physical model of the rolling rig can be represented in the form of a block diagram in which parts of the system, including the wind as a source of energy, are denoted simply by blocks as follows:-

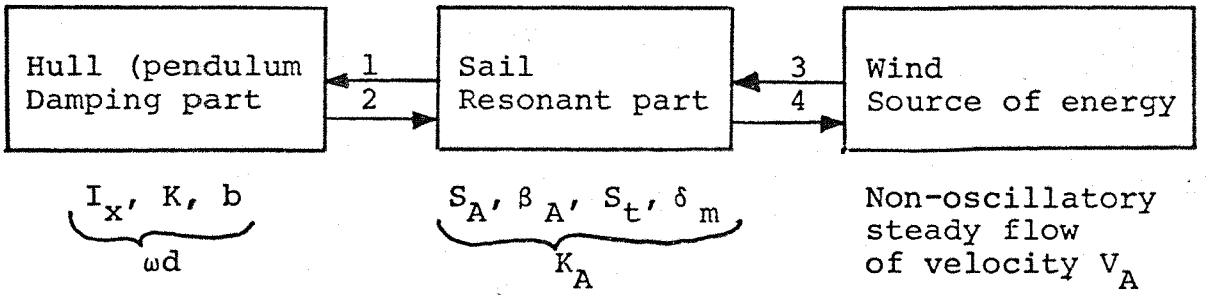

The mutual interaction or causes and effects are marked by arrows 1, 2, 3, 4, indicating the direction of action.

The rolling hull as a damping part of the system fixes the frequency of oscillation ωd which is a function of the moment of inertia I_x, the stability factor k, and the hydrodynamic damping factor b. The solution of form

$$\phi = \phi_o e^{-\frac{bt}{2I_x}} \cos\omega dt \qquad 32$$

describes the natural behaviour of this part of the system (see Eq.24 in the Appendix). Since, for moderate damping, the differences in the frequencies ω_o and ω_d are negligible (see Appendix Eq.32 and 33) we can assume that $\omega_o \simeq \omega_d$.

The sail as a resonant part of the system affects the amplitude of rolling which in turn is dependent on the internal constraints of the system, or interaction, marked by the arrows 1 and 2. The aerodynamic forcing function K_A in Eq.7, being dependent on a number of factors:- sail area S_A, course sailed β_A, Strouhal number S_t, angle of trim δ_m and so on, is such in character that it may transfer energy from the external source, i.e. the wind, to the system, as indicated by the arrows 1 and 3, or, it can extract energy from the system and dissipate it into the airstream as indicated by the arrows 2 and 4. Therefore there is a "feed back" between the hull and sail.

Let us assume as a working basis for discussion that the "driving" moment or forcing function K_A in Eq.7 (which

may be positive or negative) is proportional to the angular velocity ϕ and, for the time being, is positive

$$K_A = b_A\dot{\phi} \qquad 33$$

Positive means that the aerodynamic driving moment K_A is directed in accordance with the angular velocity $\dot{\phi}$ of the sail increasing the initial amplitude of swing.

Substituting Eq.33 into Eq.7 yields

$$I_x\cdot\ddot{\phi} + (b - b_A)\dot{\phi} + K\phi = 0 \qquad 34$$

or

$$I_x\cdot\ddot{\phi} \pm b_R\dot{\phi} + K\phi = 0 \qquad 34a$$

where the resultant coefficient b_R of the damping term is the sum of two parts: hydrodynamic damping coefficient b related to the action of hull and appendages (simulated by magnetic device in physical model) and an aerodynamic coefficient b_A. Depending on the relative values of b and b_A the resultant coefficient b_R can be negative or positive. The solution to the linear Eq.34a is of the form

$$\phi = \phi_o e^{st} = \phi_o e^{-\frac{b_R}{2I}t}\cos\omega_d t \qquad 35$$

(see Eqs.21b and 24 in Appendix). The typical, actual non-linear response of the system investigated and recorded in Fig.34 may be expressed by:

$$\phi = \phi_o e^{st} + c\,\sin\omega_m t \qquad 36$$

where the second term, with modulating frequency ω_m being random in character, contributes on average less than 10% to the linearized response expressed by Eq.35. Since in our discussion the question of most interest is that of stability or instability, that is under what conditions the system manifests the oscillations with ever increasing amplitude as time proceeds, we will ignore the relatively negligible, non-linear term in Eq.36 and concentrate our attention on linearized response expressed by Eq.35 in Fig.34.

6.1 Linear type of system behaviour

Referring to Eqs.34, 34a and 35 we can find that the solution will be sinusoidal and damped i.e. system dynamically stable if $|b_R = (b - b_A)| > 0$ with positive resultant damping coefficient b_R (which indicates that hydrodynamic damping predominates), the damping moment does negative work, always opposed to the angular velocity of the hull appendages. Positive coefficient b_R when substituted in Eq.35 will produce oscillation in which each successive rolling has less amplitude ϕ and less kinetic energy. This is shown by the curve B in Fig.33. If $|b_R = (b - b_A)| < 0$ the solution will be sinusoidal and divergent i.e. the system will be dynamically unstable. Negative damping coefficient b_R indicates that the aerodynamic excitation predominates and the self-excited oscillation shown in Fig.33 by the curve A will develop and grow in amplitude with time.

In the case of negative damping the damping moment which is now a driving moment does positive work on the system, extracting energy from the external source i.e. wind. The effect of the negative damping term in Eq.34a may be interpreted physically as an energy input term. If $b_R = (b - b_A) = 0$, the solution is simple harmonic, i.e. the rolling is of constant amplitude. This indicates that an energy balance between the dissipation and excitation elements is being reached, as shown by a sine curve C in Fig.33.

These three cases discussed above and the resulting linear pattern of model behaviour B, A and C shown in Fig.33 can be represented graphically in another way - on energy dissipation-input basis. Assuming that the system is a linear one, the dissipation of energy due to the damping action of the appendages will, according to Eq.3, follow a parabolic curve - when the energy lost per cycle is plotted against the amplitude as in Fig.35. The energy lost $E_{-(b)}$ is a function of amplitude squared ϕ^2 and the damping coefficient b. If the negative damping moment due to sail action (defined by b_A) is also linear, another parabola will designate the energy input $E_{+(b_A)}$ per cycle. The system will behave as self-excited or possibly damped according to which parabola lies higher; this in turn depends on relative values of b and b_A coefficients.

6.2 Non-linear type of system behaviour

In some cases, as illustrated in Figs.27b and 27c, the energy input to the system may not be linear and therefore one can expect that the energy input and the energy dissipation curves intersect. This is shown in Fig.36. If an initial amplitude happens to be ϕ_1, more energy is put into the system, due to sail action, than is dissipated in damping, due to hull action $E_{+(b_A)} > E_{-(b)}$, so the amplitude grows. On the other hand, if the initial displacement happens to be ϕ_2, there is more hydrodynamic damping than aerodynamic self-excitation i.e. $E_{-(b)} > E_{+(b_A)}$ and the rolling amplitude will decrease. In both cases the amplitude tends towards ϕ_3, where energy equilibrium exists. The rolling rig thus executes harmonic or steady-state limit cycle oscillations. This trend is clearly seen in Figs.27c and 27b. The actual relation between the aerodynamic damping coefficient b_A and the amplitude varies from case to case, as shown in Figs.27b, 27c, 28d, 30a and so on, however the basic reason for that type of behaviour is the same - the resultant

coefficient of damping term of Eq.34a must be negative at small amplitudes and becomes positive for larger ones. If we locate this kind of non-linearity in the aerodynamic term of the equation of motion only, the simplest mathematical expression covering the case will be:

$$K_A = (b_A' - b_A''\phi^2)\dot{\phi} \qquad 37$$

when substituted into Eq.7 gives:

$$I_x\ddot{\phi} + b\dot{\phi} - (b_A' - b_A''\phi^2)\dot{\phi} + K\phi = 0 \qquad 38$$

or

$$I_x\ddot{\phi} + (b - b_A' + b_A''\phi^2)\dot{\phi} + K\phi = 0 \qquad 38a$$

An instability will occur if $|-b_A'| > b + b_A''\phi^2$

Putting

$$b - b_A' = b_o \qquad 39$$

where b_o is a function of angular velocity $\dot{\phi}$ only, one can find that the system will be unstable at small amplitude if

$$b_o < 0 \qquad \text{and} \qquad |-b_o| > b_A''\phi^2$$

The Eq.38a can now be written:

$$I_x\ddot{\phi} + (-b_o + b_A''\phi^2)\dot{\phi} + K\phi = 0 \qquad 40$$

The damping term coefficient $(-b_o + b''_A\phi^2)$ as a function of ϕ is shown in Fig.37. The damping parabola cuts ϕ axis and zero damping occurs at a certain critical amplitude

$$\phi_{cr} = \sqrt{b_o/b''_A} \,.$$

For $\phi < \phi_{cr}$ the resultant damping $(-b_o + b''_A\phi^2)$ is less than zero, therefore unstable oscillations will be induced. When $\phi > \phi_{cr}$ damping becomes positive so the oscillations will tend to die out with time.

Referring to Fig.37 and Eq.40, one can notice that by changing the magnitude of damping coefficient b_o, which is the sum of hydro and aero coefficients b and b_A respectively, a series of damping parabolas may be drawn in such a way that they are bodily shifted up or down. For example, by gradually increasing the value of positive hydrodynamic coefficient b i.e. reducing b_o, one can plot several parabolas shifted bodily upwards as indicated by the dashed curves. This, of course, will affect both the critical amplitude ϕ_{cr} at which a balance between positive and negative damping is reached and also a final amplitude at which limit cycle steady state oscillation occurs. The experiments depicted in Figs.30a, b, c and d confirm such a conclusion. By increasing the magnetic damping from 1,0 to 3,0 (every 0,5 unit of damping), the system initially unstable within the limits of amplitude being investigated (Fig.30a), manifests less and less instability when damping increases, (reaching the limit cycle at a smaller and smaller amplitude $\phi = 17^o$, 14^o, 9^o), and finally becomes stable. The last record in this series shown in Fig.30c suggests that the damping parabola drawn in Fig.37 must cut the ordinate above the origin of coordinates, and therefore $b_o = b - b'_A$ is positive i.e. the system is positively damped from the beginning of the motion.

6.3 Generalization

From the analysis of the approximate solution to Eq.40, given by Eq.41 (see Appendix §A4, Van der Pol Equation)

$$\phi = \frac{2\sqrt{b_o/b_A''} \cdot \sin(\omega_o t + \eta)}{\sqrt{1 + e^{-\varepsilon(\omega_o t + c)}}} \qquad 41$$

where

$$\varepsilon = \frac{b_o}{I_x \omega_o} = \frac{\text{negative damping moment}}{\text{stability moment}}$$

one may infer that in the case of non-linear damping (described by the second term in Eq.40), the degree of system instability might be measured in two different ways.

Firstly, it can be measured by the final amplitude ϕ at which the limit cycle steady state oscillation is reached. This final amplitude given by the numerator in Eq.41 is twice as large as the critical amplitude

$$\phi_{cr} = \sqrt{b_o/b_A''}$$

at which negative and positive damping just balance (see Fig.37). The greater the absolute value of the aerodynamic coefficient b_A (negative damping) relative to the hydrodynamic coefficient b (positive damping) i.e. the greater the negative value of $b_o = b - b_A$, the larger will be the final amplitude. This signifies the importance of both aerodynamic and hydrodynamic factors contributing towards dynamic instability. In this particular respect, the hydrodynamic factor means mainly a damping due to the action of appendages.

Secondly, the degree of system instability can be measured by the rate of growth of the amplitude (logarithmic increment δ) before the steady final amplitude is reached. This rate, being determined by ratio $\varepsilon = \frac{b_o}{I_x \omega_o}$ located in the denominator of Eq.41, exposes clearly the significance of the moment of inertia of the system. The lower the moment of inertia, other factors being equal, the higher will be the rate of growth in amplitude during that period before the final amplitude is reached.

One may make a justifiable generalization by saying that basically the physical model of the rolling rig investigated can be considered as a non-linear system. The mathematical model expressed by a non-linear Equation 38a represents with reasonable accuracy the physical model covering both the linear type of model behaviour and non-linear as well. This point will become clear if we compare the two Equations: the linear 34 with the non-linear 38a written for convenience one under the other:

$$I_x \ddot{\phi} + (b - b_A)\dot{\phi} + K\phi = 0 \qquad 34$$

$$I_x \ddot{\phi} + (b - b'_A + b''_A \phi^2)\dot{\phi} + K\phi = 0 \qquad 38a$$

The contribution of the non-linear term $b''_A \phi^2$ in Eq.38a towards the "shape" of the oscillations depends on the magnitude of b''_A relative to b'_A. If b''_A is negligible, the influence of the non-linear term $b''_A \phi^2$ will only be noticable at a large amplitude, which for practical reasons was not investigated. There was no point in investigating the behaviour of the system much beyond a realistic amplitude $\phi = \pm 25^o$, at which the boom of a full scale boat touches the water. The non-linear Eq.38a may be regarded as a reasonable mathematical representation of the actual

behaviour of the physical model with sufficient accuracy. This becomes evident when the maximum experimental amplitude is large enough to make the non-linear response noticeable. A comparison of actual model response depicted in Figs.12 and 27b with a graphical representation of the solution to the Eq.38a (expressed in non-dimentional amplitude, see Appendix Eq.47) shown in Fig.38 should clarify further this point. One may further expect that if the hydrodynamic damping b is small relative to aerodynamic excitation coefficient b'_A the critical amplitude ϕ_{cr} may become too large, to be recorded in experiments. The maximum experimental amplitude permitted in the course of tests was $\pm$ 30 degrees.

Figs.30a and b, which are in fact regarded as self explanatory, may lead to a general conclusion that stable oscillations of final amplitude in a non-conservative system are possible only if the system is a non-linear one.

The question which might be answered now is:- why the damping due to sail action being negative at a small amplitude may become positive at a large one? The discussion incorporated in §§4.2.1 and 4.2.2 leads to a conclusion that the rolling rig will be dynamically unstable if the negative slope of the L - α curve is greater than the ordinate of the drag curve. Such a conclusion was supported by the aerodynamic characteristic of the rig shown in Fig.11. Another conclusion derived on the same basis was that the same aerodynamic forces and process which may translate energy taken from the wind into incipient rolling can also act as a suppressor.

Let us consider in detail some geometrical relations which may serve as a clue, assuming that the rolling rig is set at $\beta_A = 180^o$, $\alpha = 90^o$ and apparent wind $V_A = 3{,}05$ m/s. This simple case is shown in Fig.39. The model set in such a condition is dynamically unstable. Any departure from initial static equilibrium will immediately encourage an

alternating aerodynamic force (or moment) which will magnify the amplitude during a series of subsequent swings to port and starboard. Rolling will, of course, modify both the instant and local angle of incidence α of various sections along the sail span by an amount $\pm\Delta\alpha$, depending on amplitude ϕ, velocity V_A and a distance z from the axis of rolling.

Assuming further that ω_d = 4,35 rad/sec and $\phi = 10^o$, let us estimate the corresponding maximum variations in α for two sections of the model sail A and B, which are 0,5 and 1,0 metre above the axis of rolling. Calculations based on relations, written for convenience next to Fig.39, show that $\Delta\alpha_{max} = 7^o$ for section A and $\Delta\alpha_{max} = 14^o$ for section B, i.e. the maximum variation in α for the lower section A will be $90^o \pm \Delta\alpha_m = 83^o - 97^o$; and $76^o - 104^o$ for the upper section B.

According to Fig.11 such a variation in the angle of incidence α is still within the instability limit signified by the shaded area. One can therefore expect that there will be an energy input during the full cycle (swing). This increases the amplitude of oscillation, and the increase will continue until there is an excess of energy being tapped from the air stream. At some large amplitude, say $\pm 30^o$, the maximum variation in α for lower and upper sections of the sail A and B are $90^o \pm 17^o$ and $90^o \pm 37^o$ respectively. The upper part of the sail is now working in such a condition that near the end of each swing, or in one side swing, the energy is extracted from the wind, but in the middle of the swing, or in the course of swing to the other side, the energy may be taken away. This is due to the fact that $\frac{\partial L}{\partial \alpha} + D$ is positive at a sufficiently small and sufficiently large angle of incidence. Therefore, there must be a certain critical amplitude when the energy balance is reached, i.e. the energy extracted from the wind is equal to the energy dissipated into the airstream.

In this example, which gives a rough physical insight into the mechanisms of non-linearity in aerodynamic excitation, an emphasis was put on the significance of the instantaneous angle of incidence α in order to relate the rolling motion to the aerodynamic characteristics of the sail as represented in Figs.7 and 11. Changing the range of variation of instantaneous angles of incidence α by altering, say, course β_A or angle of trim δ_m, one may affect the rolling instability. The experiments clearly confirmed such a possibility.

Of course, according to Fig.39 the variation in V_R (ΔV_R) also matters, however, its significance is of secondary importance as compared with the effect of variation in incidence α.

7. CONCLUSION

Concentrating attention on the possible practical application of the experimental results on the rolling rig to a full scale yacht, the conclusions may be summarized as follows. The rolling instability induced by aerodynamic forces can be reduced or eliminated in various ways. Some factors affecting a boat's behaviour and her tendency towards rolling instability can be directly controlled to some extent by the crew; some other factors being predetermined on the designer's desk may be beyond the command of even the best crew. More specifically:

1. The heading angle β_A (see Fig.27f) has considerable effect on rolling. The degree of instability, being a maximum at $\beta_A = 165^o$, decreases when β_A increases. By applying a technique of sailing "by the lee" ($\beta_A = 200^o$) the rig becomes dynamically stable and rolling will die out in time.

Sailing "by the lee" is always considered to be a cardinal sin on the part of a helmsman. Yet, according to wind tunnel findings, it may eliminate rolling. The danger of an unintentional gybe can be excluded by using a combination of foreguy and preventer, or kicking-strap, to effectively lock the mainsail boom.

2. The angle of sail trim δ_m also acutely affects the rolling behaviour of the rig (see Fig.28c). The unstable rolling, being most spectacular at a large angle of trim, can be drastically reduced by hauling in the mainsail and decreasing δ_m. Pulling in the boom to $\delta_m = 65^o$ encourages a positive stability, i.e. the aerodynamic force developed on the sail acts as a suppressor of rolling in the case where the rolling is induced by wave action.

3. Wind velocity V_A (or Strouhal number $S_t = \frac{\omega \cdot c}{V_A}$) influences the instability in such a way (see Fig.29c) that there seems to be a critical wind speed for a given

rig configuration which produces most conspicuous rolling (high logarithmic increment). In other words, heavy rolling may not necessarily occur in very "strong" winds, but rather in "moderate" winds. This problem is related to the sail area.

Certainly, carrying more sail area than is prudent when running vastly increases the aerodynamic input coming from a sail - a "rolling engine". When coupled with low inertia (light displacement) and inefficient hydrodynamic damping, such a combination of factors may stimulate wild and occasionally disastrous rolling. An inspection of these factors incorporated in Eqa.38a, 40 and 41 clearly suggests such a consequence. This point may be illustrated further by an example described by Adlard Coles in his book "Heavy Weather Sailing" (p.111-112):-

> "When we came to race Cohoe II in 1952, which was a season of fresh and strong winds, we found her fast in light or moderate breezes but she proved to be overmasted and overcanvassed in strong winds, and the world's champion rhythmic roller. This was partly due to her being designed to carry a lead keel, but having had an iron one substituted, as lead reached a peak price in the year she was built.
>
> Accordingly, in consultation with her designer I had the sail plan reduced the following winter by cutting the mast at the jumpers and cutting the mainsail. The reduction in sail area was drastic, being equivalent to two reefs ..... the alteration greatly improved the yacht. From being a tender boat she became a stiff one ..... gone was the rhythmic rolling."

4. Positive hydrodynamic damping seems to be of essential importance. Fig.30d suggests that there is a certain critical damping which makes the system dynamically stable. The experiments justify the already expressed view that the modern tendency to reduce the wetted surface of the hull by cutting down the area of appendages in order to improve the boat's speed performance, may lead to a reduction of hydrodynamic damping below an acceptable minimum imposed by the dynamic stability requirements.

One can expect that the energy input per cycle and subsequent rolling instability due to aerodynamic excitation, may under certain conditions reach its maximum. The actual hydrodynamic damping of the hull may not be viscous in character, i.e. proportional to the velocity of roll but, for one reason or another, its damping efficiency is a non-linear function of such parameters as amplitude, boat's velocity, configurations of appendages, etc. It may happen that in some unfavourable conditions the maximum aerodynamic input is far greater than the hydrodynamic damping. In such circumstances, the rolling amplitude will build up into one of those nightmarish affairs that both cruising and regatta sailors know only too well.

5. Anti-rolling sail effectiveness (see Fig.32d) has been proved beyond any doubt in the course of wind tunnel tests. Experiments with anti-rolling sail together with a spinnaker of "Dragon" type (see Photo 7) and a mainsail show the same pattern of behaviour as manifested by low aspect ratio "Finn" type rig.

The device could be quite easy to fit to a full size cruising yacht and there is nothing in the International Rule to prevent its use while racing.

If full scale tests confirm the wind tunnel finding, one can expect that the hazard of being knocked down by a rolling spinnaker, a real danger almost all yachtsmen face, would be greatly reduced.

REFERENCES

1. Standard symbols - ITTC, National Phys.Lab. Ship Rep.77, 1965

2. "Hydrodynamics in ship design"
H.E. Saunders, Vol.II and III, SNAME 1957

3. D.L. Discussion of yacht research nomenclature.
Stevens Institute of Technology
(private correspondence)

4. Yacht Research Group Notation
University of Southampton

5. Report of Presentation Committee
12th International Towing Tank Conference

6. "Aircraft Stability and Control"
A.W. Babister, Pergamon Press 1961

7. "Skene's Elements of Yacht Design"
F.S. Kinney, Dodd and Mead 1962

8. "Theory of Naval Architecture"
Prof. A. McCance - Robb

9. "Effect of form on roll"
M.E. Serat, SNAME

10. "Theory of Ship Motions"
S.N. Blagovenshechensky, Dover Publ.Inc. 1962

11. "Dynamics of Physical Systems"
R.H. Cannon, McGraw Hill, 1967

12. "Mechanical Vibration"
J.P. Den Hartog, McGraw Hill 1962

13. "Dynamics", Vol.I
R. Halfman, Addison-Wesley 1962

14. "Introduction to Aeronautical Dynamics"
M. Rauscher, John Willey and Sons 1953

15. "Drgania i flatter samolotów"
R. Scanlan, R. Rosenbaum, P.W.N. 1964

16. "An Introduction to the Theory of Aeroelasticity"
Y. Fung, John Willey 1955

17. "The Aerodynamic characteristics of a 2/5th scale Finn sail and its efficiency when sailing to windward"
C.A. Marchaj, A.A.S.U. Rep.No.254 (1964)

18. "Experimental determination of the lift of an oscillating airfoil"
E.G. Reid and W. Vincenti, J.of Aer.Sc. Vol.8

19. "Growth of circulation about a wing and apparatus for measuring fluid motion"
P.B. Walker, R & M No.1402

20. "General theory of Aerodynamic Instability and the Mechanism of Flutter"
Th. Theodorsen, T.R. NACA No.496 1935

21. "General Aerodynamic Theory"
Th. Karman and I.M. Burgers in "Aerodynamic Theory" (W. Durand Vol.2), Dover Publ.

22. "Airfoil Theory for Non-Uniform Motion"
Th. Karman and W.R. Sears, J. of Aer. Sc. Vol.5, 1938

23. "The force and moment on an oscillating airfoil"
H. Glauert, R & M 1242, 1929

24. "The Elements of Aerofoil and Airscrew Theory"
H. Glauert, Cambridge 1959

25. "On the Flow of Air behind an inclined flat plate of infinite span"
A. Fage and F.C. Johansen, Proc. Royal Soc. 116, 1927

26. "Some aspects of non-stationary airfoil theory and its practical application"
W.E. Sears, J.of Aer. Sc. 1940

27. "Evaluation of High-Angle of Attack on Aerodyn. Derivatives Data and Stall-Flutter Prediction Technique"
NACA T.N. 2533, Halfman, R.L., Johnson, H.C., Haley, S.M.

28. "Experimental Aerodyn. Derivatives of a sinusoidally oscillating airfoil in two dimensional flow"
Halfman, R., NACA Rep.1108

29. "Vortex formation behind obstacles of various section"
E. Tyler, Phil. Mag. Vol.XI, 1931

30. "Elementary Mechanics of Fluids"
H. Rouse, John Willey, 1946

31. "Applied hydro and aerodynamics"
L. Prandtl and O.G. Tietjens, Dover Publ.

32. "Photographic evidence of the formation and growth of vorticity behind plates"
D. Perce, J.Fluid Mech. Vol.II, 1961

33. "A survey of correlatiCn length measurements of the vortex shedding process behind a circular cylinder"
C. Graham, MIT - T.R. 76028-1

34. "The Lift and drag forces on a circular cylinder in a flowing fluid"
R. Bishop and A. Hassan, Proc. Royal Soc. of London Vol.277A

35. "Ordinary Non-linear Differ. Equations"
McLachlan, Clarendon Press

36. "Non-linear Oscillations in Physical Systems"
Ch. Hayashi, McGraw Hill

37. "Non-linear Oscillations"
N. Minorsky, Van Nostrand Co.

38. "On relaxation oscillations"
Van der Pol, Phil.Mag.2, 1926

39. "On the stability of the solutions of Matheu's Equations"
Van der Pol and M.J. Strutt, Phil.Mag.7-5, 1928

40. "Introduction to Non-linear Analysis"
W. Cunningham, McGraw Hill

TABLE III.

„FINN" Run VII
Small model 1/5 scale
V = 7.62 m/sec = 25 ft/sec
$\Delta D = + 0.1$
$D_{cor} = D - \Delta D$

α^c	L_I	L_{II}	D	$L_I + L_{II}$	D_{cor}	$\frac{dL}{dx}$
15	0.65	0.90	0.50	1.55	0.40	8.6
20	1.00	1.30	0.65	2.30	.55	9.75
25	1.40	1.75	0.90	3.15	.80	8.6
30	1.75	2.15	1.20	3.90	1.10	5.15
35	1.95	2.40	1.60	4.35	1.50	−0.57
40	1.95	2.35	1.90	4.30	1.80	−5.15
45	1.80	2.05	2.10	3.85	2.00	−1.72
50	1.75	1.95	2.40	3.70	2.30	−1.15
55	1.75	1.85	2.80	3.60	2.70	−2.30
60	1.70	1.70	3.15	3.40	3.05	−2.86
65	1.60	1.55	3.45	3.15	3.35	−2.86
70	1.50	1.40	3.75	2.90	3.65	−3.44
75	1.35	1.25	4.00	2.60	3.90	−3.44
80	1.25	1.05	4.30	2.30	4.20	−4.02
85	1.10	0.85	4.45	1.95	4.35	−4.58
90	.95	.60	4.60	1.55	4.50	−4.58
95	.75	.40	4.70	1.15	4.60	−4.58
100	.55	.20	4.80	0.75	4.70	−5.15
105	.30	.0	4.85	.30	4.75	−5.15
110	.10	− .25	4.90	− .15	4.80	−5.15
115	− .15	− .45	4.90	− .60	4.80	−5.15
120	− .40	− .65	4.90	−1.05	4.80	−4.58
125	− .60	− .85	4.85	−1.45	4.75	−4.58
130	− .85	−1.00	4.80	−1.85	4.70	−4.58
135	−1.05	−1.15	4.70	−2.25	4.60	−4.58
140	−1.30	−1.35	4.50	−2.65	4.40	−4.02
145	−1.50	−1.50	4.25	−3.00	4.15	−4.02
150	−1.75	−1.60	4.00	−3.35	3.90	−3.44
155	−1.95	−1.70	3.65	−3.65	3.55	−1.72
160	−2.10	−1.70	3.20	−3.80	3.10	−1.15
165	−2.20	−1.70	2.75	−3.90	2.65	
170	−2.15	−1.60	2.15	−3.75	2.05	

TABLE IV.

„FINN" Run VIII (Twist reduced)
Big model 2/5 scale
V = 7.32 m/sec = 24 ft/sec (4 Beaufort Sc)

α	L_I	L_{II}	D	$L_I + L_{II}$
17½	4.70	10.60	3.20	15.30
20	5.35	11.25	3.85	16.70
25	6.15	12.50	5.50	18.65
30	6.00	12.50	7.50	18.50
35	5.55	11.60	9.10	17.15
40	–	–	–	–
45	5.35	11.25	12.30	16.60
50	5.30	11.20	14.25	16.50
55	5.15	11.00	16.25	16.15
60	4.90	10.75	18.15	15.65
65	4.40	10.30	20.35	14.70
70	3.65	9.75	22.35	13.40
75	2.75	8.90	24.35	11.65
80	1.70	8.10	26.00	9.80
85	0.40	7.15	27.60	7.55
90	−0.90	6.10	28.70	5.20
95	−2.35	4.85	29.50	2.50
100	−3.75	3.65	29.80	−0.10
105	−5.20	2.40	29.80	−2.80
110	−6.75	1.15	29.60	−5.60
115	−7.90	0.00	28.30	−7.90

TABLE V.

„FINN" Run IX
Big model – 2/5 scale
V = 7.32 m/sec = 24 ft/sec (4 Beaufort Sc)

α	L_I	L_{II}	D	$L_I + L_{II}$
17½	2.15	6.15	2.65	8.30
20	2.85	7.65	2.90	10.50
25	4.20	9.60	3.85	13.80
30	5.35	11.15	5.05	16.50
35	6.10	12.30	6.35	18.40
40	6.10	12.15	8.05	18.25
45	5.85	11.50	9.90	17.35
50	5.80	11.10	11.30	16.90
55	5.70	10.90	13.10	16.60
60	5.55	10.60	14.60	16.15
65	5.15	10.15	16.40	15.30
70	4.65	9.65	18.35	14.30
75	4.00	8.95	20.10	12.95
80	3.15	8.25	21.90	11.40
85	2.25	7.40	23.50	9.65
90	1.15	6.40	25.10	7.55
95	0.00	5.55	26.30	5.55
100	−1.40	4.40	27.00	3.00
105	−2.70	3.20	27.40	0.50
110	−4.00	2.10	27.40	−1.90
115	−5.25	0.90	26.80	−4.35

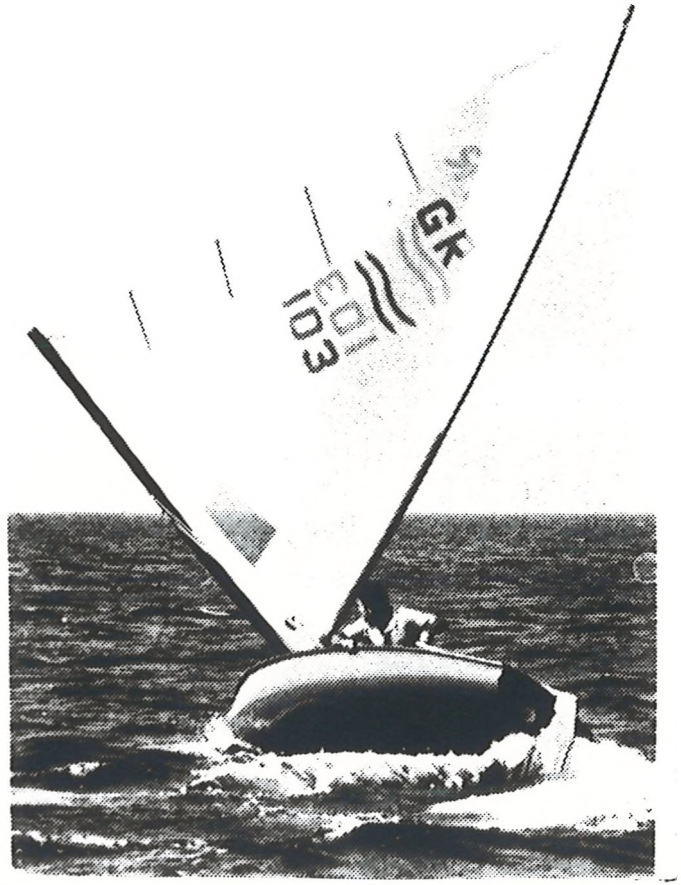

Full scale 'Finn' rolling downwind and the 1/5 scale model of the 'Finn' rig manifesting the same kind of instability during initial test in the wind tunnel.

Photo 1

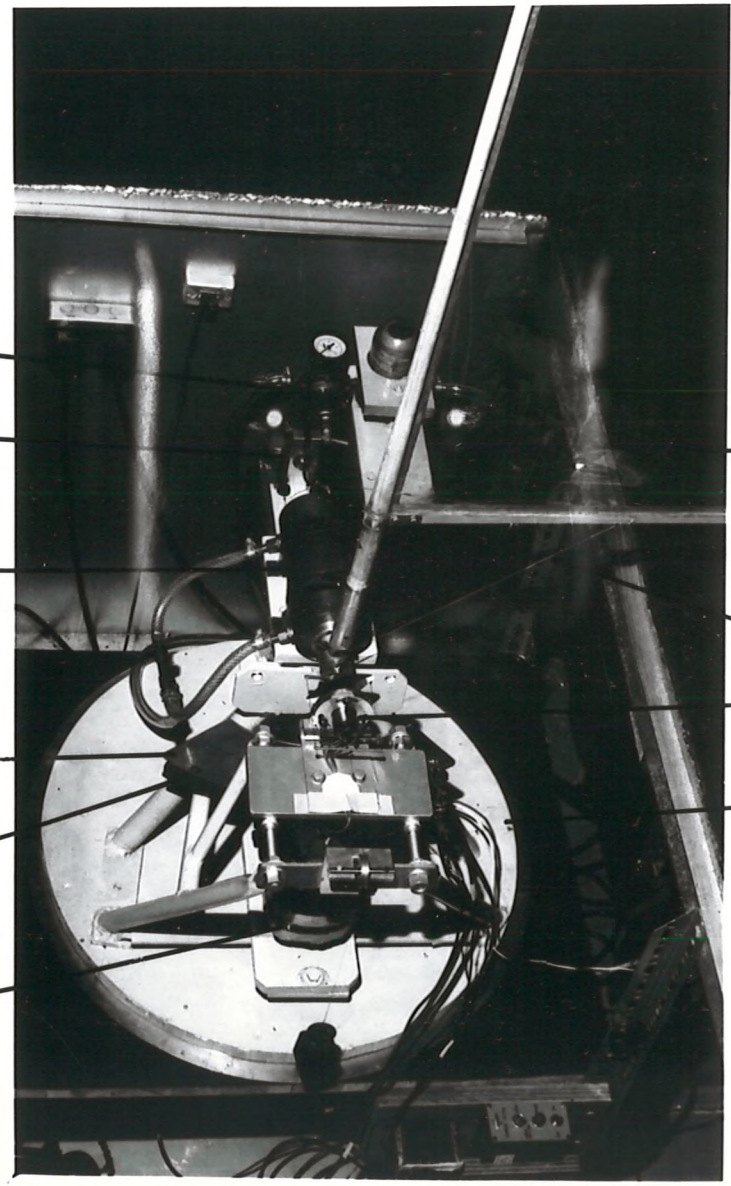
Pressure gauge
Transducer and flexure to measure drag component
Air bearing
Aluminium disc swinging between magnet poles
Movable ballast attached to the disc
Electro-magnet
1/5 Scale model of the 'Finn' rig
Kicking strap
Rotary pick-up
Rotating base of the apparatus

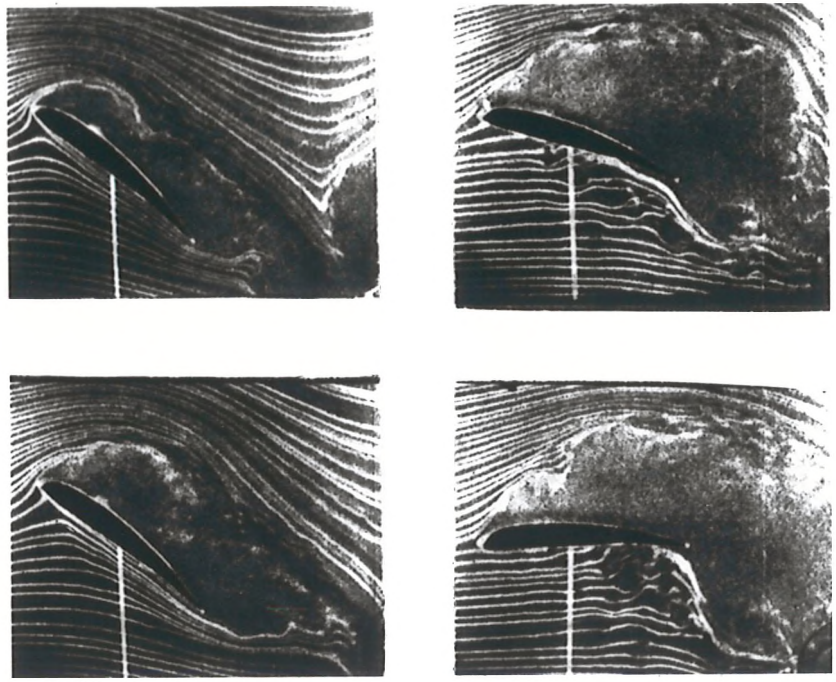

Photo 3 (Above) Hysteresis effect on the flow round the airfoil

Photo 4 (Right side) An enlarged view of the vortex sheet being developed into circular vortex

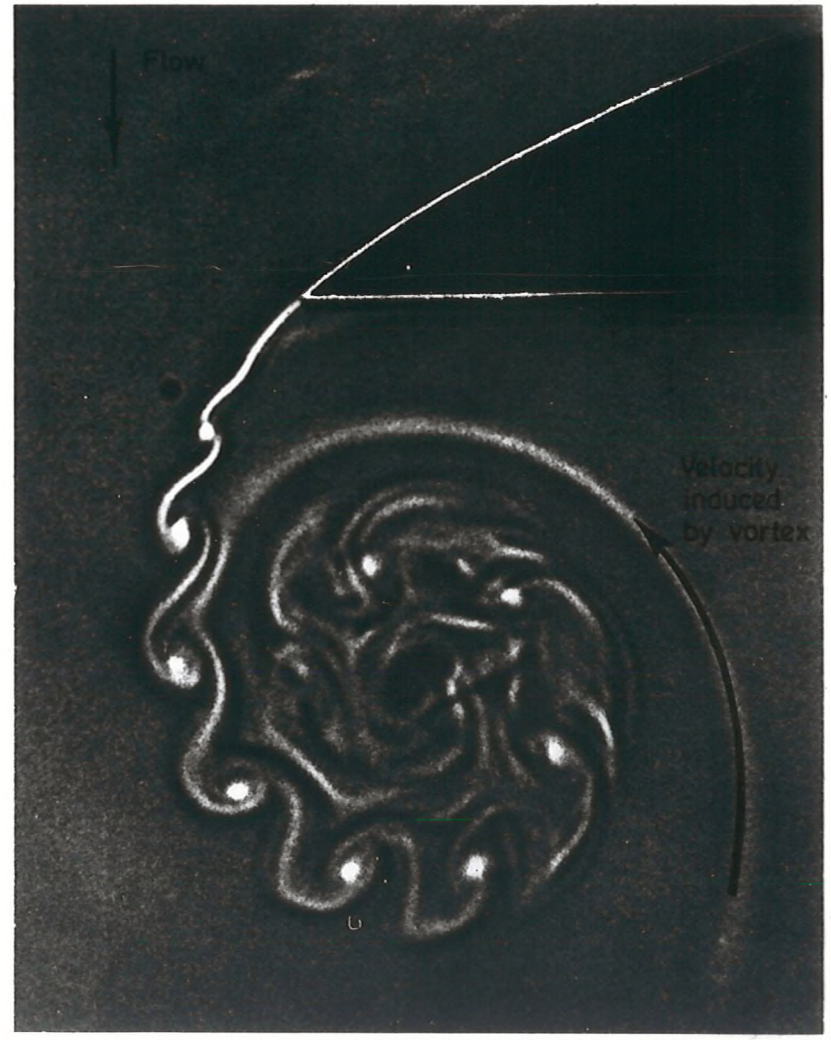

WATER CHANNEL EXPERIMENTS

LOWER VELOCITY ($\beta = 180°$)

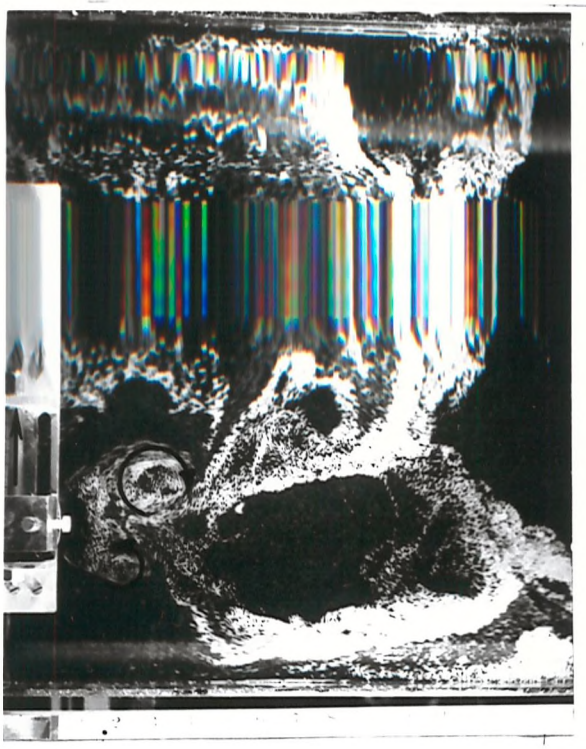

1

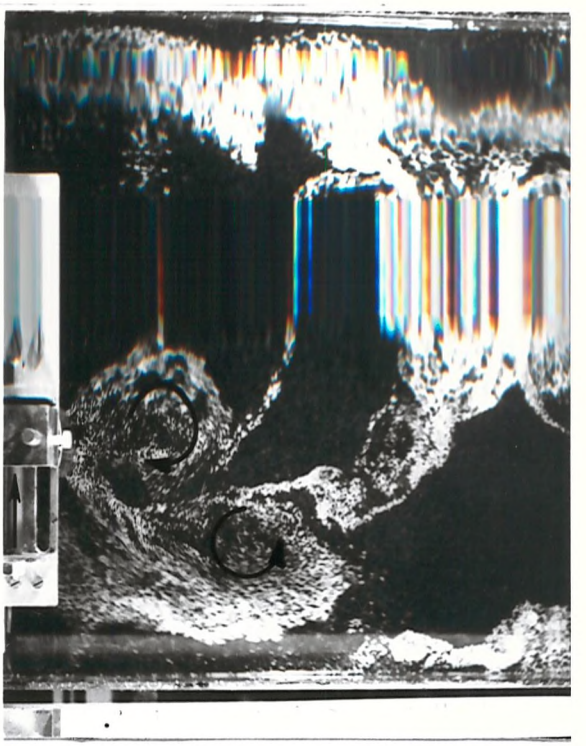

2

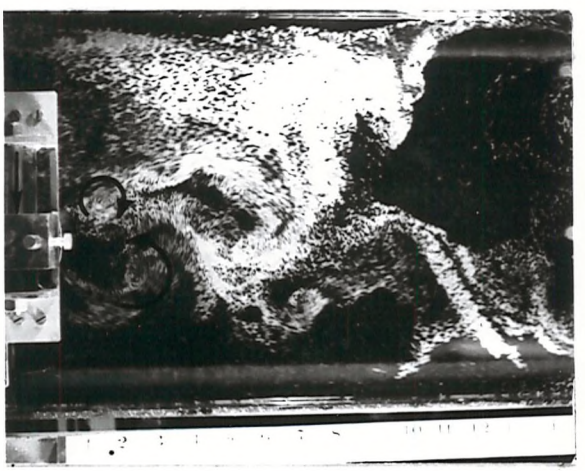

3

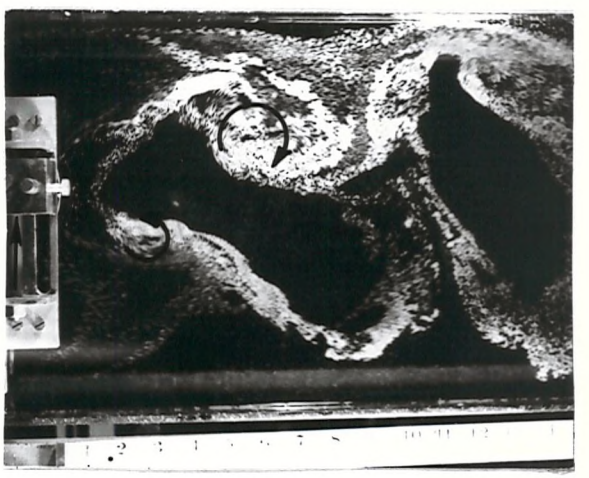

4

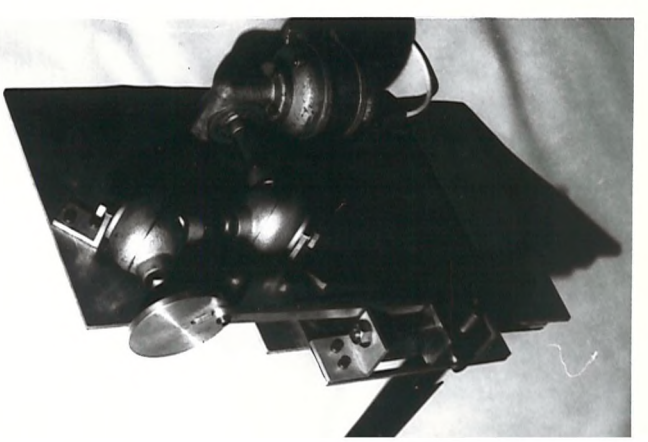

Photo 5

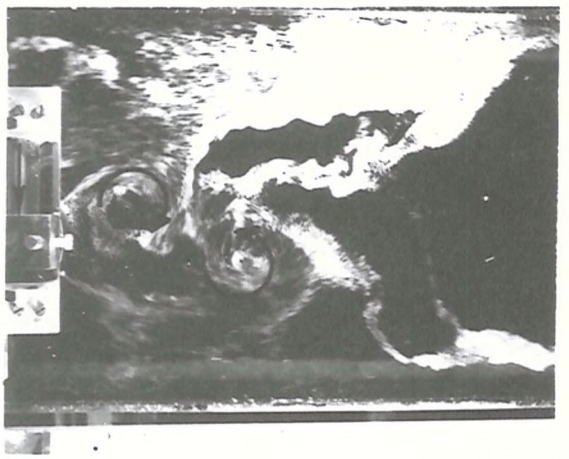

1

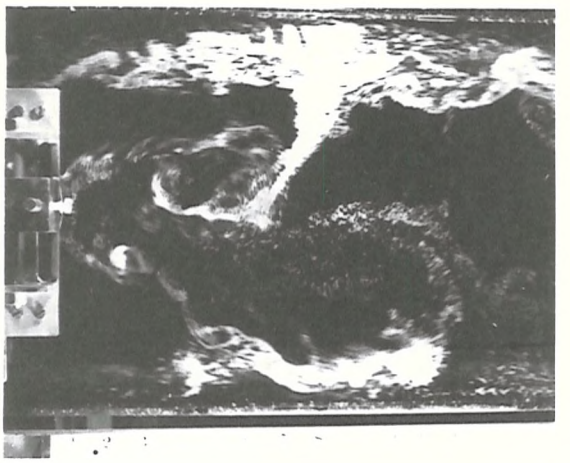

2

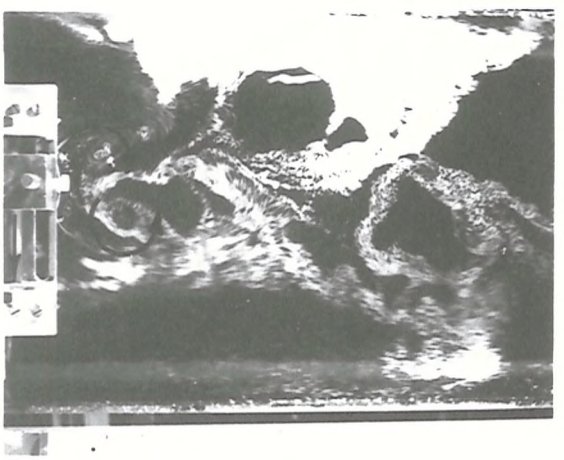

3

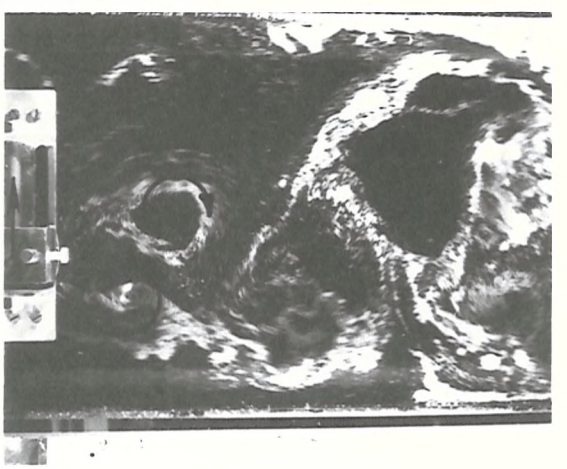

4

WATER CHANNEL EXPERIMENTS

HIGHER VELOCITY ($\beta = 180°$)

Photo 6

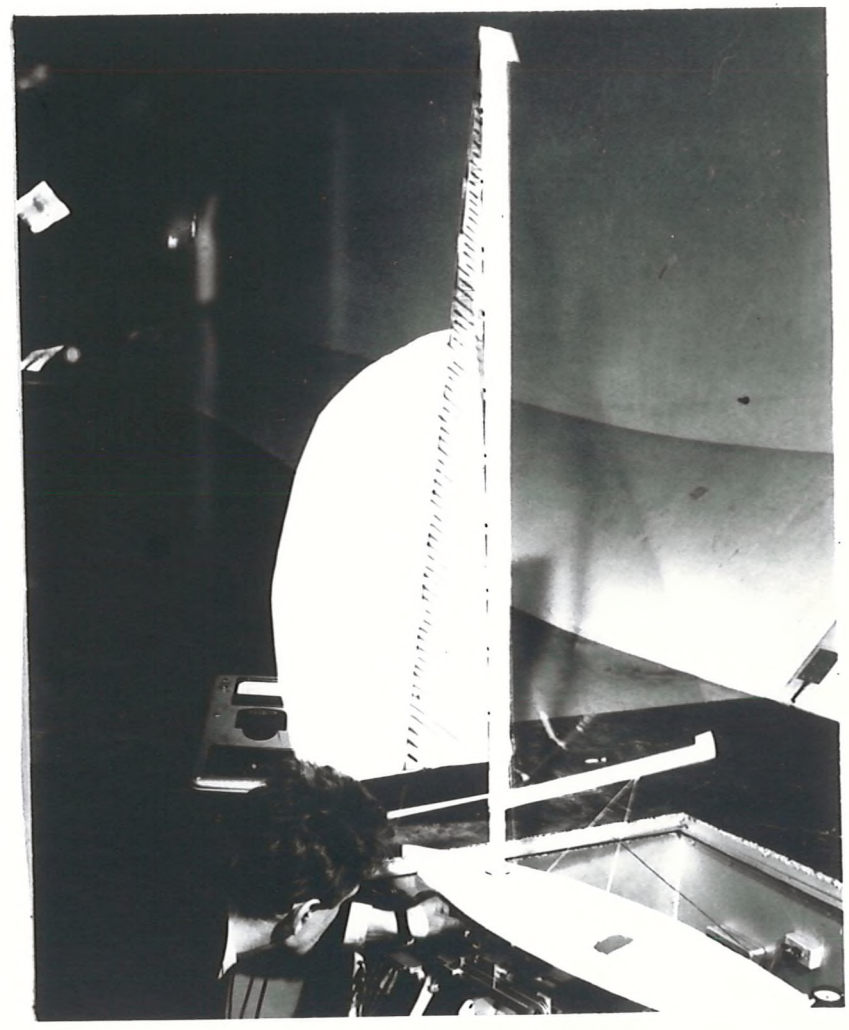

Photo 7

Model of the 'Dragon' rig
(without and with anti-rolling sail)

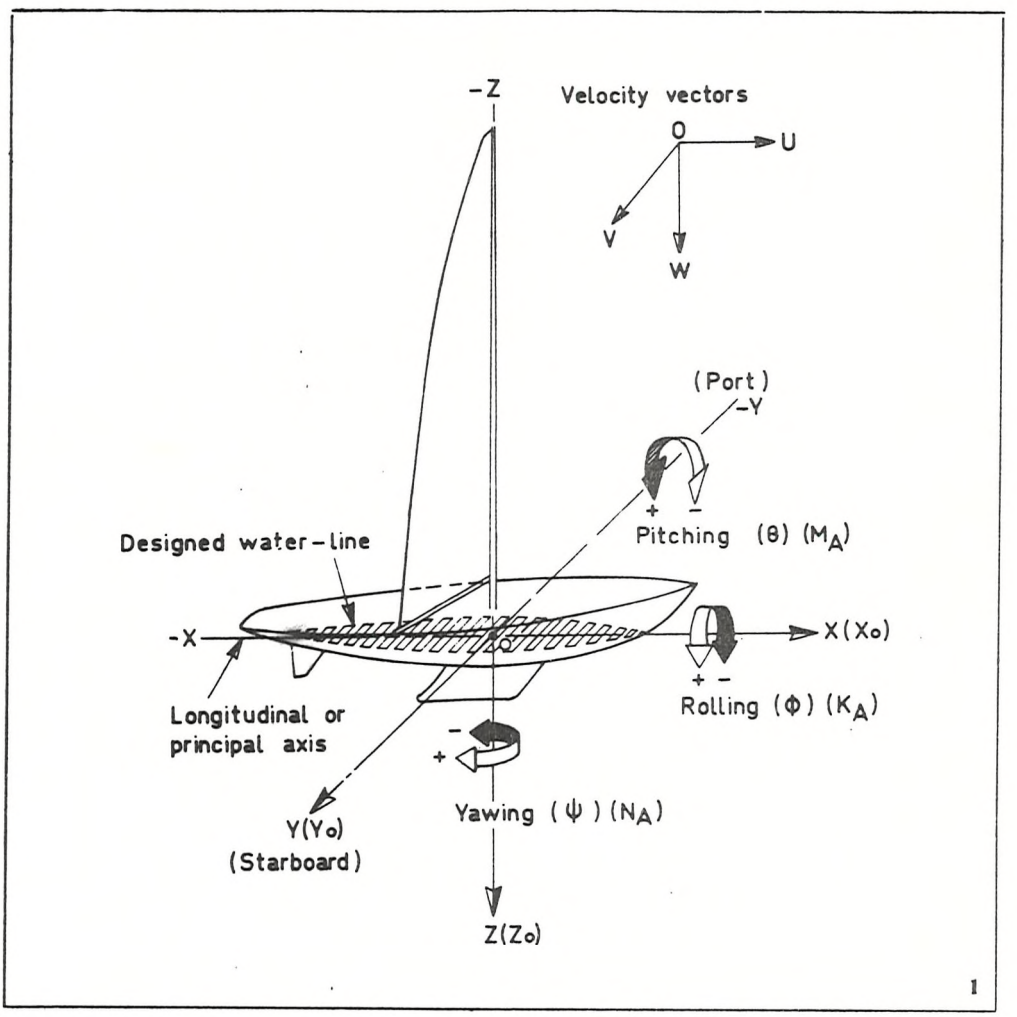

figure 1
Sailboat nomenclature. The fixed and body axes (Sign convention)

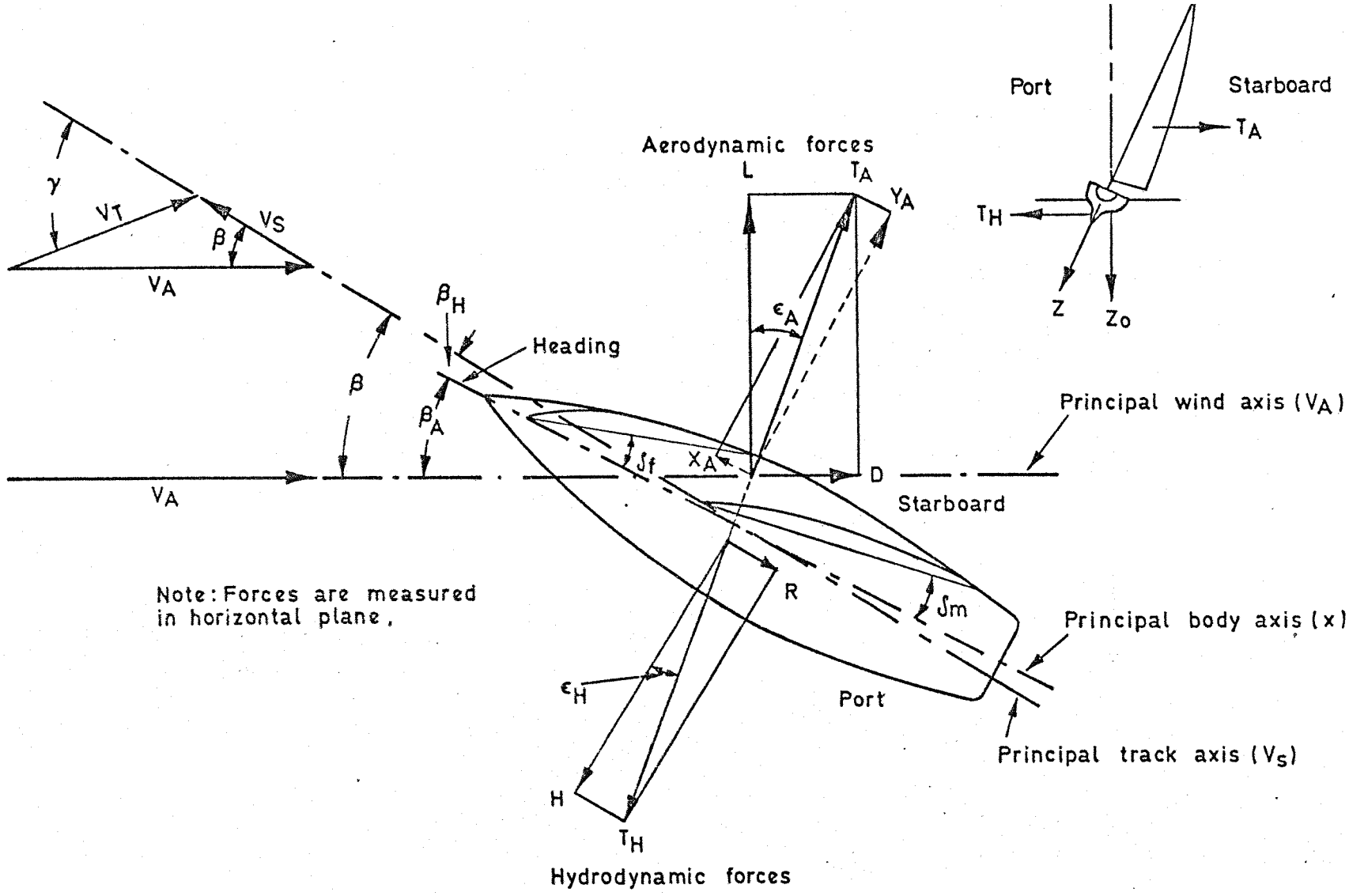

Fig 2 Sailboat nomenclature
Track and wind axis co-ordinate system

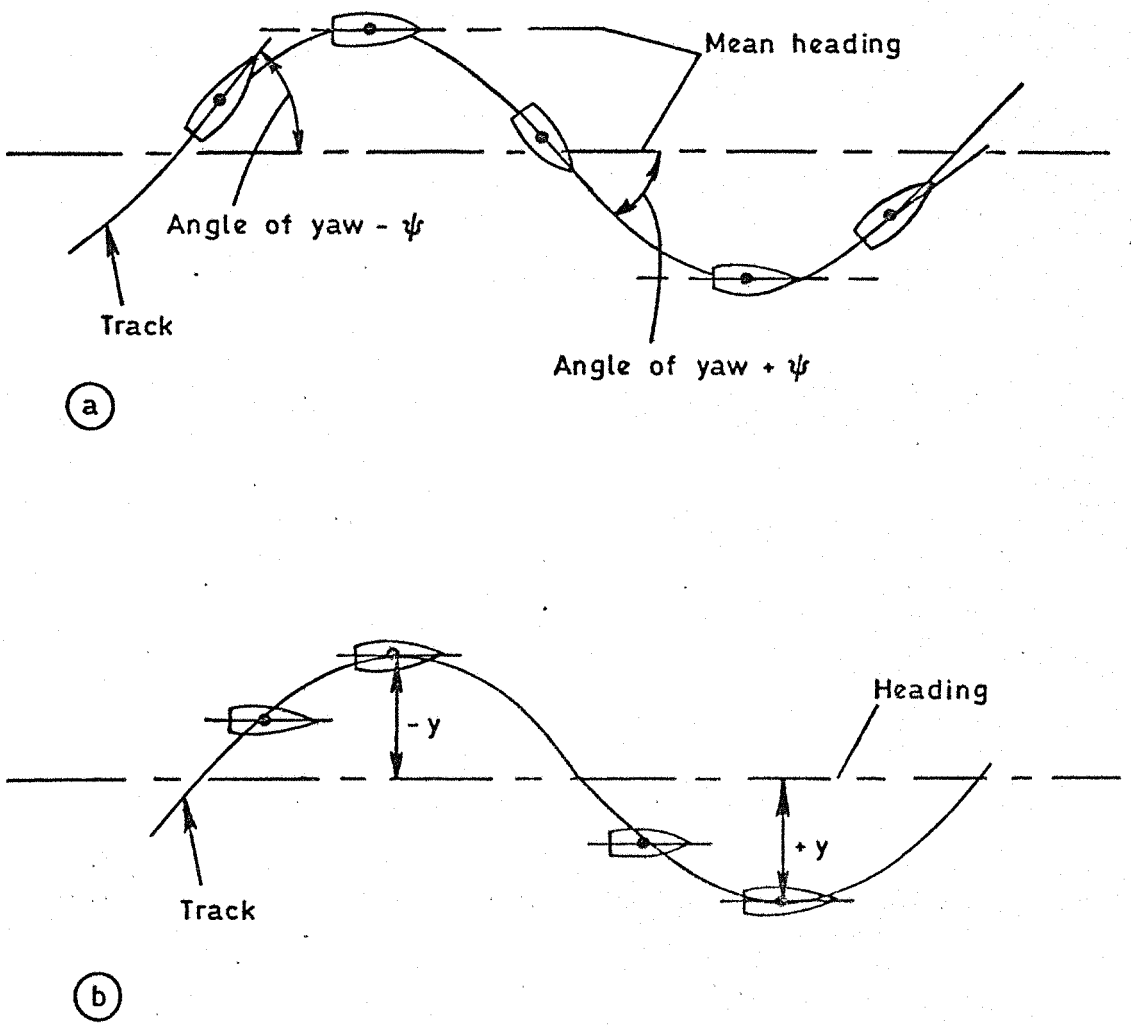

Fig 3 Sailboat nomeclature
Pure yawing and swaying motion,
(Sign convention)

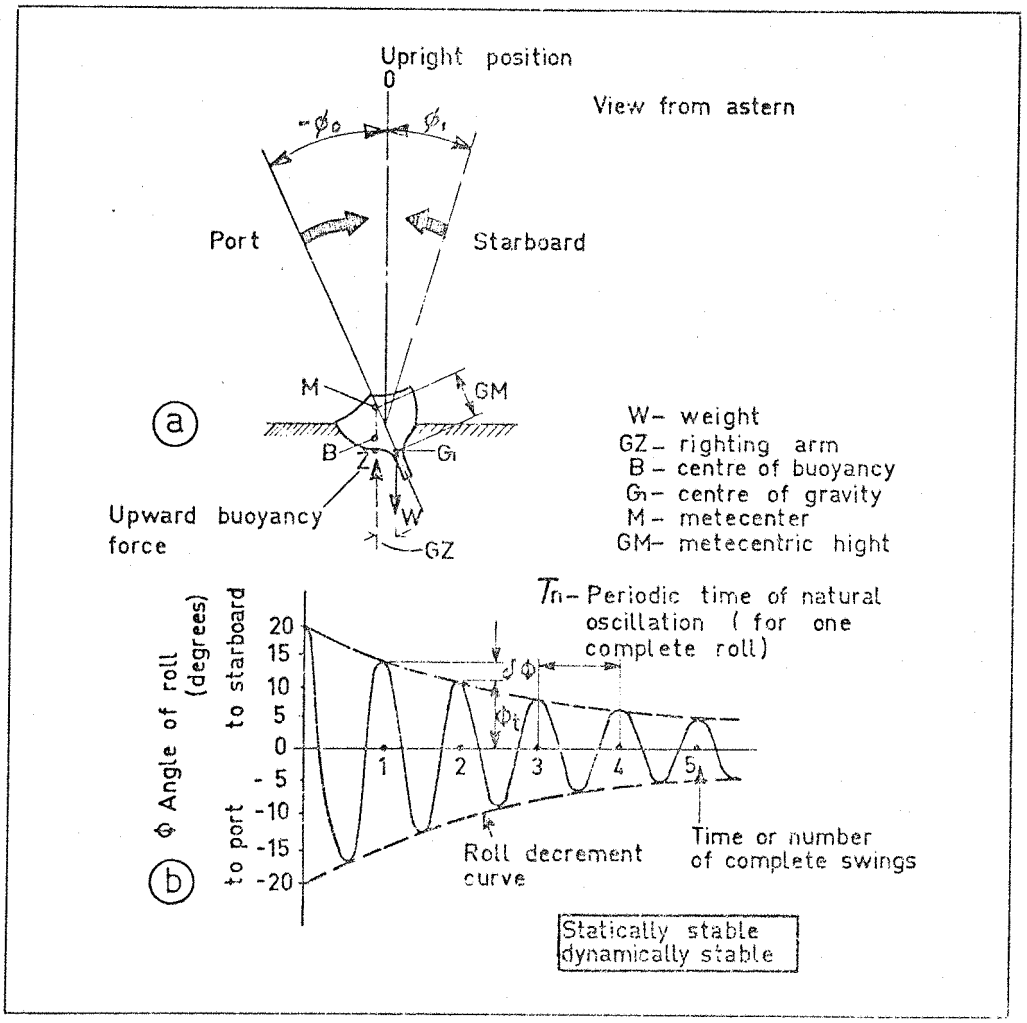

Fig. 4. Statically and dynamically stable rolling motion.

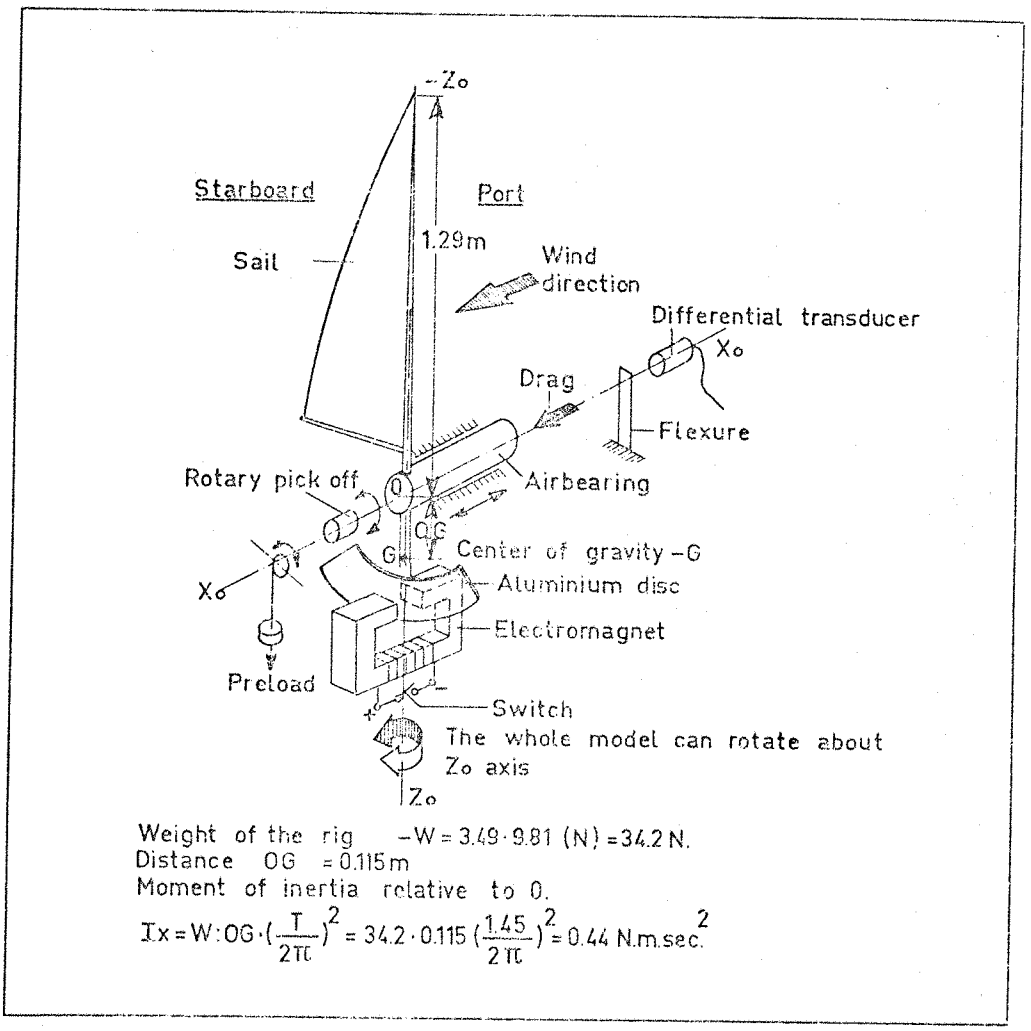

Weight of the rig $-W = 3.49 \cdot 9.81\ (N) = 34.2\ N.$

Distance $OG = 0.115\ m$

Moment of inertia relative to O.

$$Ix = W \cdot OG \cdot \left(\frac{T}{2\pi}\right)^2 = 34.2 \cdot 0.115 \left(\frac{1.45}{2\pi}\right)^2 = 0.44\ N.m.sec.^2$$

Fig. 5 Wind tunnel model of the rolling rig.

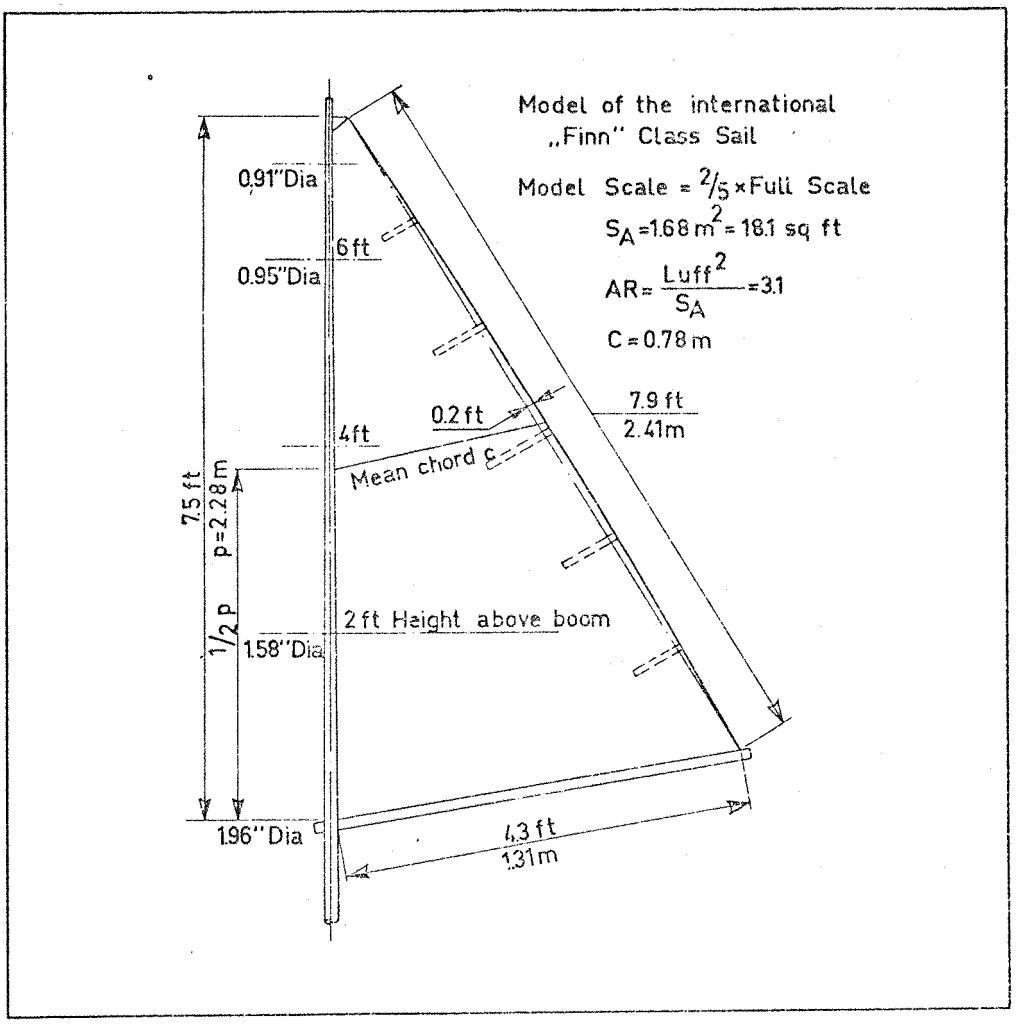

Fig. 6 Finn type Sail Model used in rolling experiments.

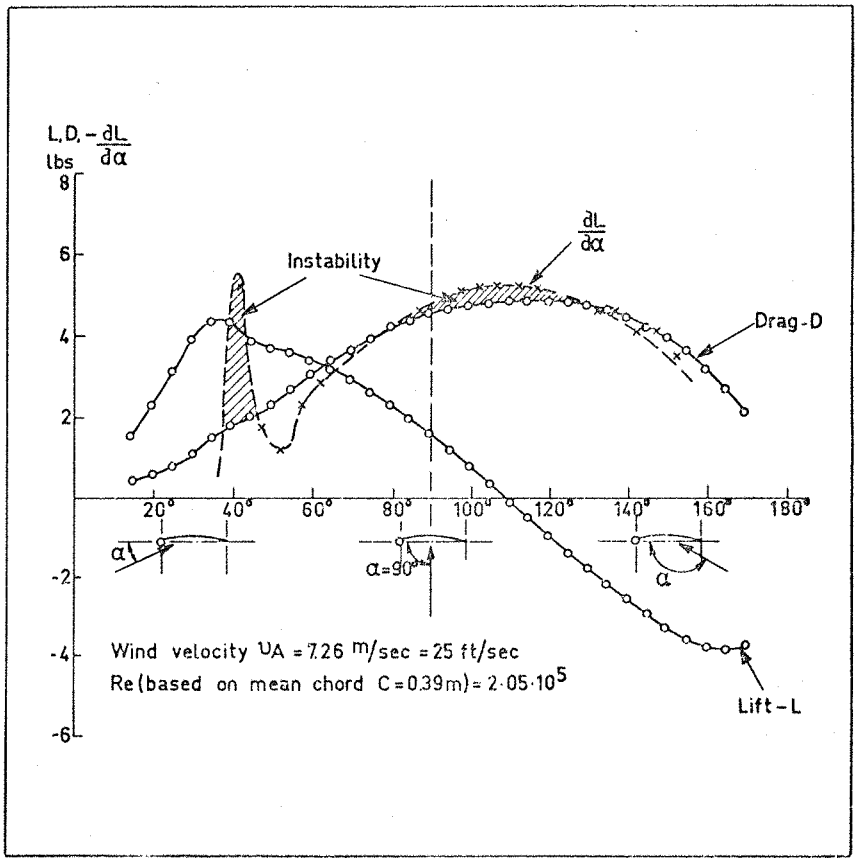

Figure 7.
Run VII Small model, 1/5 Scale (Melinex).

Wind velocity V_A = 7.26 m/sec = 25 ft/sec
Re (based on mean chord C = 0.39 m) = $2.05 \cdot 10^5$
Note : In order to facilitate an immediate comparison of $\frac{\partial L}{\partial \alpha}$ and D values the graph of $\frac{\partial L}{\partial \alpha}$ is plotted with the negative values above the abscissa.

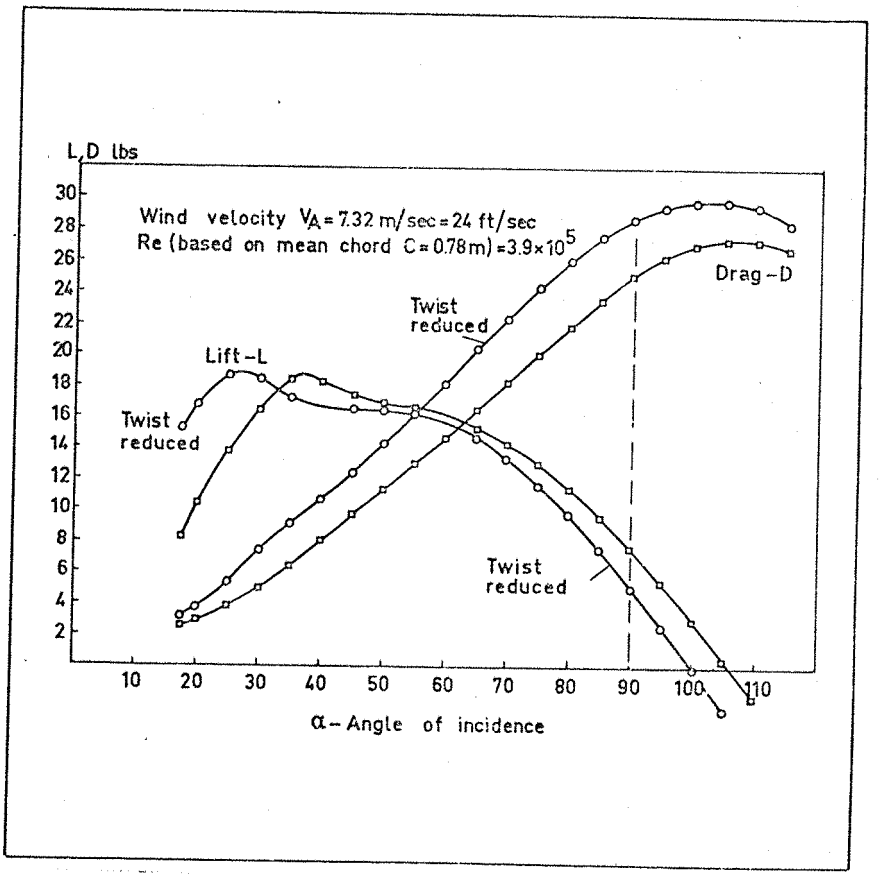

Figure 8
Runs VIII and IX Big model, 2/5 Scale (Terylene).

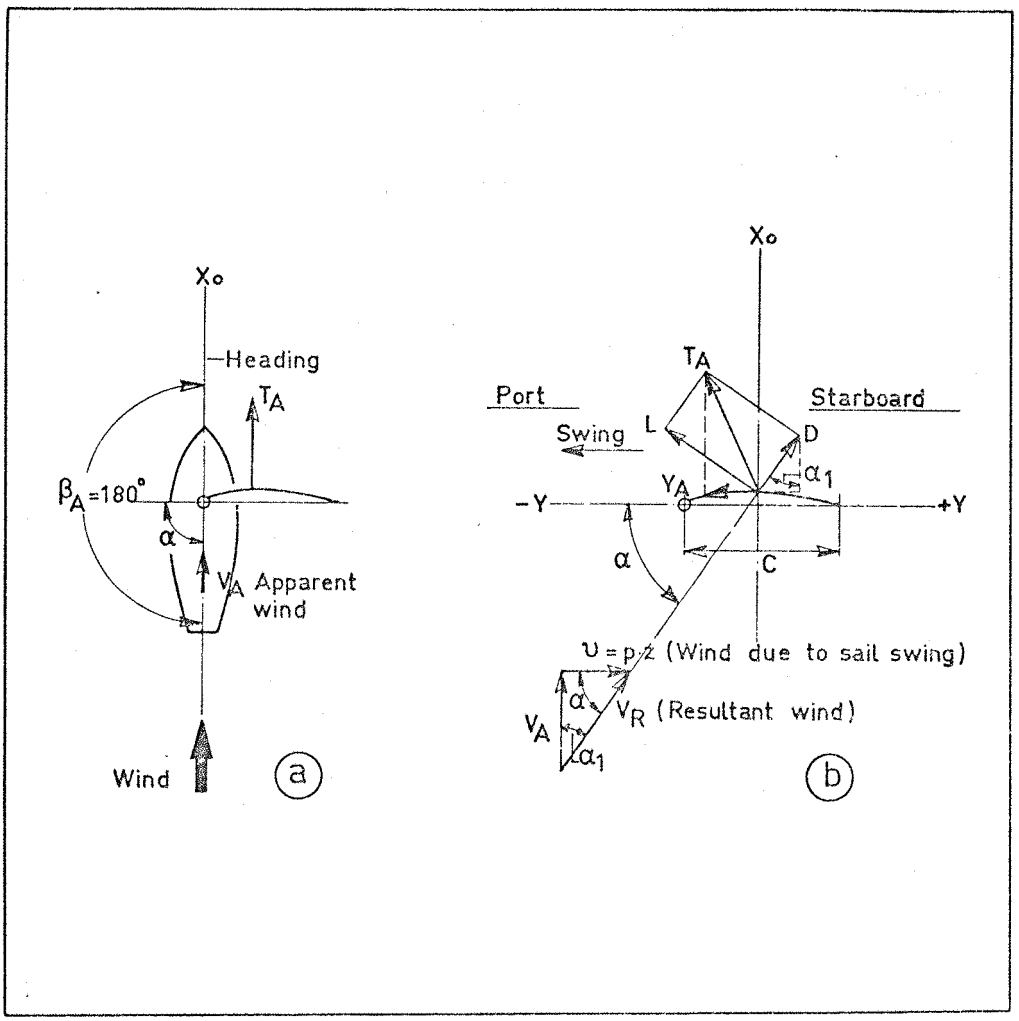

Fig. 9 Diagram of forces and velocities ; running before the wind, without and with swinging motion.

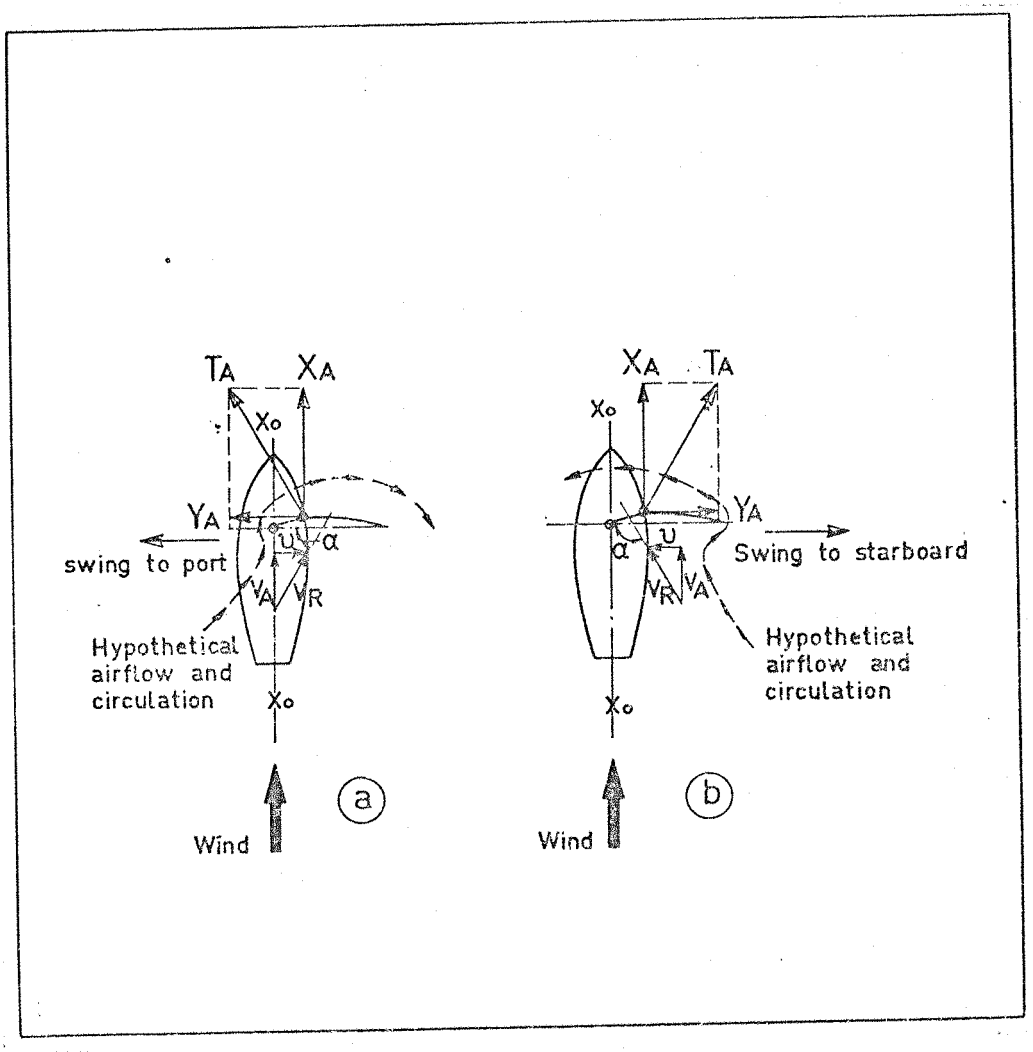

Fig. 10 Illustration of circulation reversal due to swinging motion.

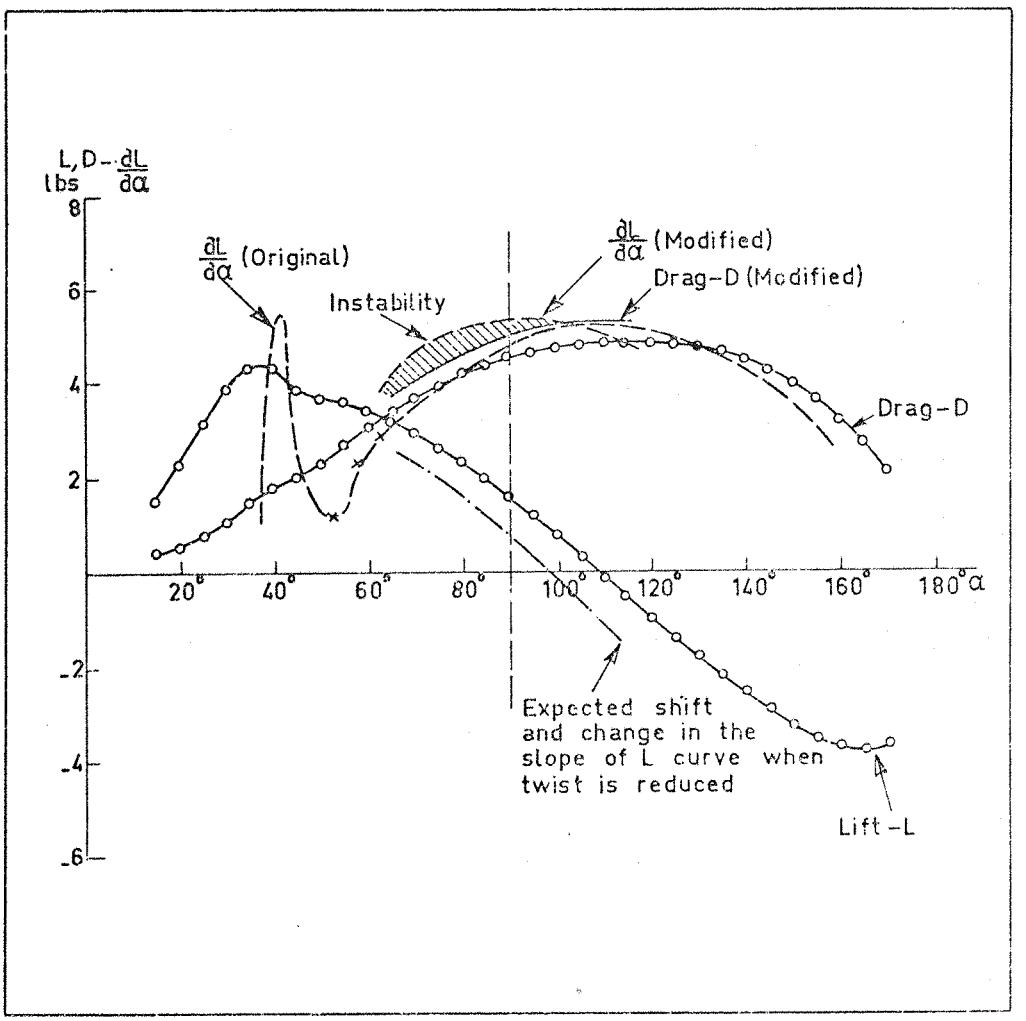

Fig. 11 Modified aerodynamic properties of the small model (see Fig.7) at incidence α = 70 - 110 degrees.

Note : In order to facilitate the immediate comparison of $\frac{\partial L}{\partial \alpha}$ and D values the graph of $\frac{\partial L}{\partial \alpha}$ is plotted with the negative values above the abscissa.

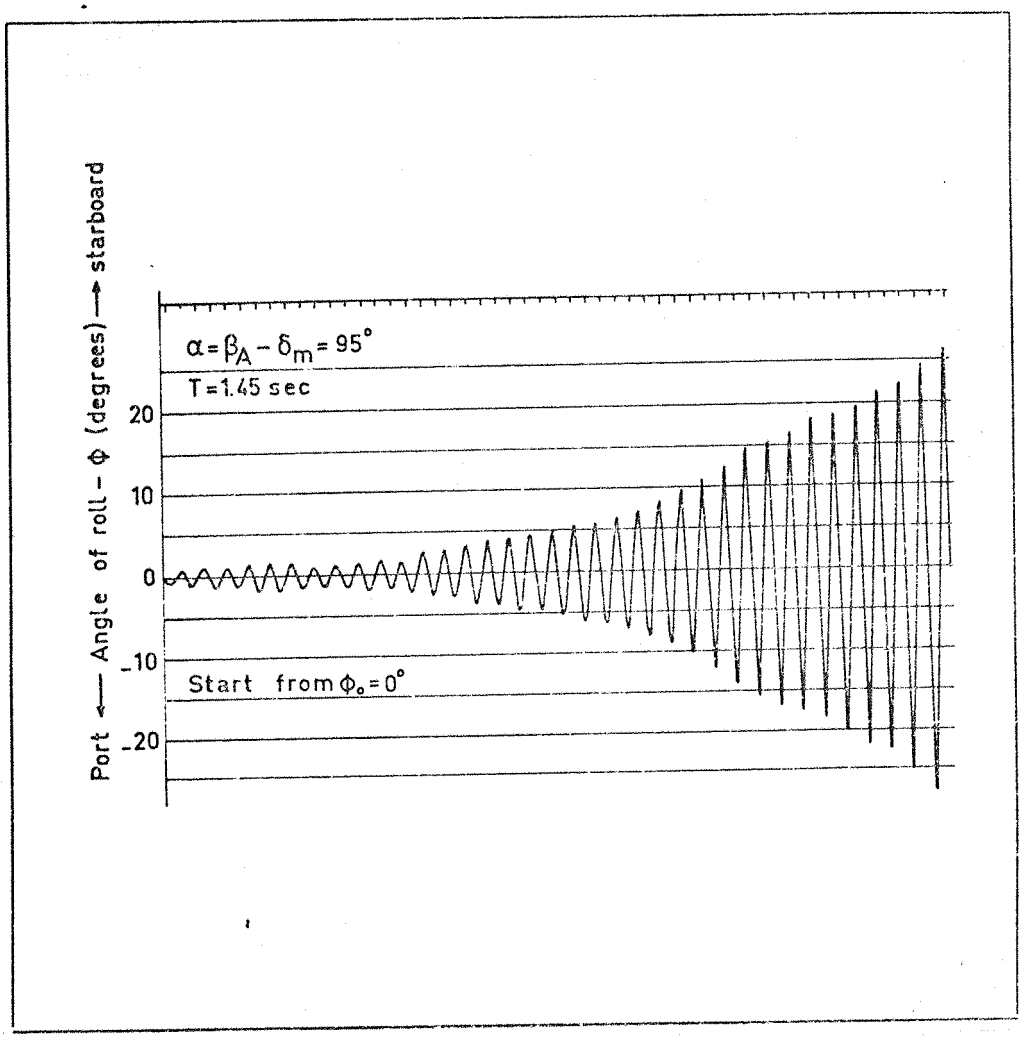

Fig. 12 Recorded oscillation of the 1/5 scale Finn rig.
Dynamically unstable rolling motion.

V_A = 3.05 m/sec

S_t = 0.55

β_A = 180°

δ_m = 85°

Magnetic damping = 1.0

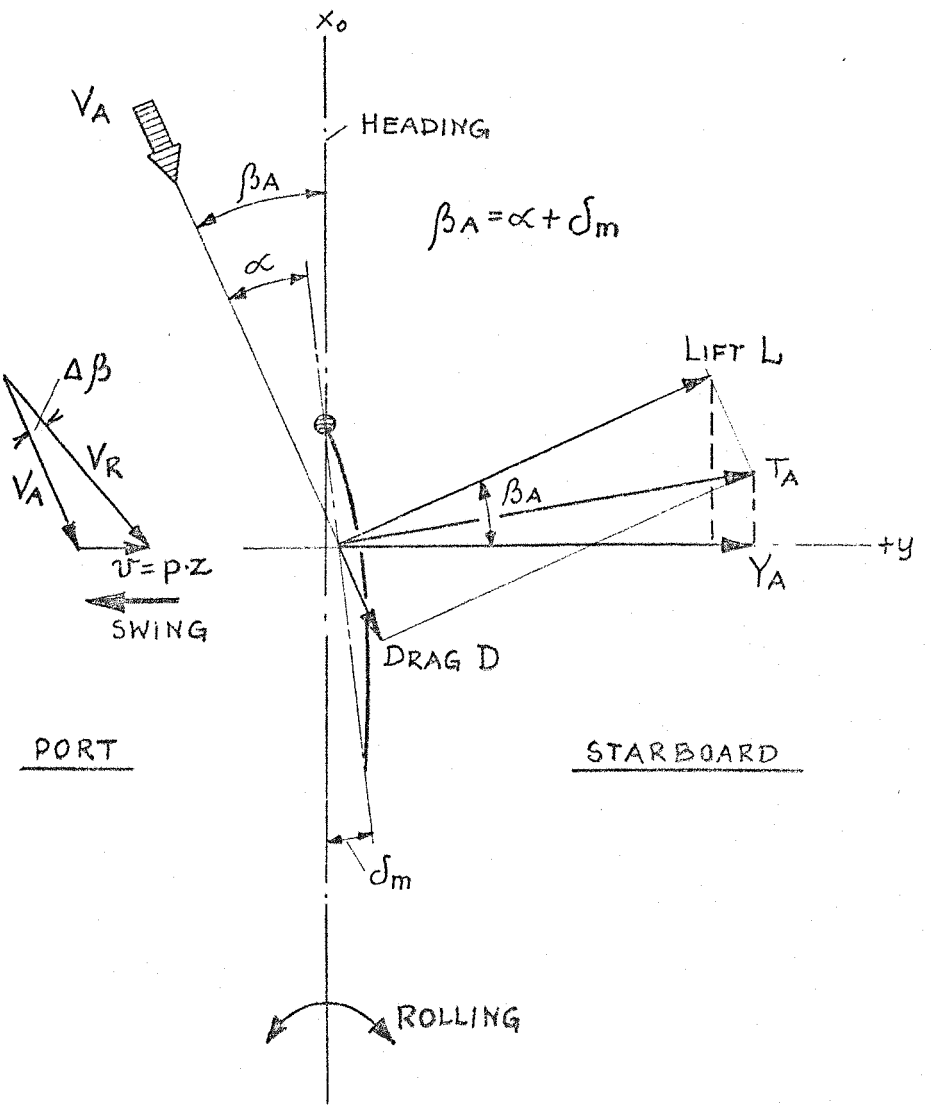

Fig. 13 Geometry of forces and wind velocities in close-hauled rolling condition.

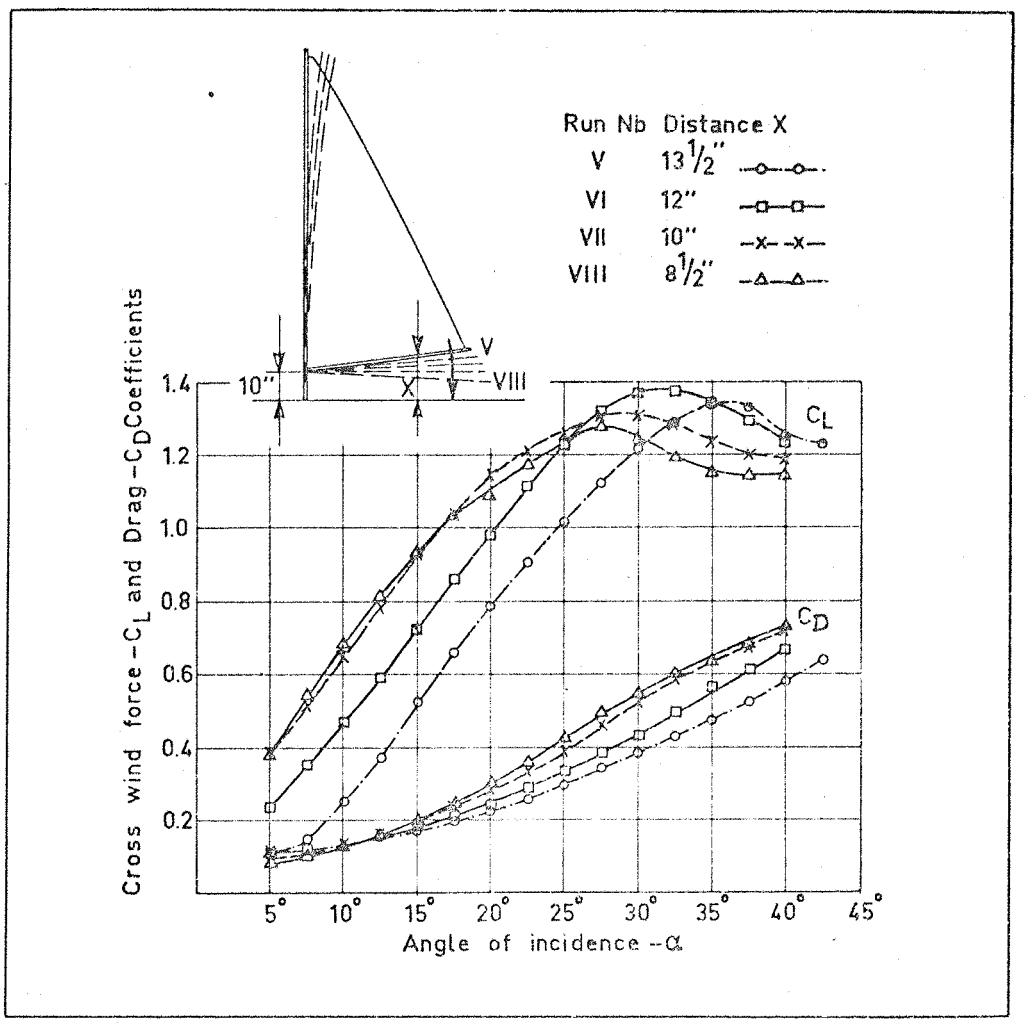

Fig. 14 Close hauled force characteristics of Finn rig with different vertical positions of the boom.

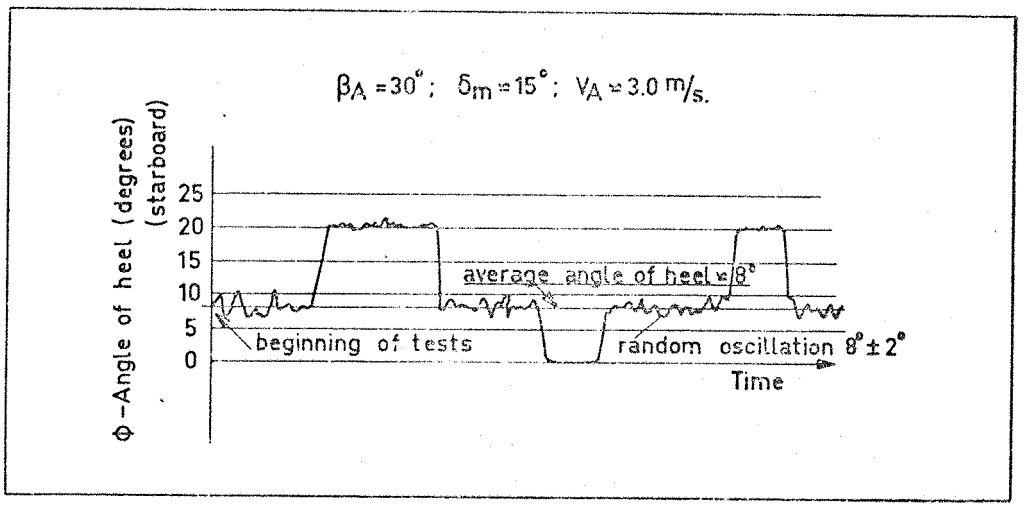

Fig. 15 Rolling in a close hauled condition.

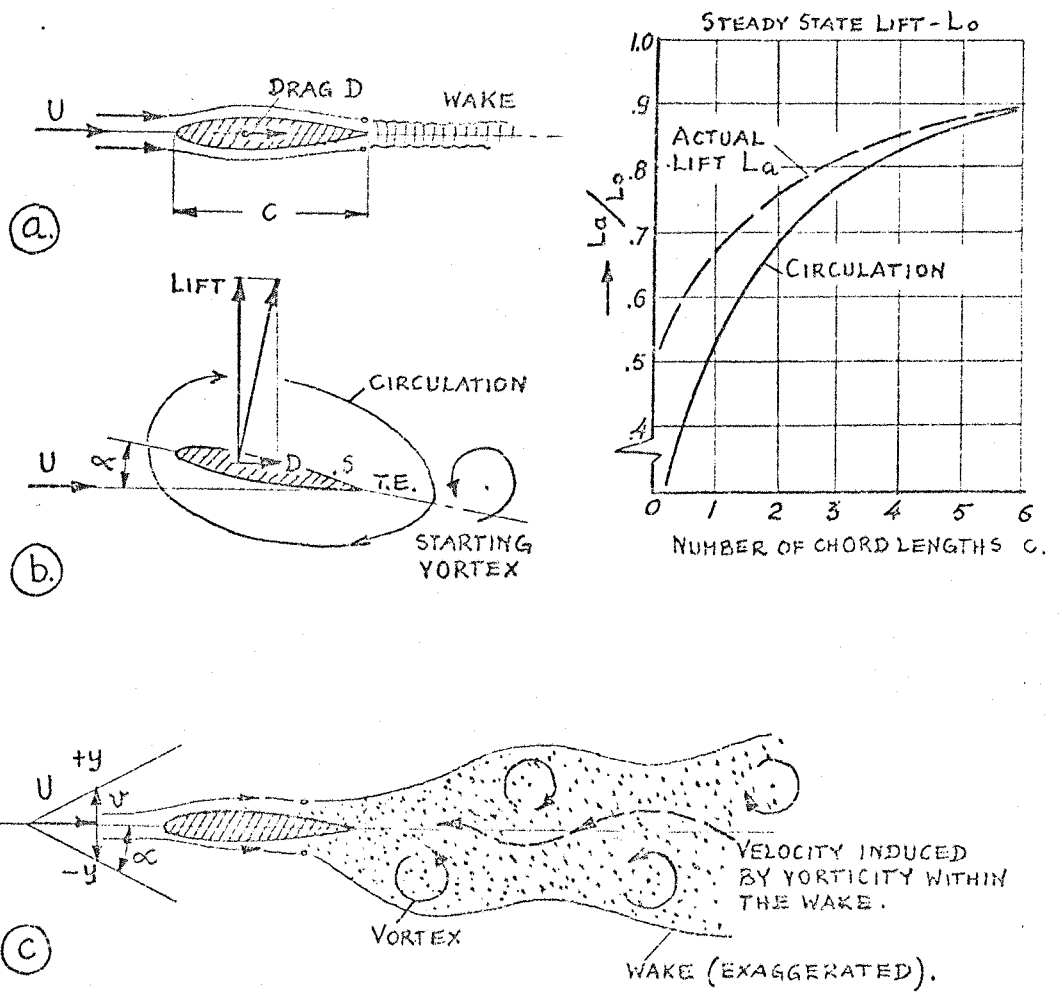

Fig. 16

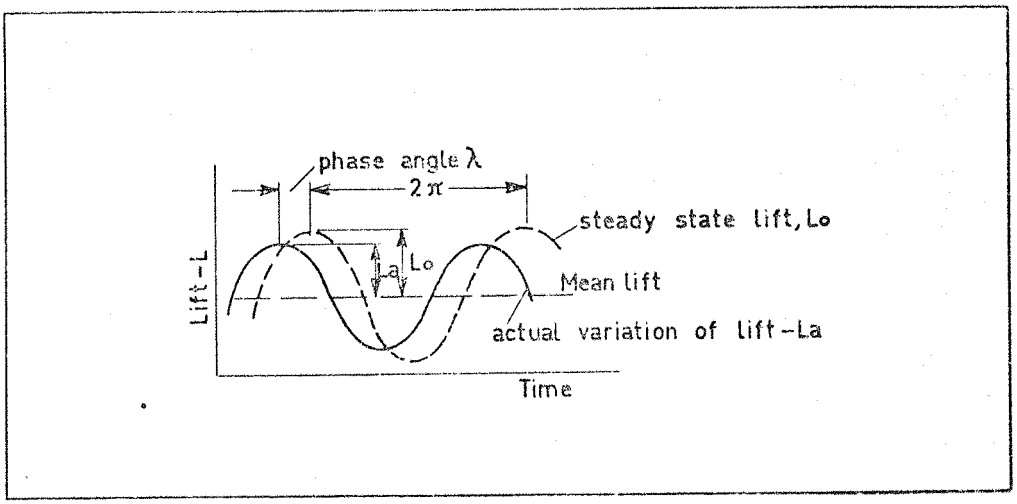

Fig. 17 Phase λ and Lift relations in a case of oscillating airfoil.

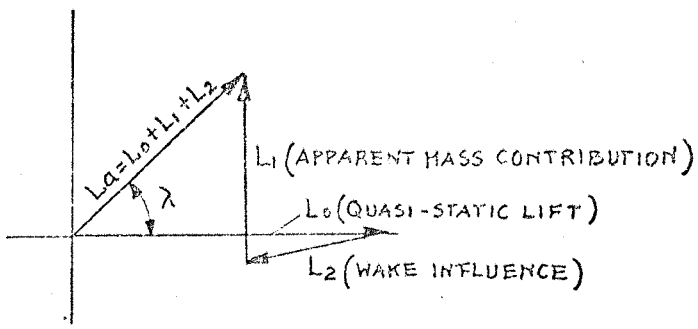

Fig. 18 Vector diagram for the Lift of an oscillating airfoil.

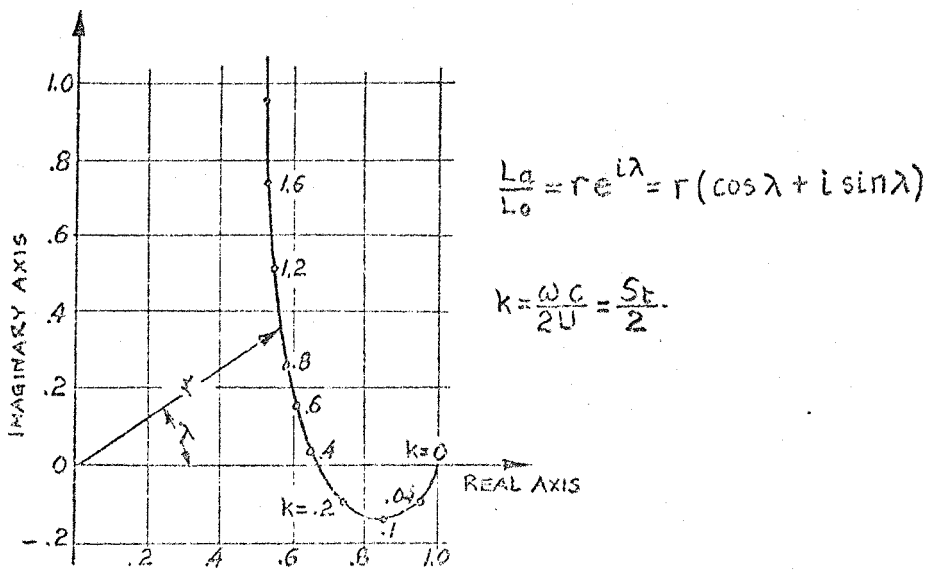

Fig. 19 Vector diagram for the lift (translatory oscillation)

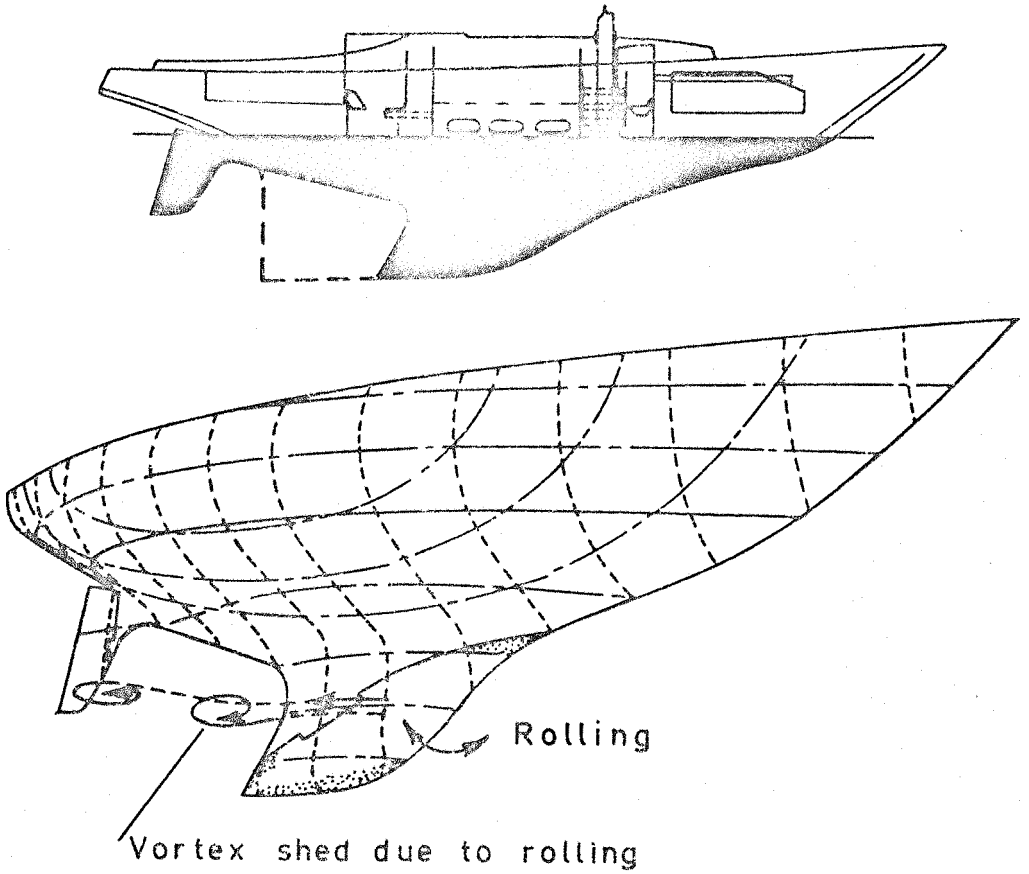

Fig. 20

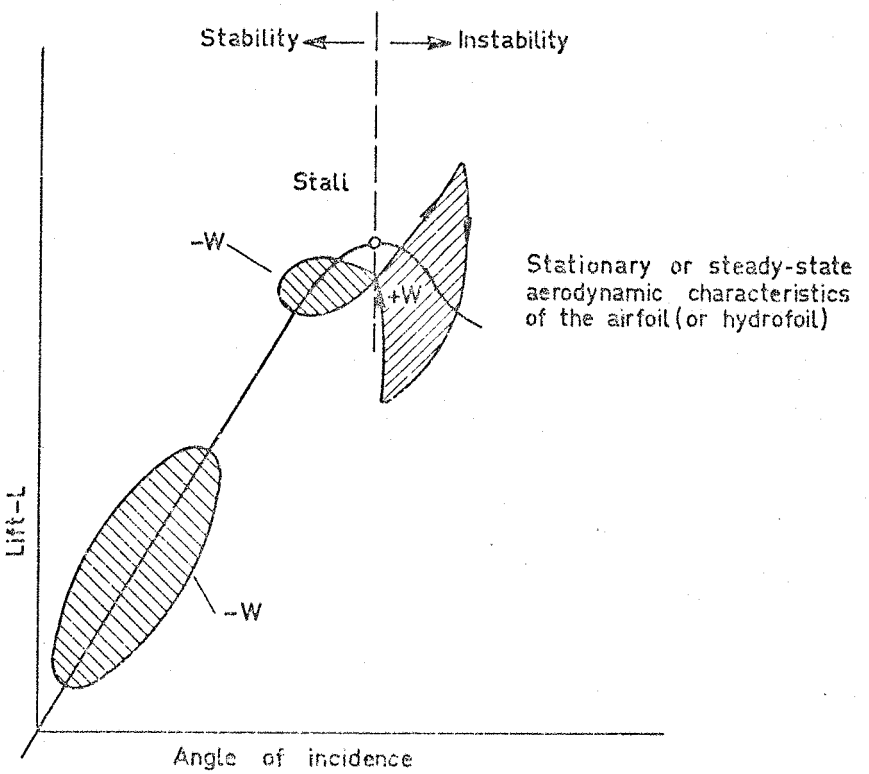

Fig. 21 Effect of aerodynamic hysteresis on dynamic stability of an oscillating airfoil (hydrofoil).

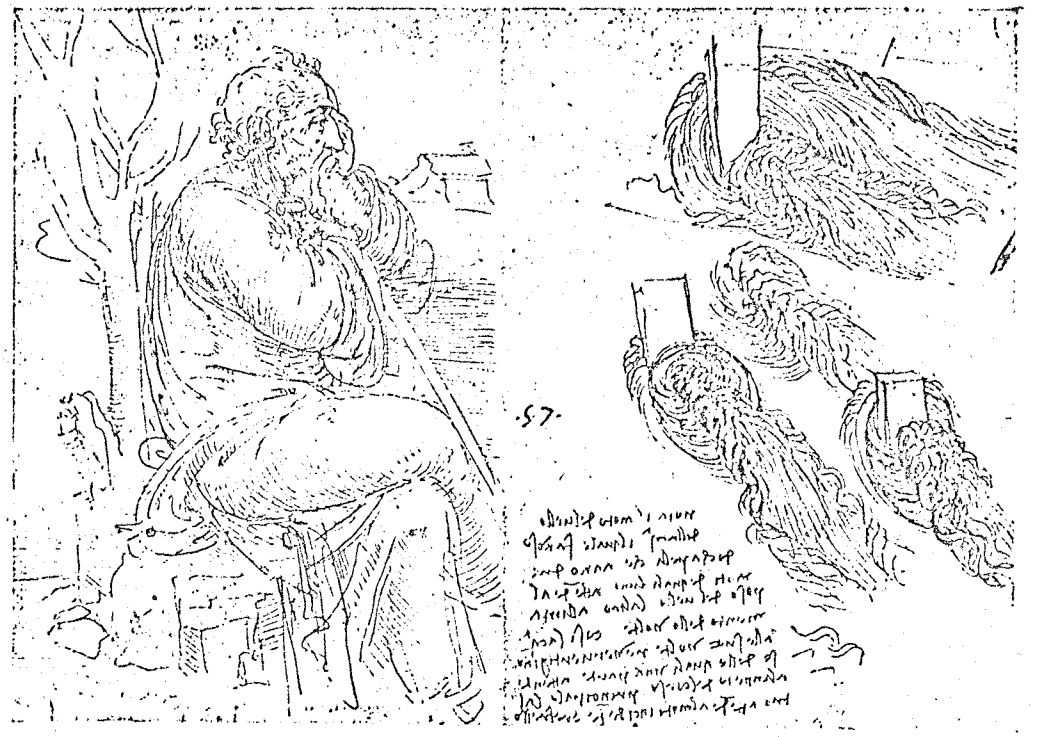

Fig. 22. Vortex shedding studies by Leonardo da Vinci.

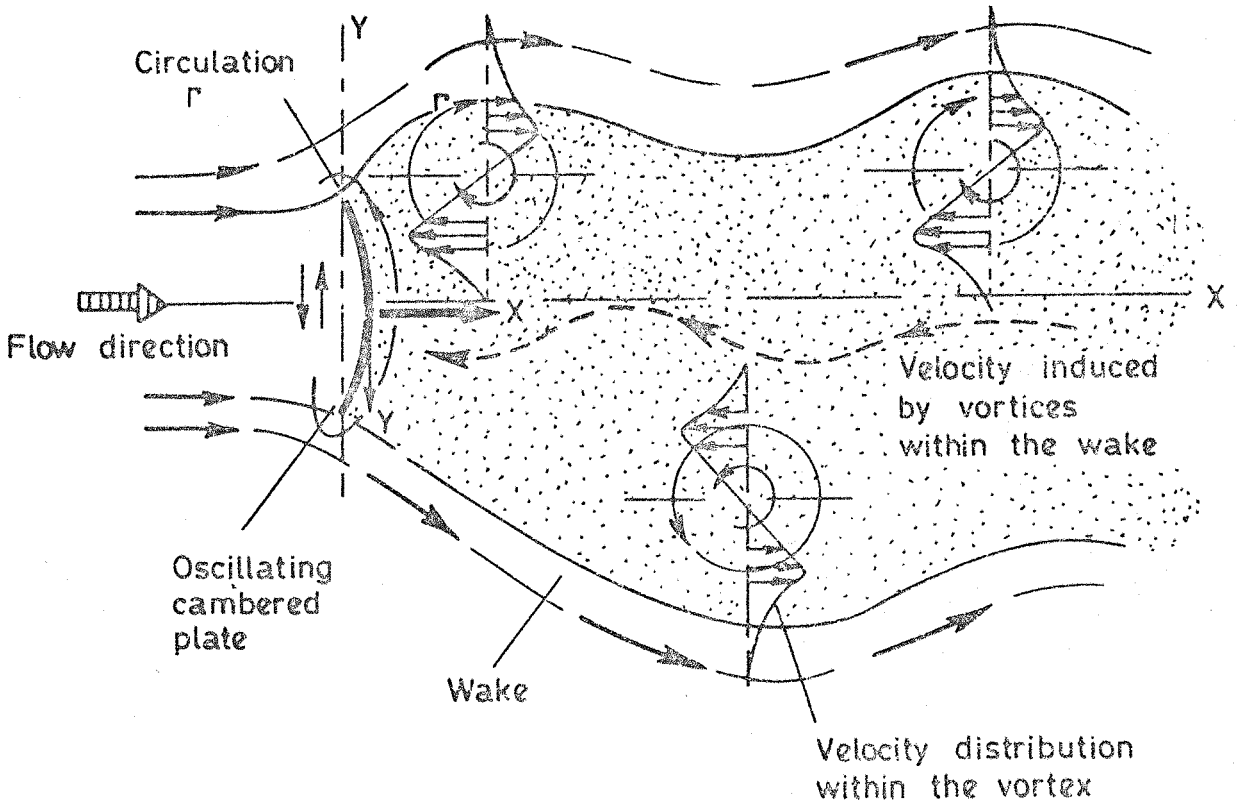

Fig. 23. Water channel experiments.
Wake behind the oscillating plate and vortex distribution in two dimensional flow.

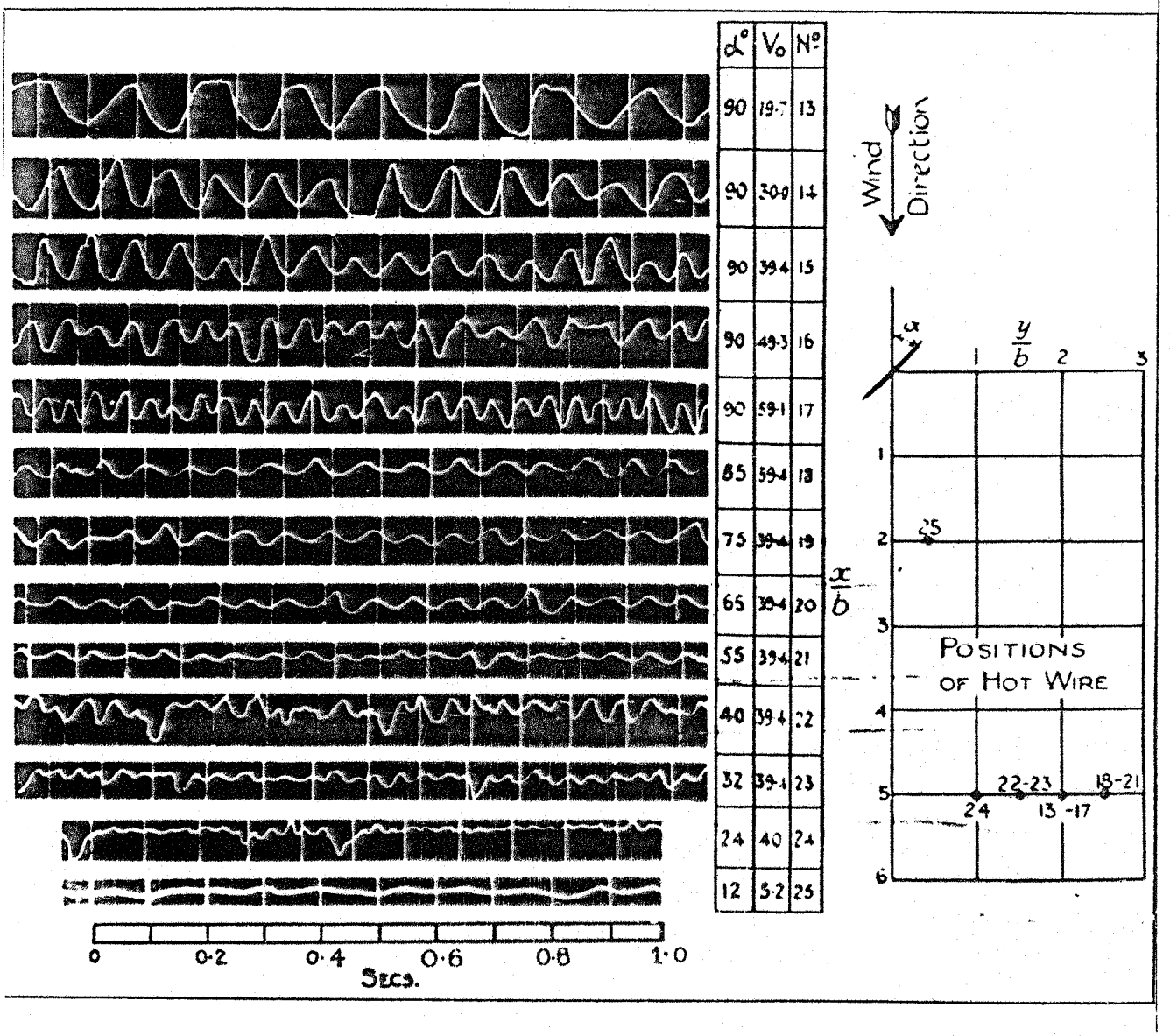

Fig.24. Velocity fluctuation in the wake behind the plate (measured by hot-wire anemometer).

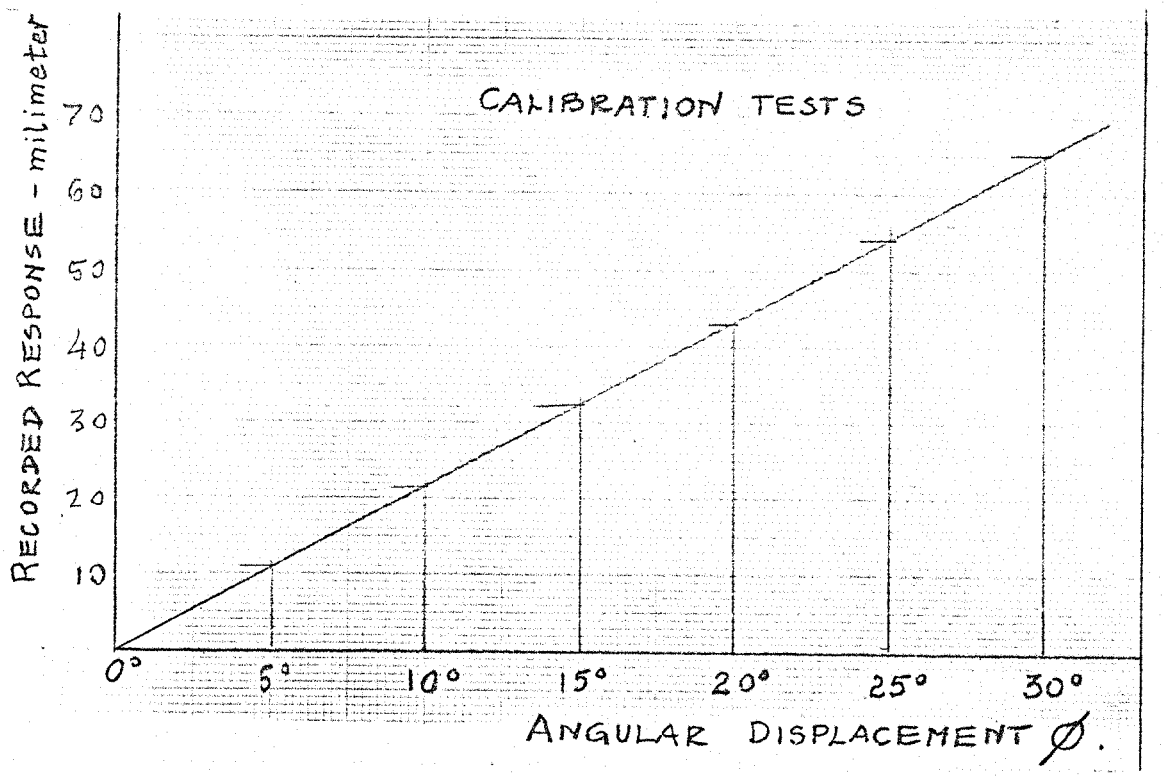

Fig.25.Angular Displacement ϕ of the mast against the recorder response.

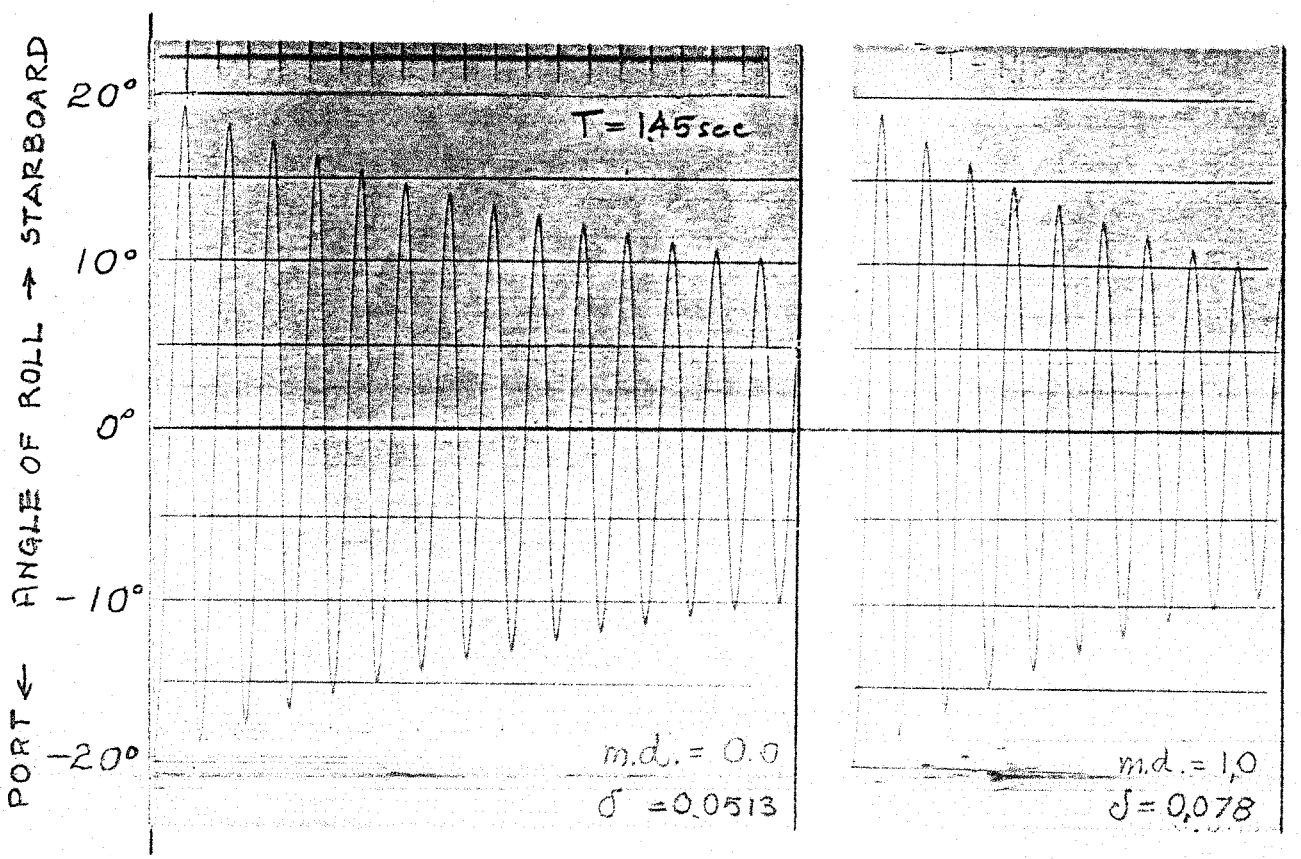

Fig.26.Decrement curves for various degrees of magnetic damping m.d.(in arbitrary units).

$\delta_m = 85^\circ$, no wind , ϕ_o(initial displacement) $= -20^\circ$

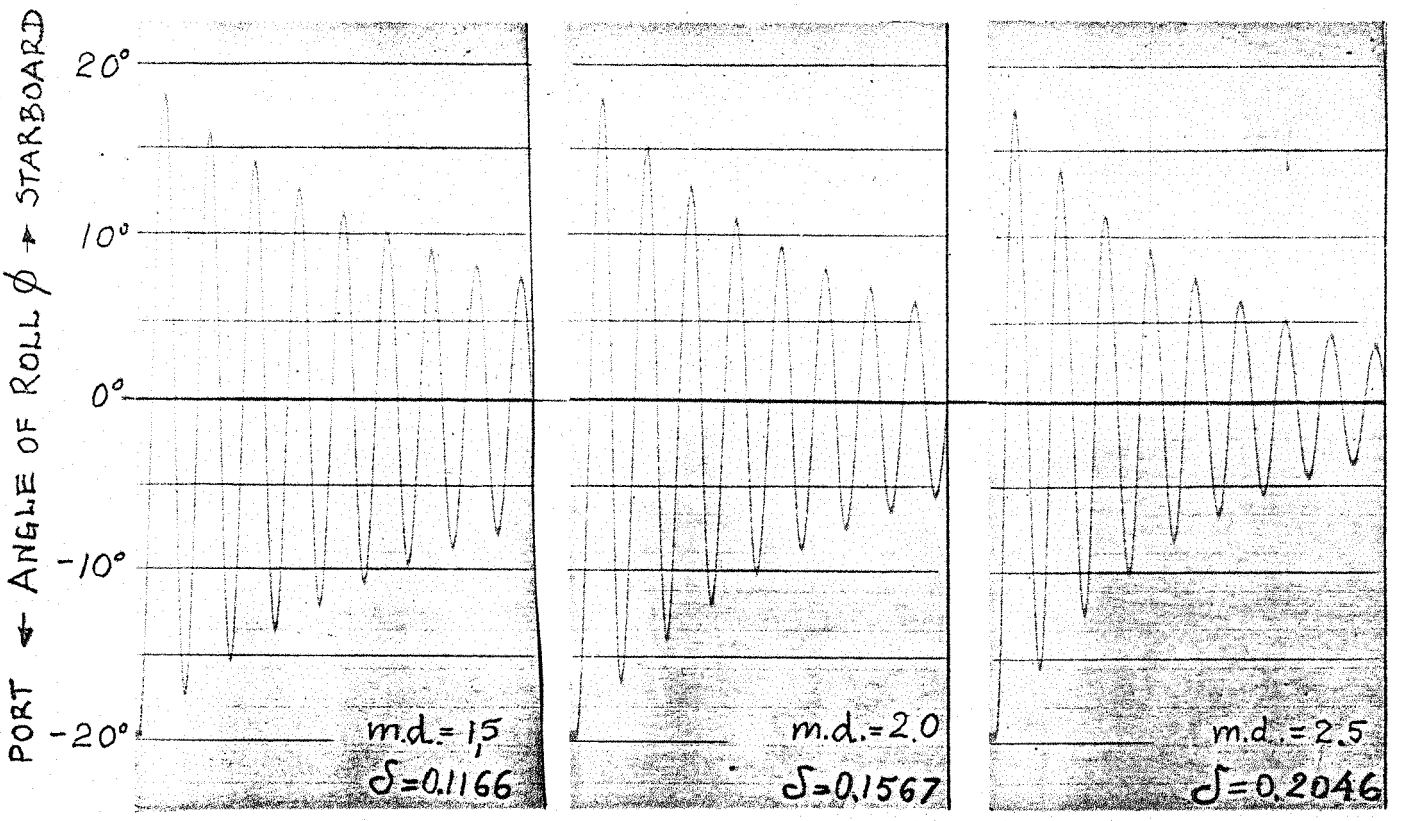

Fig.26 a.

Note: Calculation of the logarithmic decrement is based on Eq. 28 , Appendix.

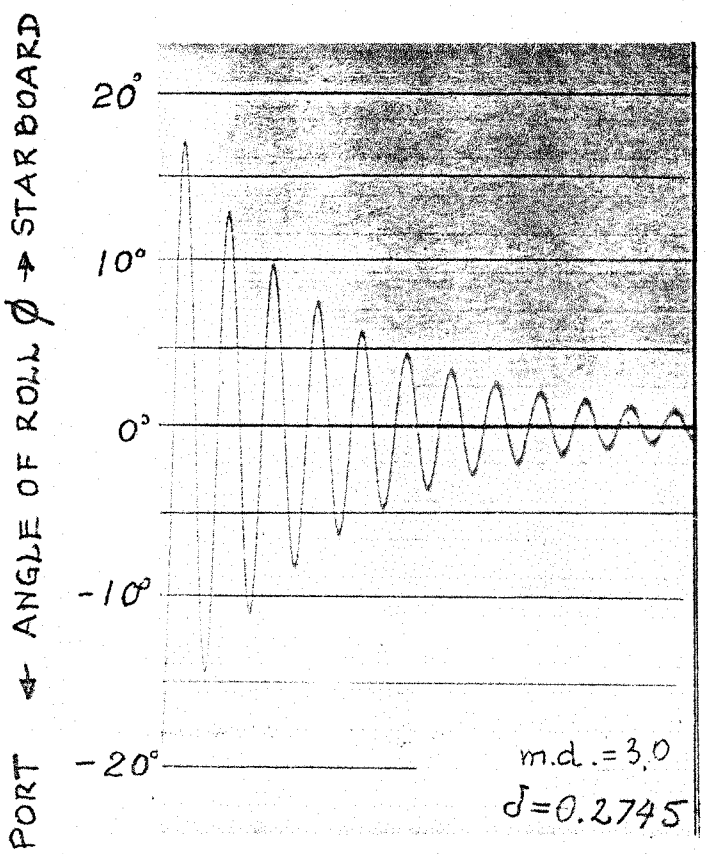

Fig.26 b .

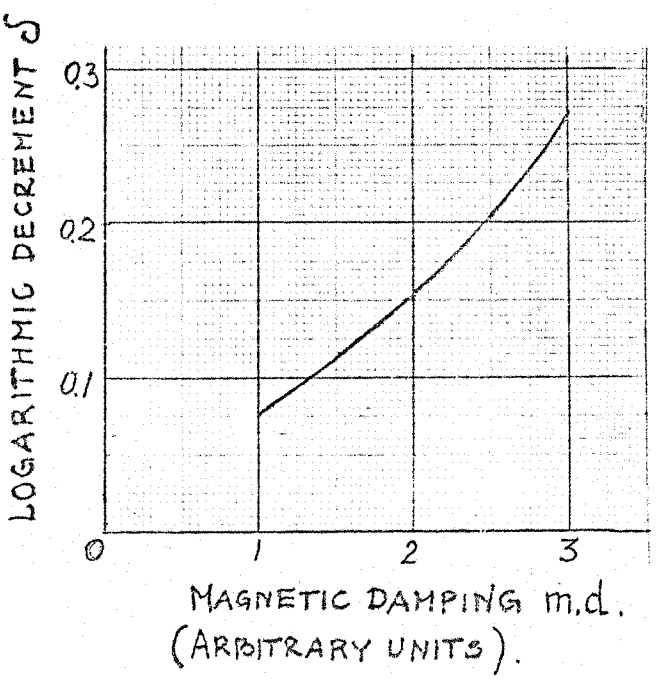

Fig.26 c .

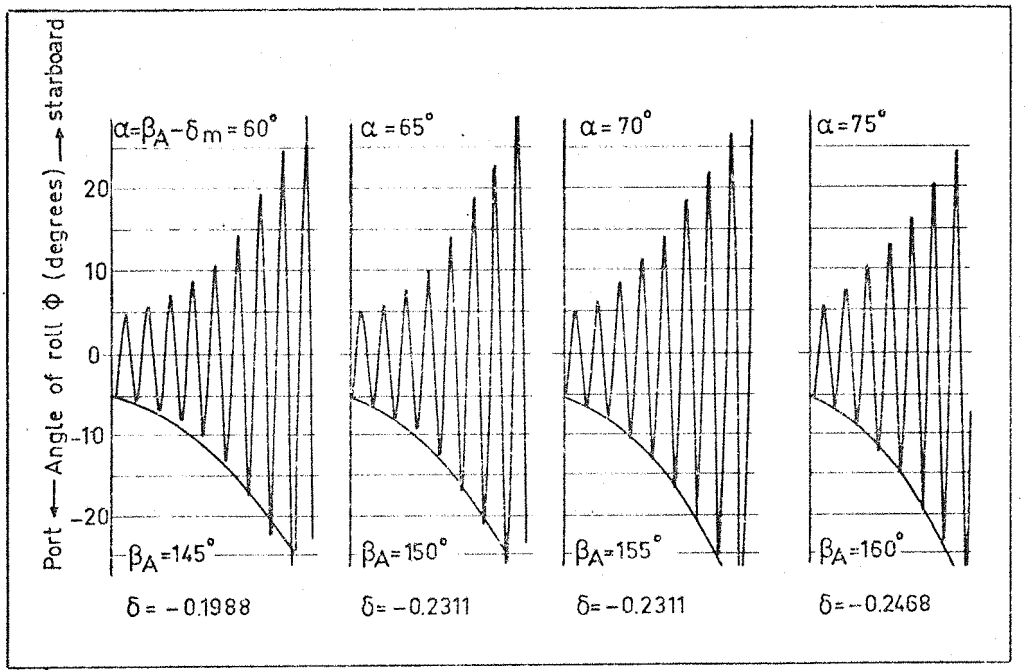

Fig. 27

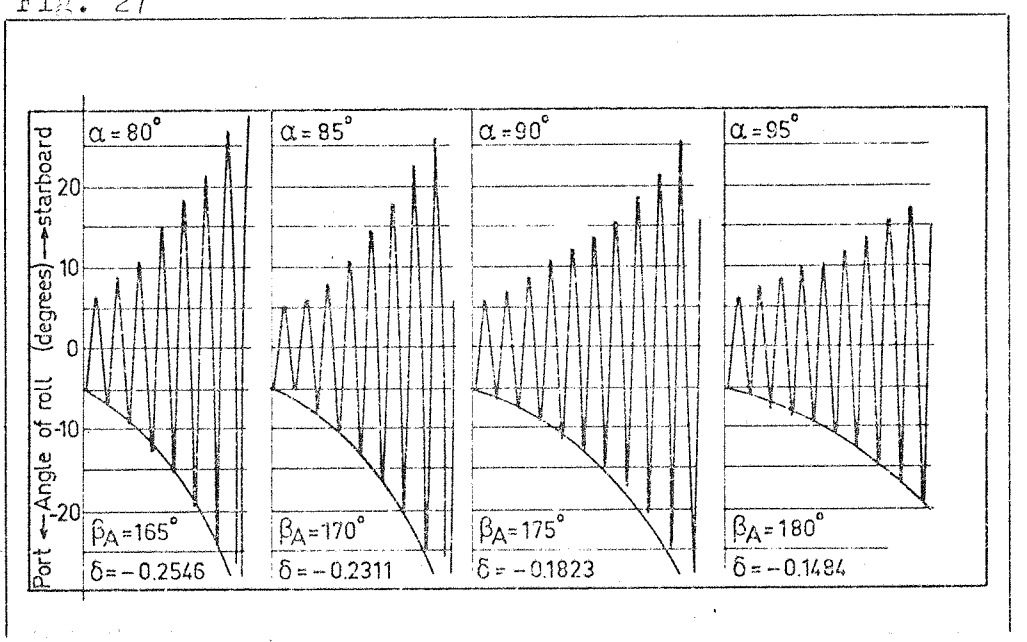

Fig. 27a Recorded oscillations of the 1/5 scale Finn rig.

V_A = 3.05 m/sec = 10 ft/sec
S_t = 0.55 (based on mean chord of the sail) } constant
δ_m = 85°
Magnetic damping = 1.0
β_A variable

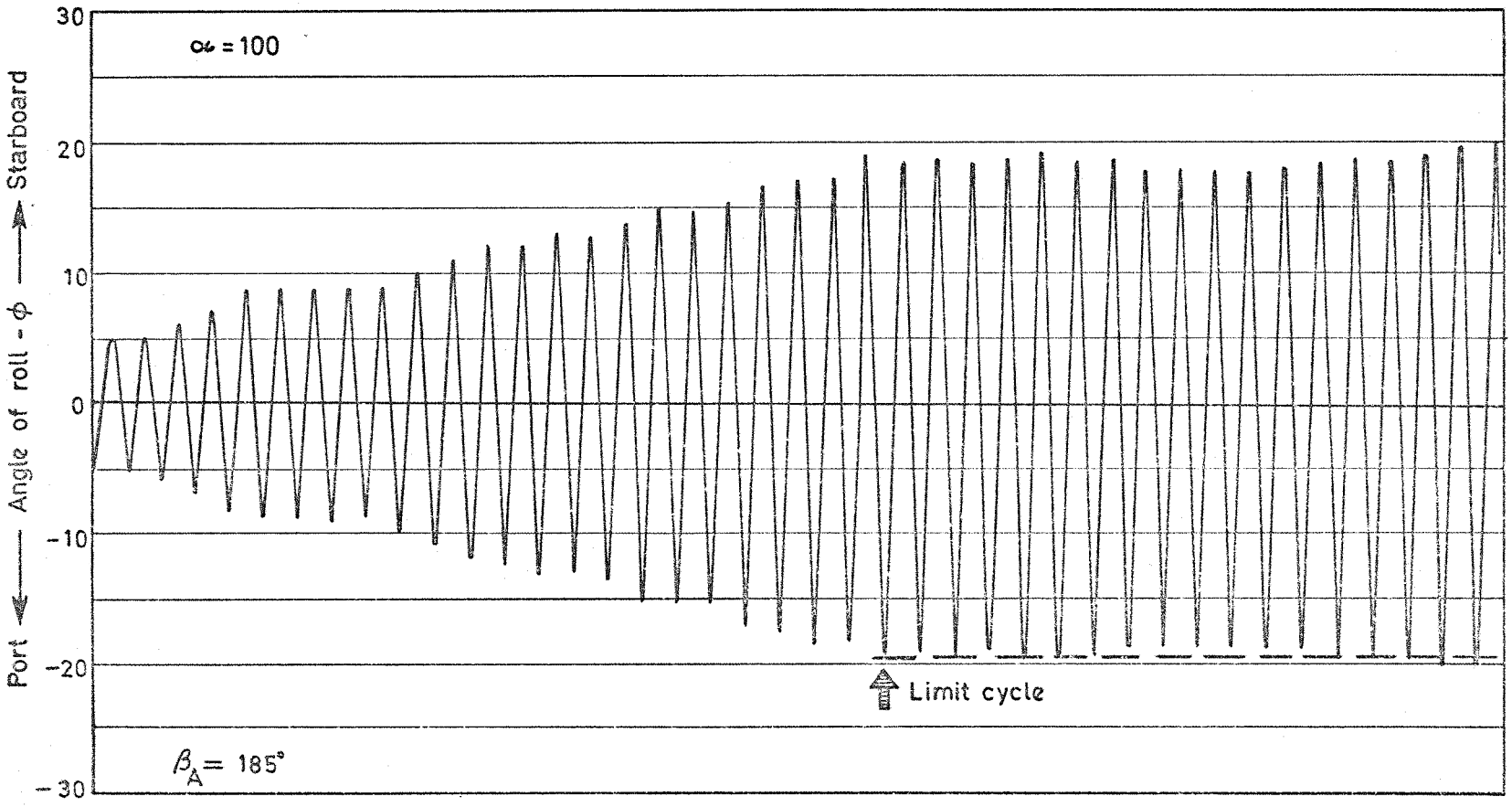

Recorded oscillation of the 1/5 scale 'FINN' rig. β_A - varable

Fig 27b

V_A = 3,05 m/s = 10 ft/s
St = 0,55
δm = 85° Magn. damping = 1.0
} constant

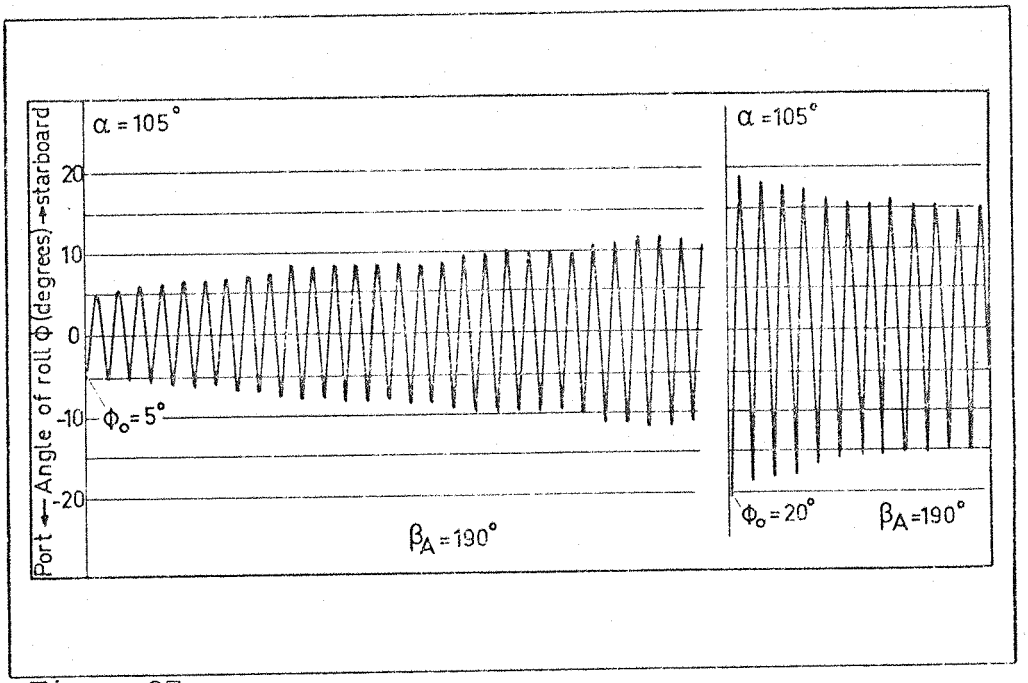

Fig. 27 c

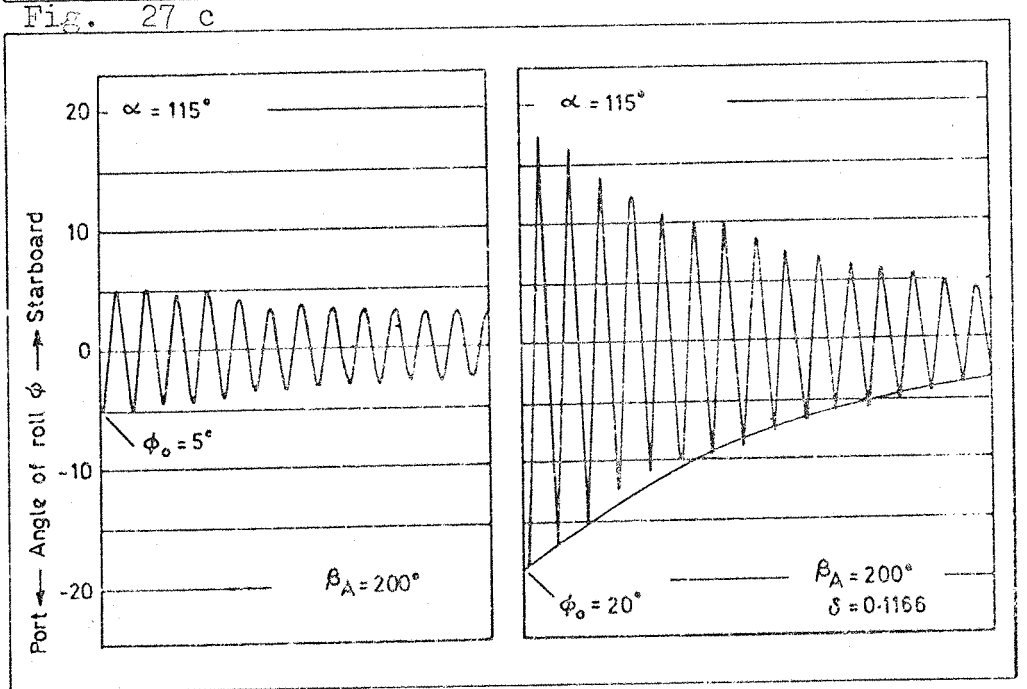

Fig. 27 e

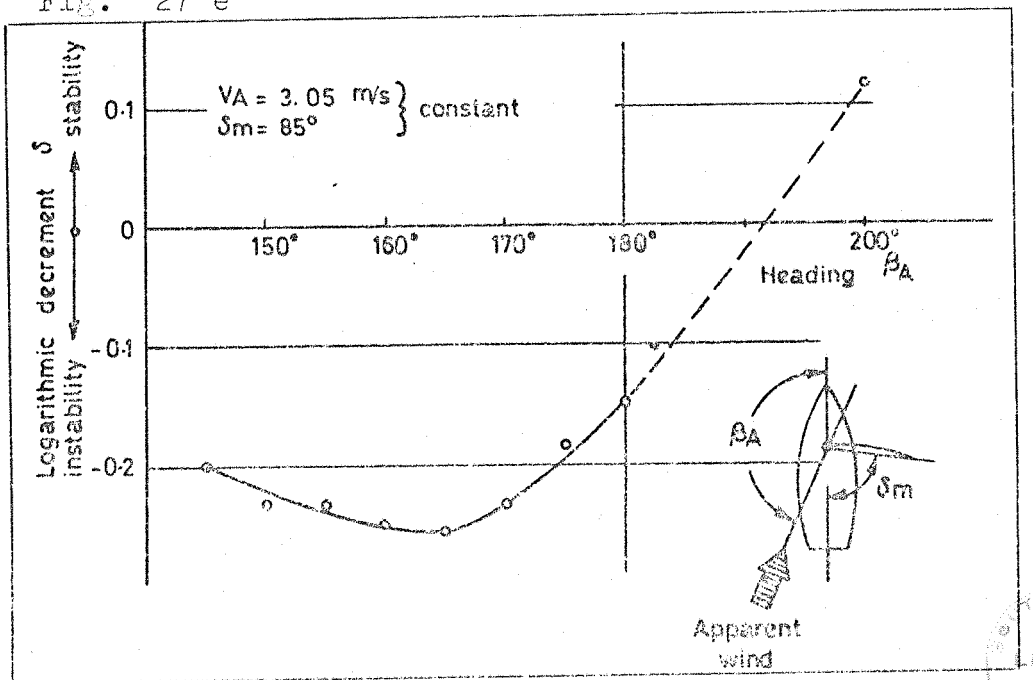

Fig. 27 f

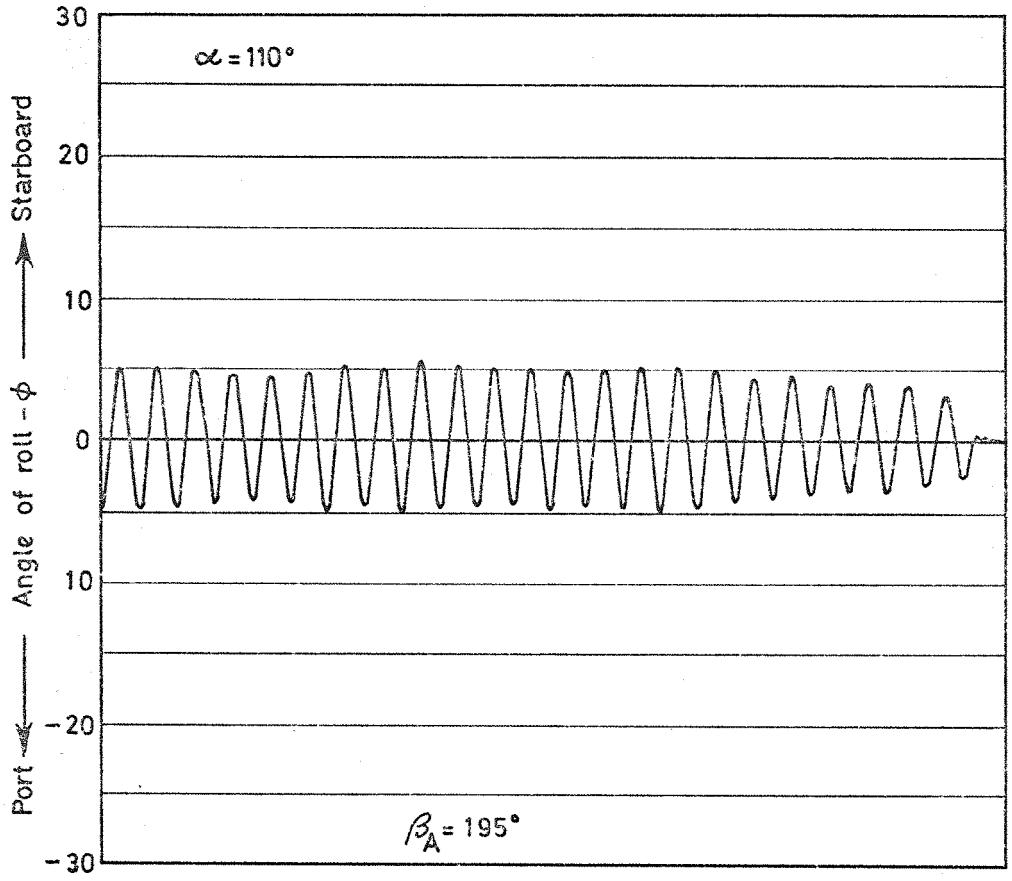

Fig. 27d

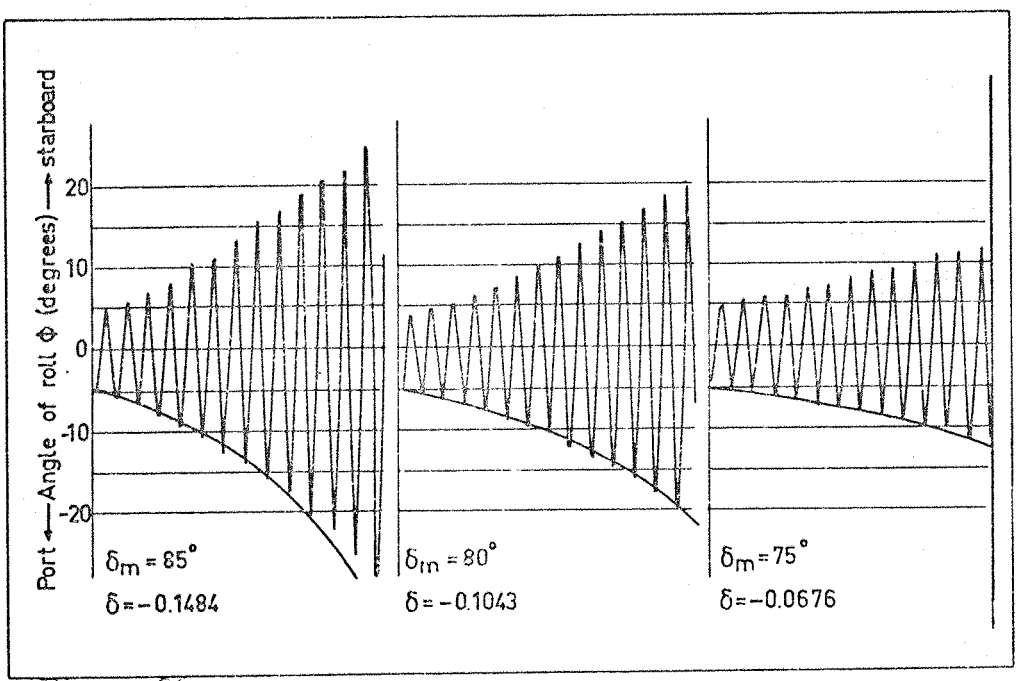

Fig. 28 a

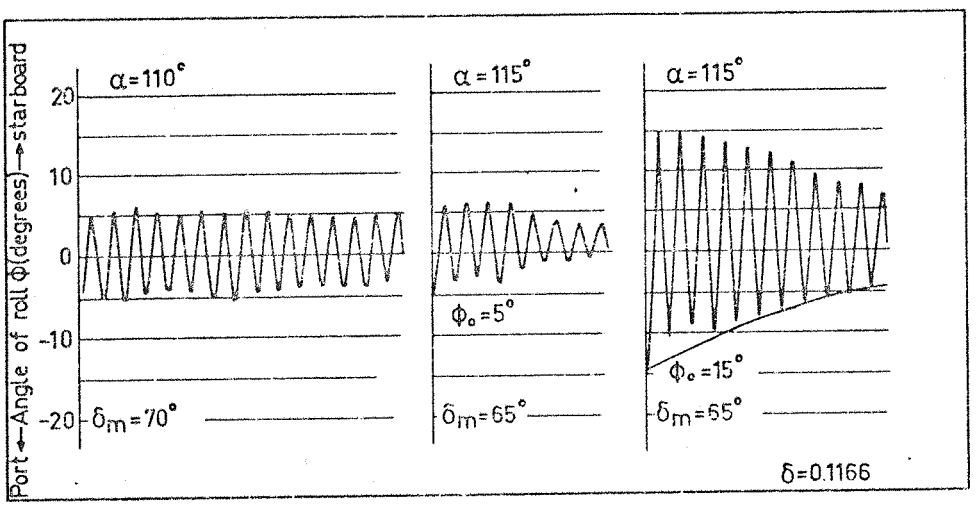

Fig. 28 b

Recorded oscillations of the 1/5 scale Finn rig.

V_A = 3.05 m/sec = 10 ft/sec
S_t = 0.55
β_A = 180°
Magnetic damping = 1.0
} constant

δ_m - variable

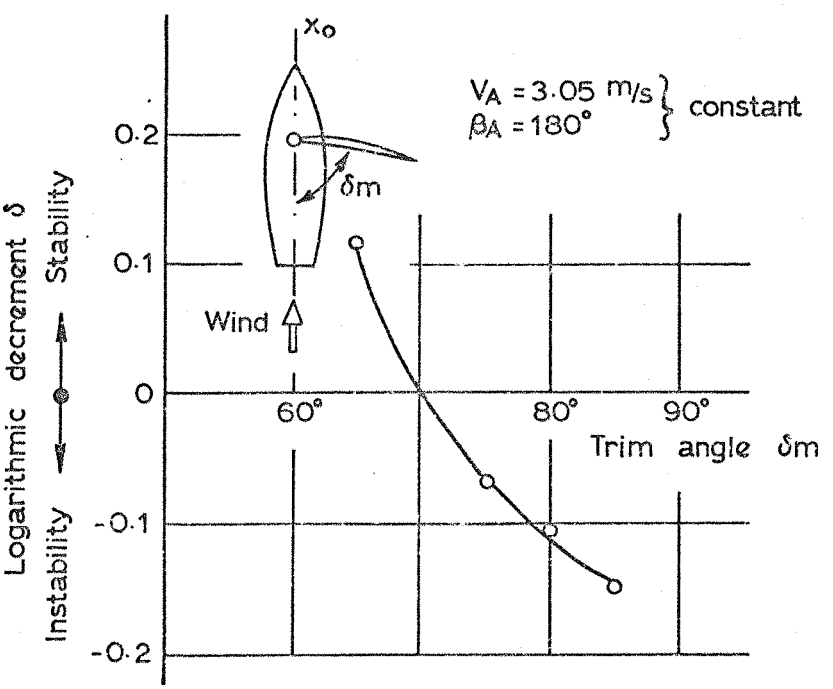

Fig 28c

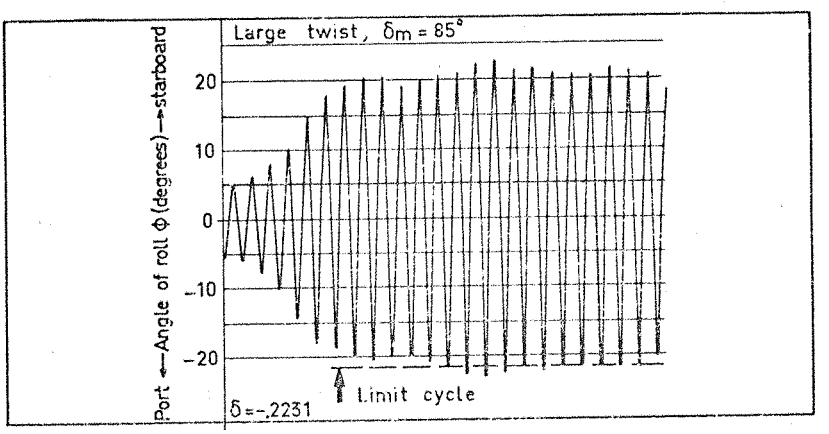

Fig. 28 d

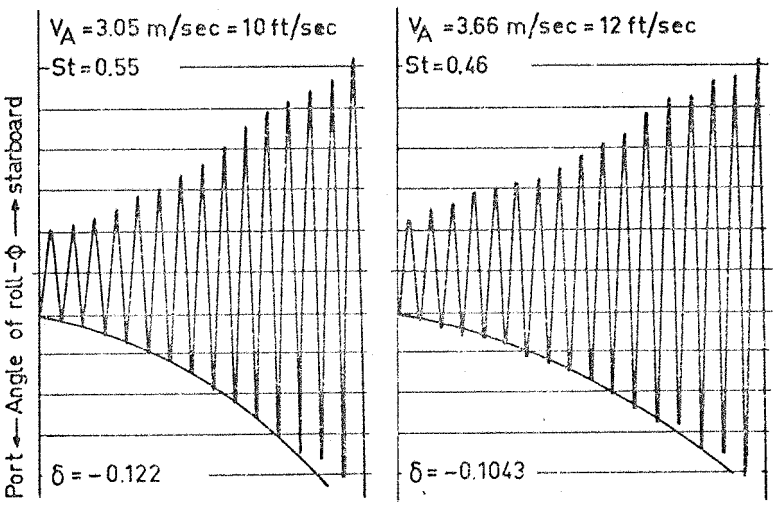

Fig. 29 a. Recorded oscillations of the 1/5 Finn rig.

β_A = 180° }
δ_m = 85° } constant
Magnetic damping = 1.0 }

V_A - variable

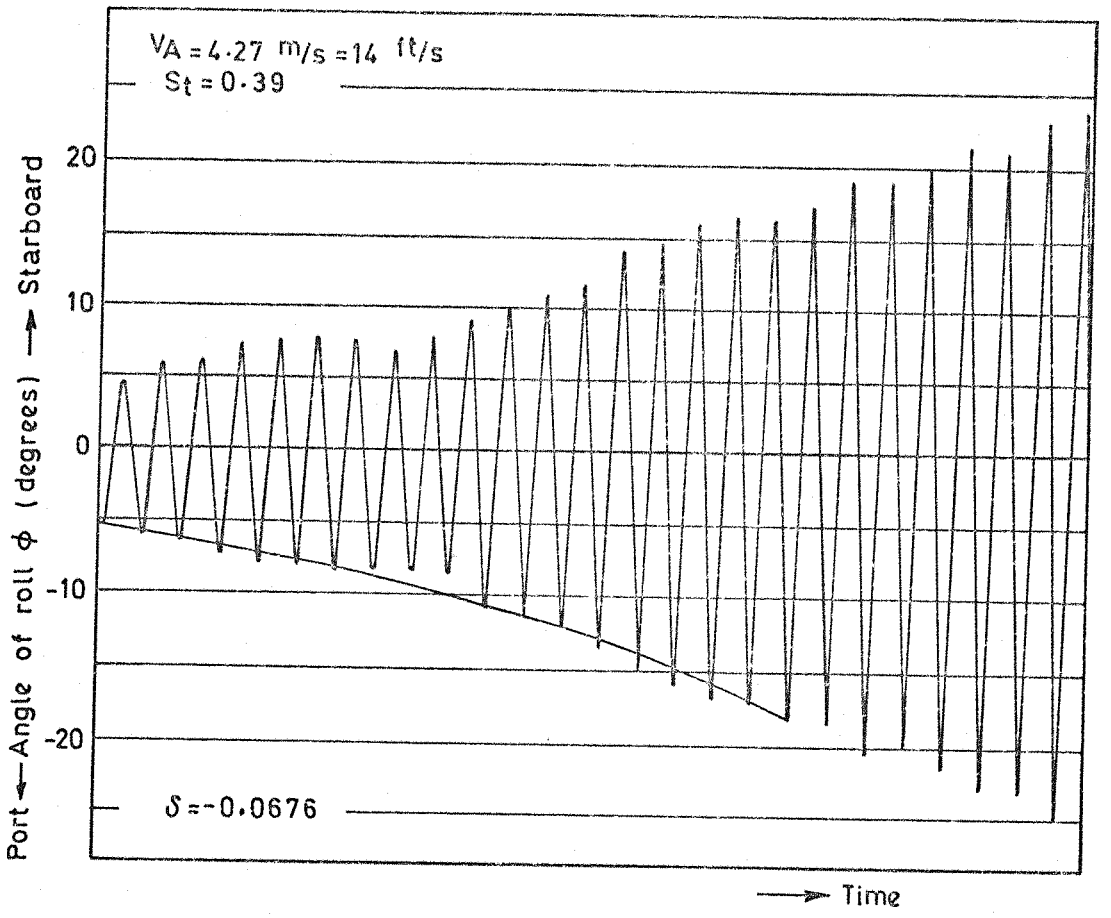

Fig 29b

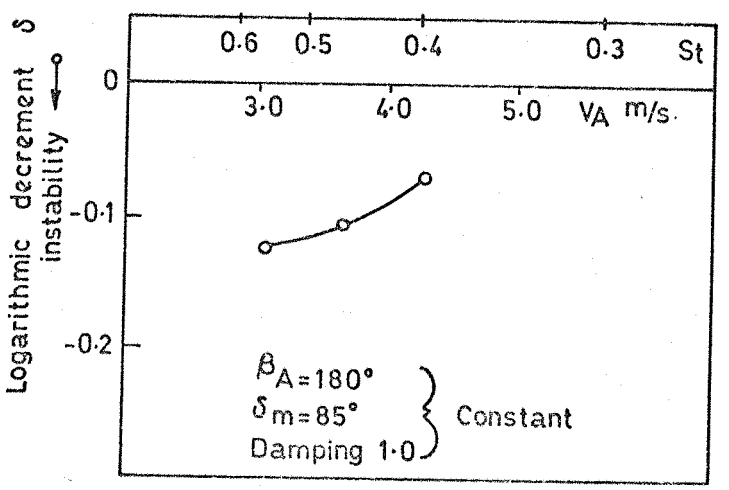

Fig 29c

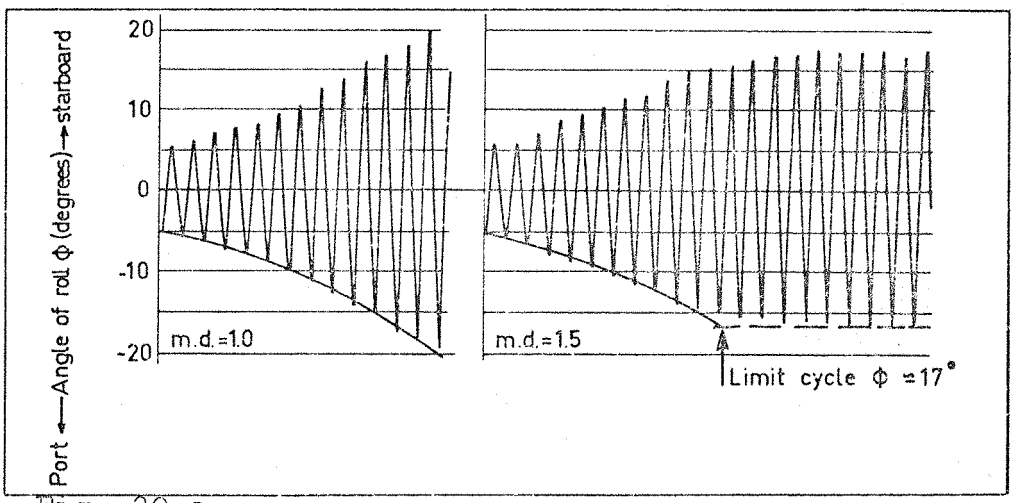

Fig. 30 a

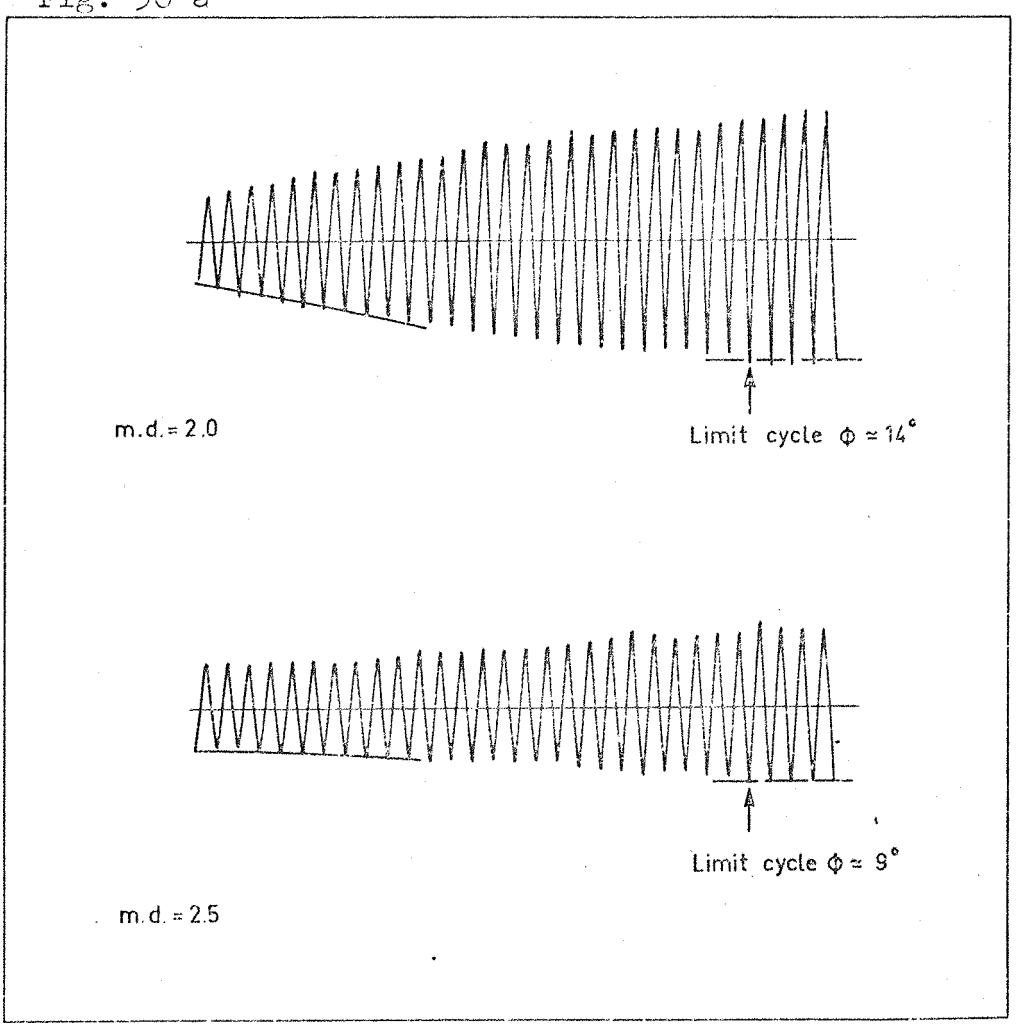

Fig. 30 b

V_A = 3.05 m/sec
S_t = 0.55
β_A = 180°
δ_m = 80°
} constant

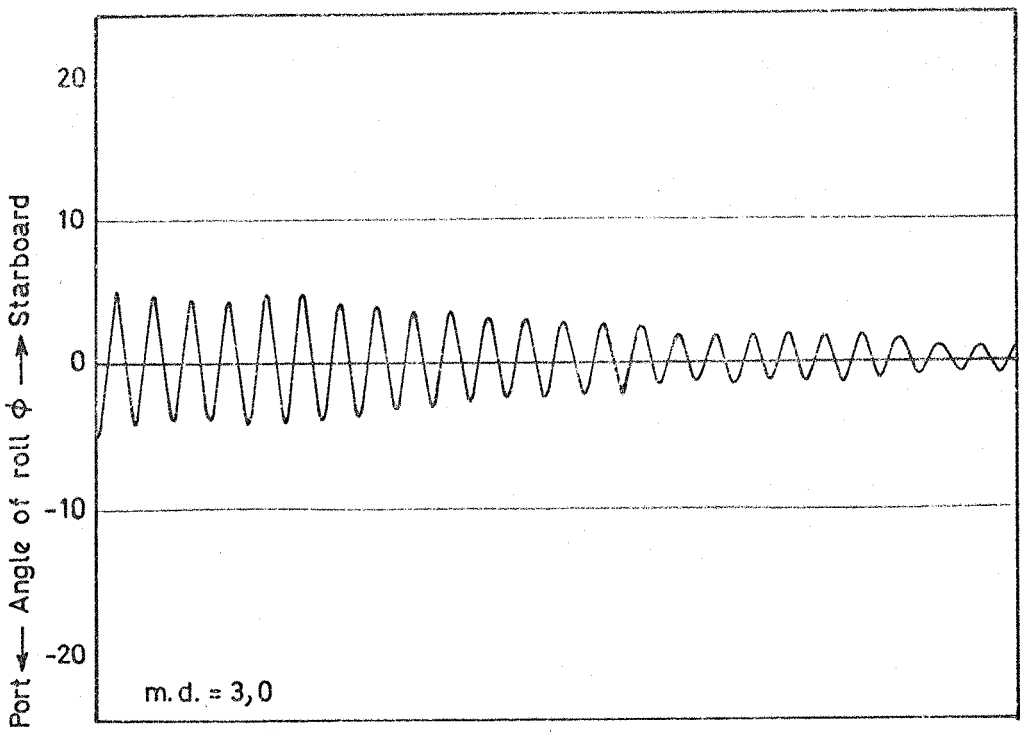

Fig 30c

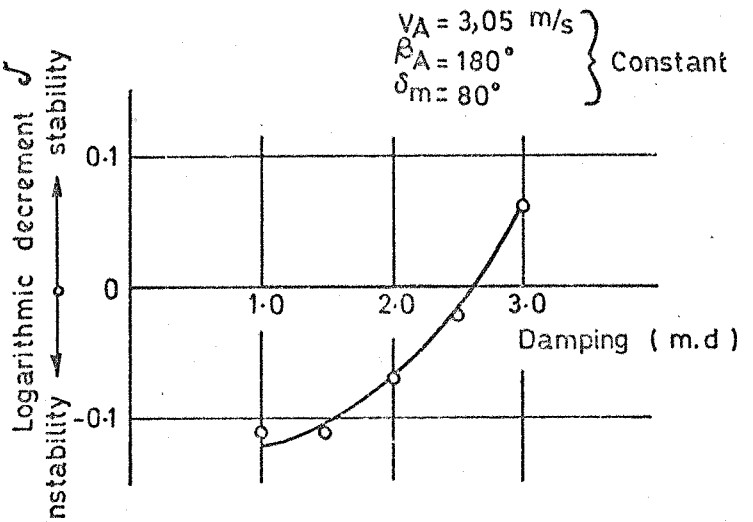

Fig 30d

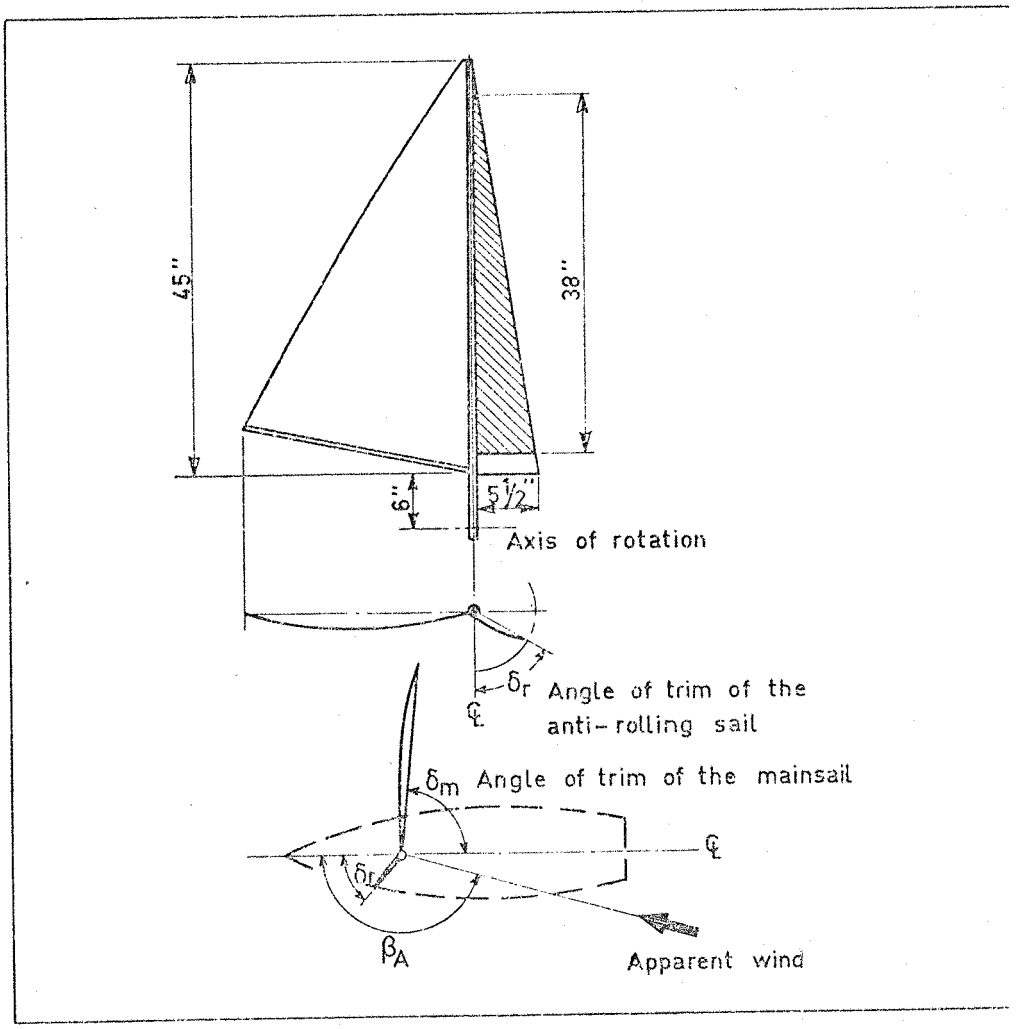

Fig. 31 Anti-rolling sail configuration.

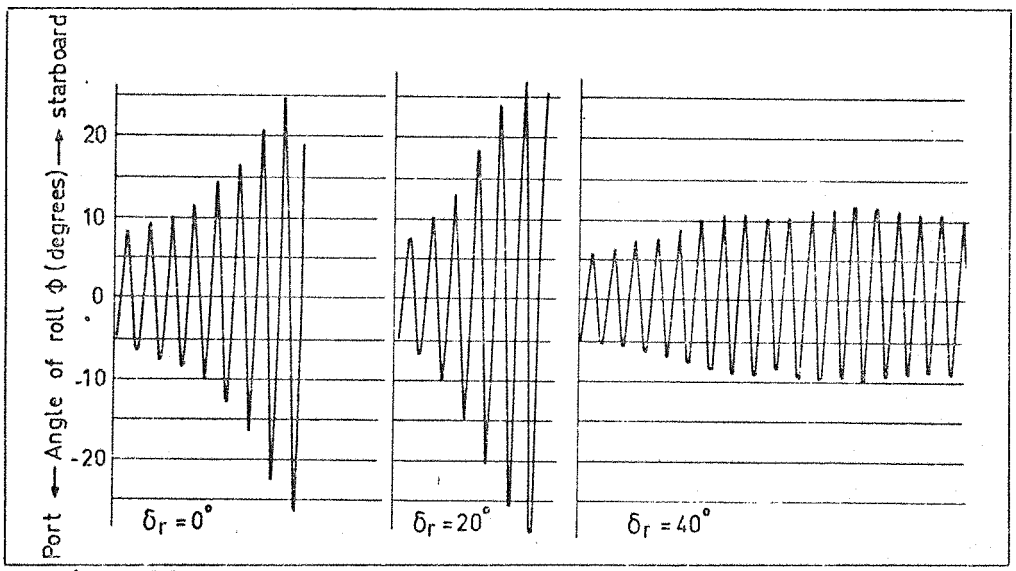

Fig. 32 a

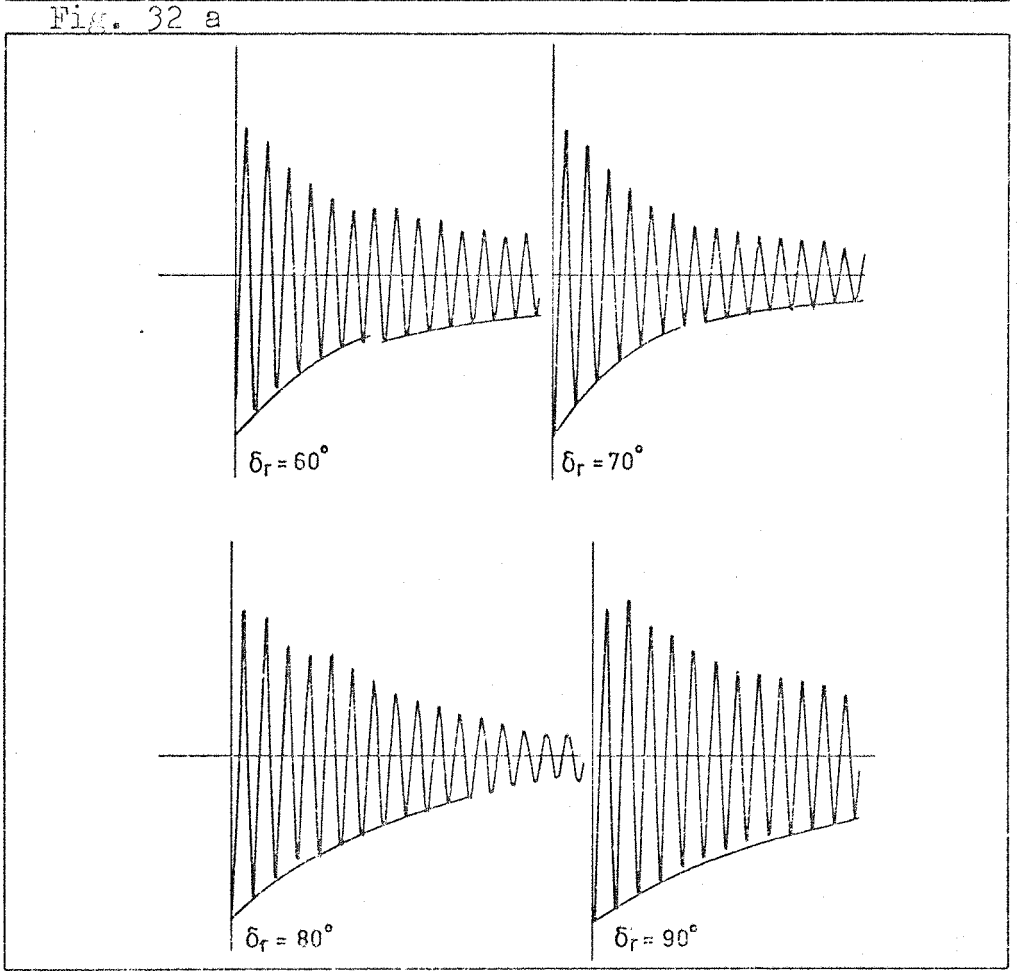

Fig. 32 b Anti-rolling sail.

V_A = 3.05 m/sec
S_t = 0.55
β_A = 180°
δ_m = 85°
} constant

δ_r - variable

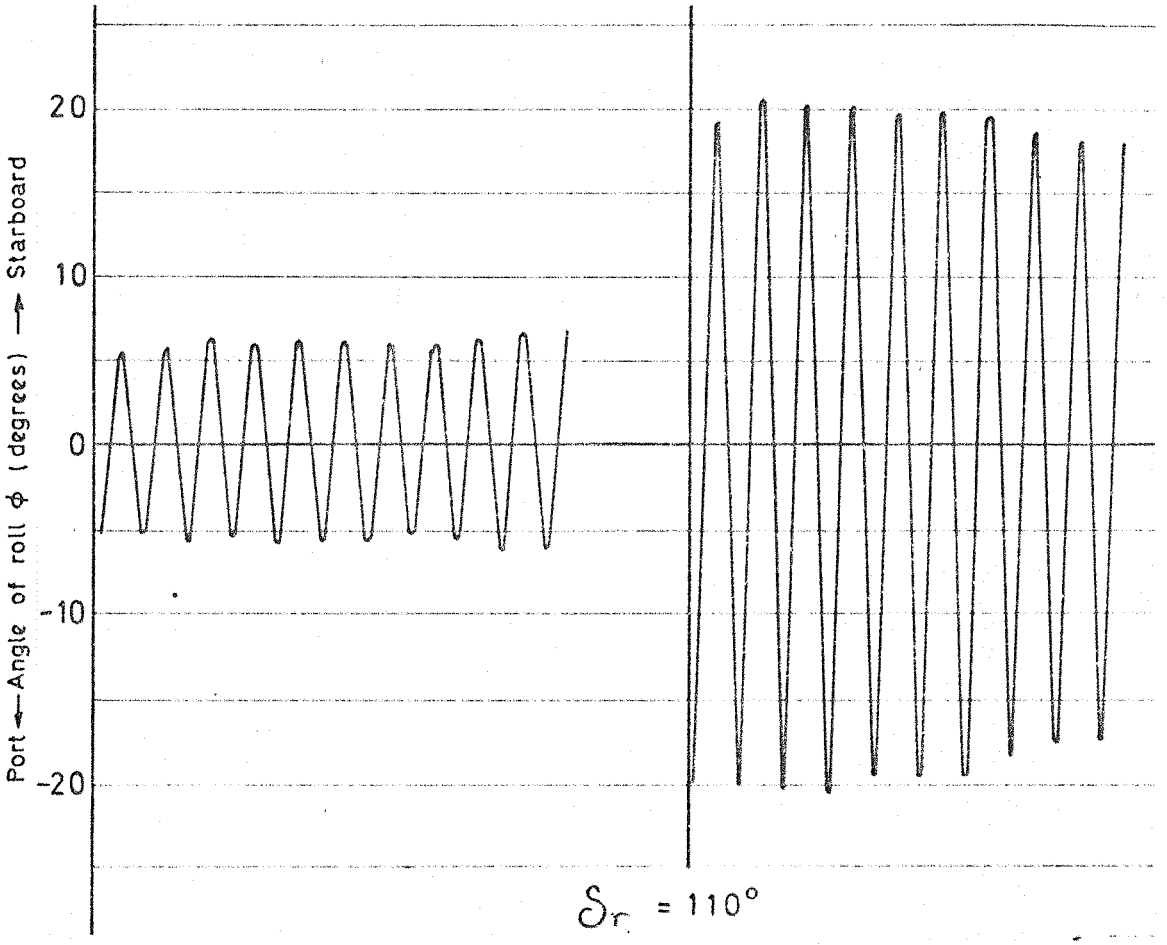

Fig. 32 c

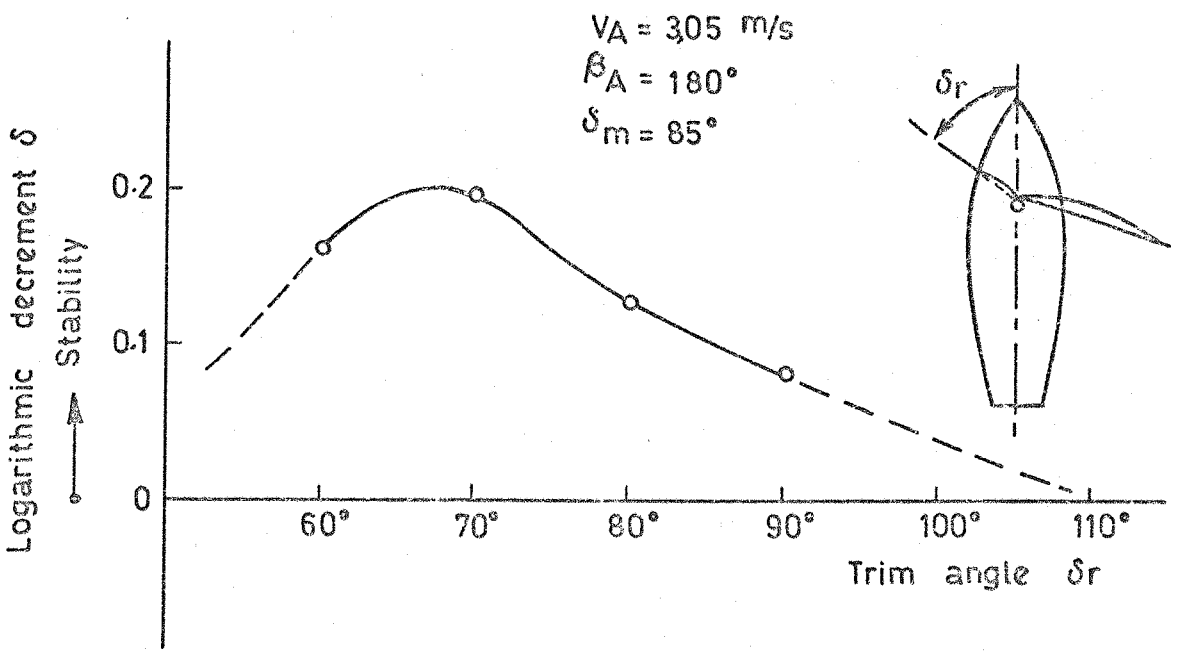

Fig 32d

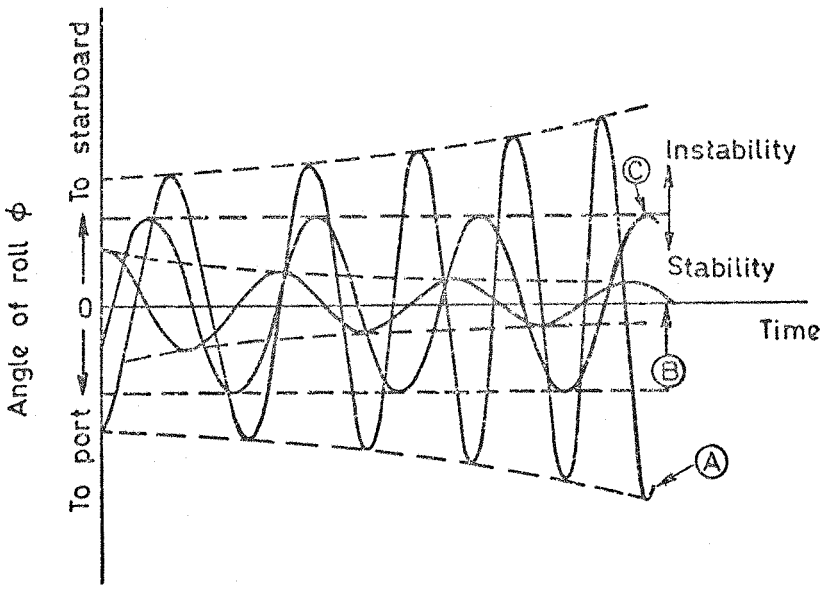
Angle of roll φ
To starboard
0
To port
Instability
Stability
Time
C
B
A

Fig 33

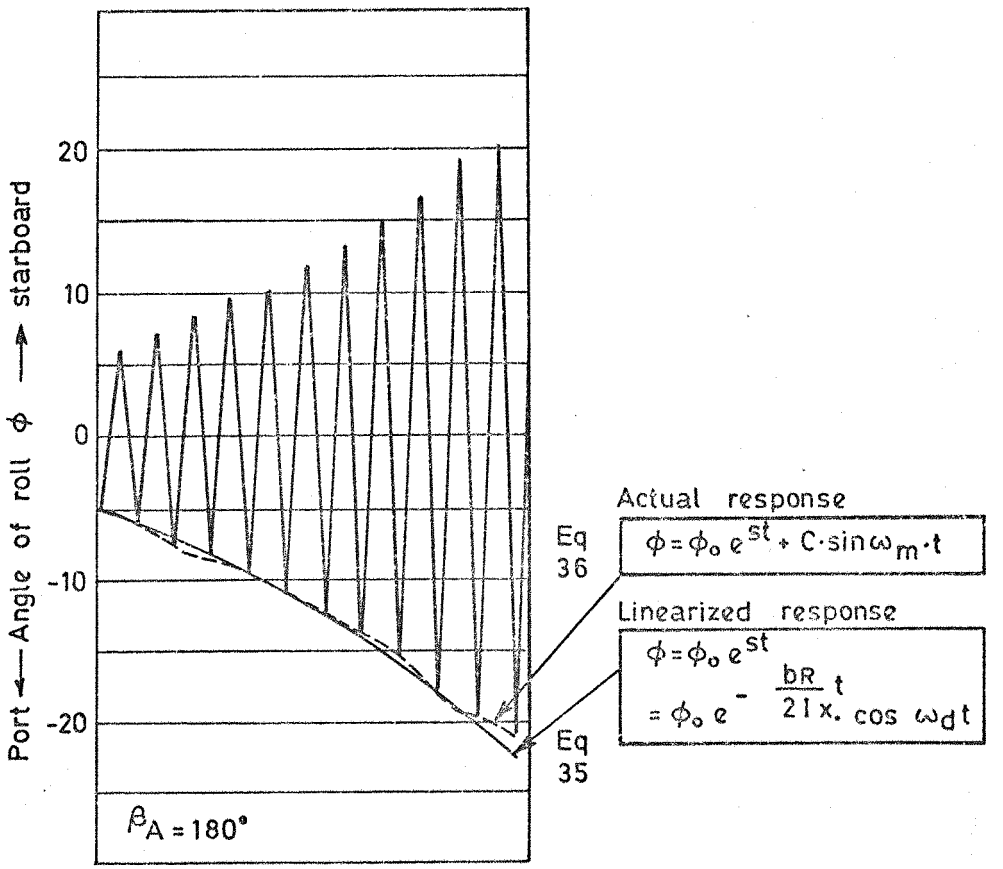
Port ← Angle of roll φ → starboard
20
10
0
-10
-20
$\beta_A = 180°$
Actual response
$\phi = \phi_o e^{st} + C \cdot \sin \omega_m \cdot t$
Eq 36
Linearized response
$\phi = \phi_o e^{st}$
$= \phi_o e^{-\frac{bR}{2Ix.}t} \cos \omega_d t$
Eq 35

Fig 34

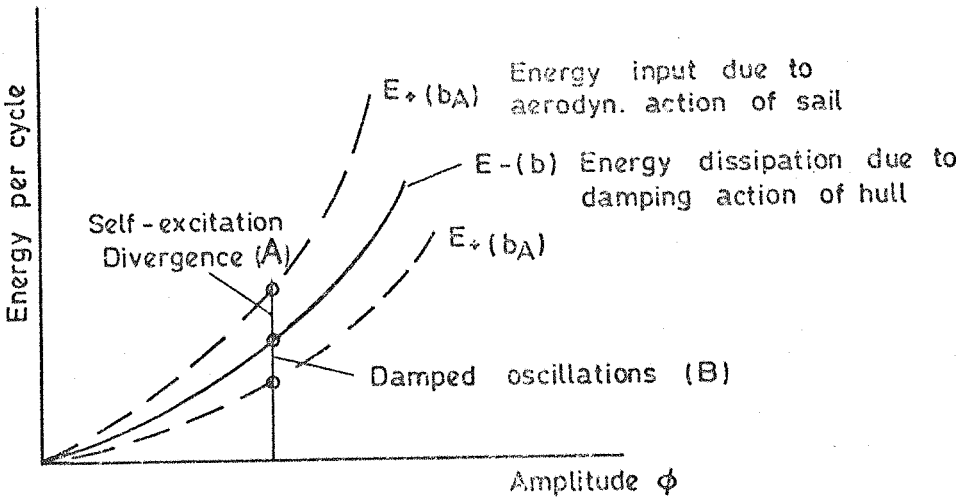

Fig 35

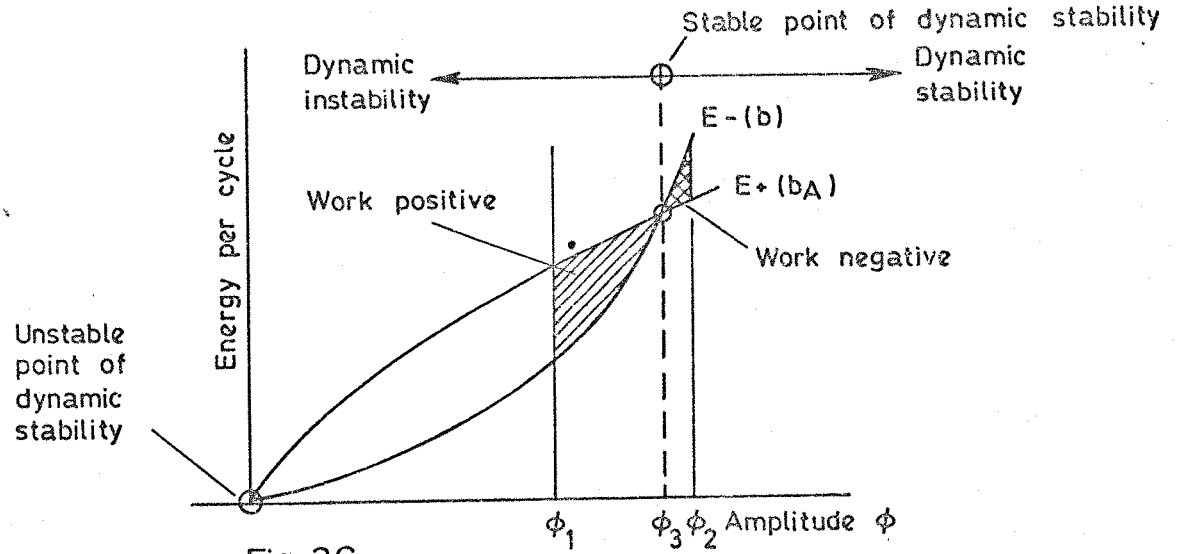

Fig 36

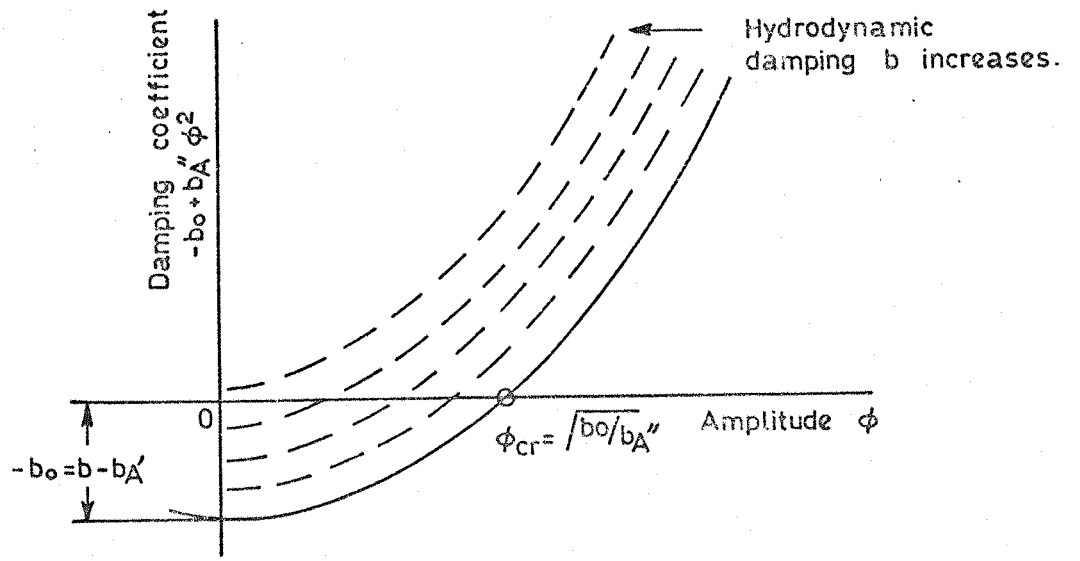

Fig 37

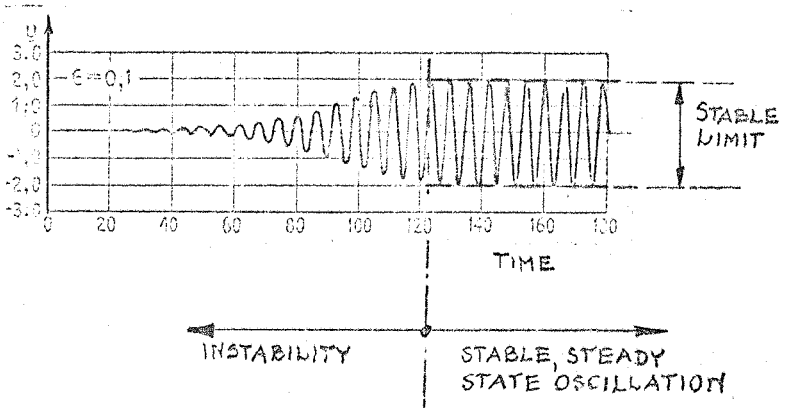

Fig.38. Graphical representation of the solution to the Eq.47, (Appendix - non-dimensional amplitude) showing the non-linear oscillation reaching its final amplitude.

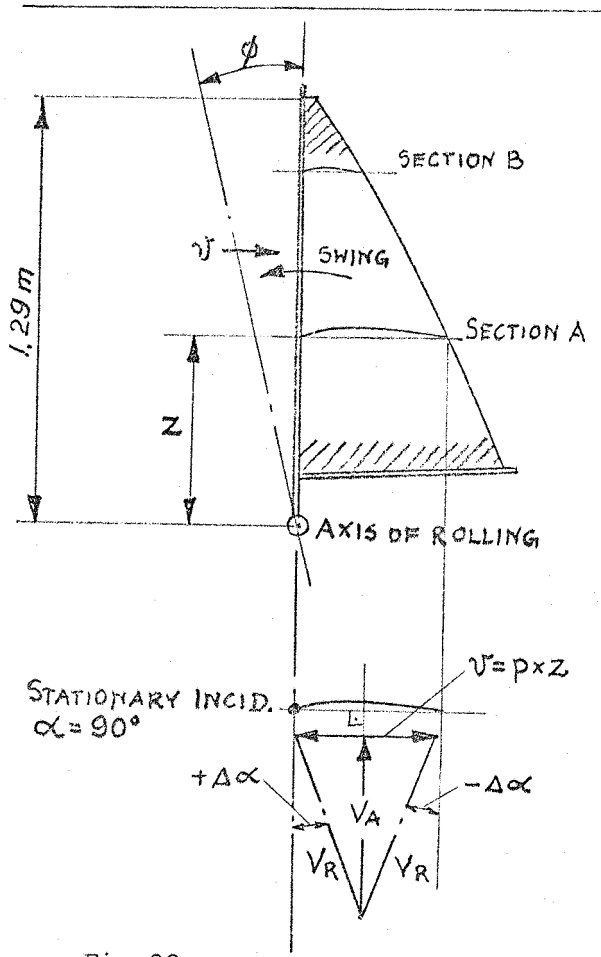

Fig.39.

Circular frequency of damped motion

$$\omega_d = \frac{2\pi}{T} = \frac{2\pi}{1.45} = 4.35 \text{ rad/sec.}$$

Maximum angular velocity at $\phi = 10°$

$$p_m = \omega_d \phi \frac{\pi}{180} = 0.76 \text{ rad/sec.}$$

Maximum linear velocity due to roll

$$v = p_m \cdot z = 0.76\, z$$

Maximum variation in

$$\Delta_m \alpha = tg^{-1} \frac{p_m \cdot z}{V_A}$$

Instant incidence angle

$$\alpha \pm \Delta\alpha$$

APPENDIX

The following brief summary of the chief ideas and formulae of the linear theory of oscillation serves as a reference when analyzing the behaviour of a physical model of the rolling yacht. Although the aerodynamic forcing function, self-excited in character, is in many cases under investigation, non-linear at large amplitudes the solution to the rolling phenomenon can be made on the basis and sequence of linear approximations. The non-linear Van der Pol equation is also introduced as a plausible mathematical representation of the combined, hydro-aerodynamic system simulated by the physical model investigated in the wind tunnel. (Refs.11-15).

A.1. Conservative second order system

A compound pendulum swinging back and forth, shown in Fig.1A, performs sinusoidal oscillations which, with some reservations expressed earlier in §3, may represent the dynamic behaviour of the rolling hull in still water. It can also be used to study the dynamic behaviour of linear systems.

If the damping term and the forcing function are zero, the differential equation of motion for a "free" oscillation is:

$$-W \cdot \ell \sin\phi = I\ddot{\phi} \qquad 1$$

or

$$I\ddot{\phi} + W \cdot \ell \sin\phi = 0 \qquad 2$$

For small values of ϕ, say less than ½ radian, one may approximate $\sin\phi$ by the first term in its series expansion

$$\sin\phi = \phi - \frac{\phi^3}{3!} + \frac{\phi^5}{5!} - \frac{\phi^7}{7!} + \ldots\ldots$$

with an error less than 4 per cent.

Letting $W \cdot l = k$, equation 2 can be written as:-

$$I\ddot{\phi} + K\phi = 0 \qquad 3$$

The constant coefficient of the restoring moment (or stiffness) k is defined by the equation

$$k = \frac{M}{\phi}$$

where M is the moment (in Newton metre) necessary to produce an angular deflection of the pendulum of ϕ radians. The units of k are therefore Newton metre per radian.

Eq.3 may be arranged in the form:

$$\ddot{\phi} + \frac{k}{I}\phi = 0 \qquad 4$$

The solution to this equation is given by:

$$\phi = A\cos\omega_o t + B\sin\omega_o t \qquad 5$$

where A and B are constants of integration which can be established from initial conditions.

$$\omega_o = \pm\sqrt{\frac{k}{I}} \text{ (rad/s)} \qquad 6$$

is called natural circular frequency of the undamped free oscillation, measured in radians per second.

The period of oscillation is given by:

$$T_o = \frac{2\pi}{\omega_o} = 2\pi\sqrt{\frac{k}{I}} \quad \text{(seconds)}$$

The frequency f_o is the reciprocal of the period:-

$$f_o = \frac{1}{T_o} = \frac{\omega_o}{2\pi} = \frac{1}{2\pi}\sqrt{\frac{I}{k}} \quad \text{(cycles/seconds)}$$

If at the beginning of counting time (t = 0), the starting conditions are $\phi = \phi_o$ and $\dot{\phi} = 0$, then the solution to the equation of motion is:-

$$\phi = \phi_o \cos\omega_o t \qquad 7$$

One can find that by giving the pendulum an initial angular velocity $\dot{\phi}_o$ when t = 0 and $\phi_o = 0$, the solution is

$$\phi = \frac{\dot{\phi}_o}{\omega_o} \sin\omega_o t \qquad 8$$

A more general starting condition is to let the pendulum have both angular displacement ϕ_o and angular velocity $\dot{\phi}_o$ when t = 0. The solution:

$$\phi = \phi_o \cos\omega_o t + \frac{\dot{\phi}_o}{\omega_o} \sin\omega_o t \qquad 9$$

is graphically represented in Fig.2A.

A study of Fig.2A suggests that the motion of the pendulum can also be expressed by the equation

$$\phi = \Phi_o \cos(\omega_o t - \eta) \qquad 10$$

where Φ_o and η are the constants which describe the starting conditions.

These constants are obtainable directly from the geometry of Fig.2A.

$$\Phi_o = \sqrt{\phi_o^2 + (\frac{\dot{\phi}_o}{\omega_o})^2} \; ; \quad \eta = \tan^{-1} \frac{\dot{\phi}_o}{\omega_o \phi_o}$$

The angle η, called the phase angle, denotes the angular lag of the motion with respect to the cosine function.

The eq.10 may be rewritten in another form:

$$\phi = \sqrt{\phi_o^2 + (\frac{\dot{\phi}_o}{\omega_o})^2} \cos(\omega_o t - \eta) = \Phi_o(\cos\omega_o t - \eta) \qquad 11$$

The motion as represented in Fig.2A can also be expressed using a complex number notation

$$\vec{\Phi} = \Phi_o e^{i\omega_o t} = \Phi_o(\cos\omega_o t + i\sin\omega_o t) \qquad 12$$

Fig.3A explains, in a "complex plane", the relationship between the exponential function $e^{i\omega_o t}$ and the relevant trignometrical representation of motion.

If the system performs oscillatory motion of the form given by Eq.11, the analysis can be carried out using exponential function taking the real part Re of the solution. The correlation between Eq.11 and 12 is given by:

$$\Phi_o \cos(\omega_o t - \eta) = \mathrm{Re}\left|\Phi_o e^{i(\omega_o t - \eta)}\right| \qquad 13$$

If the initial conditions are such that the phase angle $\eta = 0$, i.e. no initial velocity is given, then Eqs.11 and 13 take forms:-

$$\phi = \phi_o \cos\omega_o t \qquad 11a$$

and

$$\phi_o \cos\omega_o t = \mathrm{Re}\left|\phi_o e^{i\omega_o t}\right| \qquad 13a$$

When Eq.7 is substituted into 3, it yields

$$I(-\phi_o \omega_o^2 \cos\omega_o t) - k(\phi_o \cos\omega_o t) = 0$$

or

$$I\omega_o^2 \phi_o = k\phi_o \qquad 14$$

This shows that the first term, which is the maximum acceleration moment, is equal to the maximum restoring moment.

In a conservative system represented by Eq.2 (without dissipative moments acting), the total energy must be constant, i.e. the total energy = $E_{k_{max}} = E_{p_{max}}$ = const

$$= \tfrac{1}{2} I \dot{\phi}_o^2 = \tfrac{1}{2} k \phi_o^2$$

$$= \tfrac{1}{2} I(-\omega_o \phi_o)^2 = \tfrac{1}{2} k \phi_o^2 \qquad 15$$

The term ϕ_o designates maximum angular displacement.

A.2. Nonconservative second order system

By adding the damping term, which is proportional to the angular velocity $\dot{\phi}$, to the Eq.3 the following equation is obtained:

$$I\ddot{\phi} + b\dot{\phi} + k\phi = 0 \qquad 16$$

The constant damping coefficient b (in Newton-metre-second per radian) is defined by:

$$b = \frac{M}{\dot{\phi}}$$

where M is a moment necessary to produce an angular velocity $\dot{\phi}$.

The dissipation function of the system due to damping b has the dimension of energy per unit time and is given by $\frac{1}{2}b\dot{\phi}^2$.

Following the classical mathematical routine, by assuming that the solution to the homogeneous Eq.16 is of form $\phi = \phi_o e^{st}$ one obtains:

$$I(\phi_o s^2 e^{st}) + b(\phi_o s e^{st}) + k(\phi_o e^{st}) = 0$$

Cancelling out the common factor $\phi_o e^{st}$ the characteristic equation of the system is derived:

$$Is^2 + bs + k = 0 \qquad 17$$

The roots s (eigenvalues) of this characteristic equation may be given in two forms:

$$s_{1,2} = -\frac{b}{2I} \pm \sqrt{\left(\frac{b}{2I}\right)^2 - \frac{k}{I}} \qquad \text{for } \frac{k}{I} \leq \left(\frac{b}{2I}\right)^2 \qquad 17a$$

or

$$s_{1,2} = -\frac{b}{2I} \pm i\sqrt{\frac{k}{I} - \left(\frac{b}{2I}\right)^2} \qquad \text{for } \frac{k}{I} \geq \left(\frac{b}{2I}\right)^2 \qquad 17b$$

$$= -\frac{b}{2I} \pm i\sqrt{\omega_o^2 - \left(\frac{b}{2I}\right)^2}$$

depending on the relative values of I, b, and k. It is convenient to maintain the expression under the radicals in a more lucid form by factoring out $\sqrt{-1} = i$.

The value of the damping coefficient b, which makes the radical of Eq.17a,b zero, is significant and is called the critical damping (b_c). Substituting b_c for b yields:

$$\frac{b_c}{2I} = \sqrt{\frac{k}{I}} = \omega_o \qquad \text{or} \qquad b_c = 2I\omega_o \qquad 18$$

Introducing for convenience shorthand symbols:-

$$\sigma = \frac{b}{2I} \; ; \quad \sigma = \xi \cdot \omega_o$$

$$\omega_d = \sqrt{\omega_o^2 - \sigma^2} = \omega_o\sqrt{1 - \xi^2}$$

$$\xi = \frac{b}{b_c} = \frac{\sigma}{\omega_o} = \frac{b}{2I\omega_o} \qquad 19$$

the Eq.16 can be expressed:

$$\ddot{\phi} + 2\xi\omega_o\dot{\phi} + \omega_o^2\phi = 0 \qquad 20$$

The corresponding roots (Eq.17a and b) may be modified as follows:

$$s_{1,2} = (-\xi \pm \sqrt{\xi^2 - 1})\omega_o = -\sigma \pm \omega_o\sqrt{\xi^2 - 1} \qquad 21a$$

which is applicable in the case when the actual damping b is larger than the critical b_c, so $\xi > 1$ and the system is overdamped; or

$$s_{1,2} = (-\xi \pm i\sqrt{1 - \xi^2})\omega_o = -\sigma \pm i\omega_o\sqrt{1 - \xi^2} \qquad 21b$$

which is applicable when damping is less than critical and $\xi < 1$, i.e. the system is underdamped.

Since the rolling yacht, considered as a dynamic system, is never overdamped, one may limit attention to the underdamped motion, including the marginal case when the damping ratio $\xi = \frac{b}{b_c} = 1$

The standard solution to Eq.16 can also be written

$$\phi = Ae^{s_1 t} + Be^{s_2 t} \qquad 22$$

where s_1 and s_2 are the two roots given by Eq.21b and A and B are two constants depending on the initial conditions of motion. A substitution of the roots to Eq.22 and a simple transformation give:

$$\phi = \phi_o e^{-\xi\omega_o t}\cos(\sqrt{1 - \xi^2}\,\omega_o t - \eta) \qquad 22a$$

if $\eta = 0$

$$\phi = \phi_o e^{-\xi\omega_o t} \cos\sqrt{1 - \xi^2}\ \omega_o t \qquad 23$$

or

$$\phi = \phi_o e^{-\sigma t} \cos\omega_d t = \phi_o e^{-\frac{b}{2I}t} \cos\omega_d t \qquad 24$$

The damped oscillation is therefore made up of the product of two terms or curves as shown in Fig.4A.

The frequency ω_d of the damped system is less than that of ω_o, of an undamped system, and is given by the factor $\sqrt{1 - \xi^2}$ i.e.

$$\omega_d = \omega_o\sqrt{1 - \xi^2} = \sqrt{\frac{k}{I} - \left(\frac{b}{2I}\right)^2} \qquad 25$$

Fig.5A indicates the manner in which the frequency ratio ω_d/ω_o varies with damping ratio $^b/_{b_c} = \xi$.

The natural period of damped oscillation is

$$T_d = \frac{2\pi}{\omega_d} = \frac{2\pi}{\omega_o\sqrt{1 - \xi^2}} \qquad 26$$

Damping is thus seen to have the effect of reducing the circular frequency and lengthening the period of motion. These effects are however very small as long as the damping is not too severe.

The values of roots given in Eq.21b for an underdamped system may graphically be represented in the complex plane known as s- plane (Fig.6A).

The length of the complex s-vector (phasor) is ω_o and the angle between the phasor and i-axis is the angle whose sine is $\xi = \frac{\sigma}{\omega_o}$. One can see that σ is a number related to s by $Re|s| = -\sigma$ and similarly ω_d is related to

s by $J_m|s| = \pm i\omega_d$. In other words, in the case of an undamped system, the solution of the form e^{st} produces characteristic equation whose roots $s = -\sigma \pm i\omega_d$ are complex numbers. The real part σ specifies the damping rate and ω_d is the damped frequency in radians per sec.

The corresponding relationship between the s-plane and the time response for various damping is illustrated in Fig.7A. It is seen that the damping ratio ξ is a very convenient index of system stability. If ξ is negative the system is unstable and the amplitude grows without bound. When ξ is zero, the system is just neutrally stable (the amplitude neither growing nor decaying) and as ξ is increased towards 1, the relative damping of the system increases. The quantity $1/\sigma$ indicates the time required for the motion to damp to $1/e$th its original value. This time

$$T = \frac{1}{\sigma}$$

is known as the damping time constant of the system. Fig.8A represents a plot in which miniature pictures of time response are spotted on the s-plane, each at the coordinates of its characteristics.* On the real axis the motion is always a pure exponential; the further from the origin the faster is the response (2, 3, 4). In the right half-plane the motion grows, therefore the system is unstable (5). Thus, the fundamental criterion of stability in a linear system is that the roots of the characteristic equation (Eq.27) have a negative real part, thereby producing decaying oscillation.

Along the imaginary axis the motion is always an undamped oscillation, the further from the origin, the higher the frequency (6, 7, 12). A constant distance from

---

*Fig.7A and 8A adopted from "Dynamics of Physical Systems" by R.H. Cannon - MacGraw Hill - 1967.

the real axis (12, 13, 14, 15) means a constant frequency ω, but variable decay time or, in the right half-plane (11) growth time.

A constant distance from the imaginary axis (3, 9, 14) means a constant decay time $1/\sigma$ but variable frequency. Along the straight ξ line (8, 14) the number of cycles required to damp the oscillation is constant, but in general, the further from the origin, the faster the whole response.

The rate of decay of the damped free oscillation can be determined from the amplitudes of any two consecutive peaks. This rate may be measured by the ratio between the maximum displacement ϕ_t at the time - t and the displacement ϕ_{t+T_d} later when the cycle has been completed.

Modifying Eq.23 one can write:

$$\frac{\phi_t}{\phi t+T_d} = \frac{\phi_o e^{-\xi\omega_o t}.\cos\omega_d t}{\phi_o e^{-\xi\omega_o (t+T_d)}.\cos(t + T_d)} \quad ;$$

since $\omega T = 2\pi$

and $\cos(\alpha + 2\pi) = \cos\alpha$

then

$$\frac{\phi_t}{\phi_{t+T_d}} = e^{\xi\omega_o T_d}$$

and

$$\ell n\left(\frac{\phi_t}{\phi_{t+T_d}}\right) = \ell n(e^{\xi\omega_o T_d}) = \xi\omega_o T_d = \delta \qquad 28$$

Logarithmic decrement of motion denoted by δ can be expressed by:

$$\delta = \frac{2\pi\xi}{\sqrt{1 - \xi^2}}$$

therefore

$$\frac{\phi_t}{\phi_{t+T_d}} = e^{\delta} \qquad 29$$

Since the period of damped oscillation is given by:

$$T_d = \frac{2\pi}{\omega_o \sqrt{1 - \xi^2}}$$

then

$$\delta = 2\pi\xi \qquad 30$$

For the oscillating system which has small damping, (Fig.4A) there is another way of determining the logarithmic decrement from the time response curve namely:

$$\delta = \log\left(\frac{\phi_t + \Delta\phi}{\phi_t}\right) = \log\left(1 + \frac{\Delta\phi}{\phi_t}\right) = \frac{\Delta\phi}{\phi_t} + \tfrac{1}{2}\left(\frac{\Delta\phi}{\phi_t}\right)^2 + \frac{1}{3}\left(\frac{\Delta\phi}{\phi_t}\right)^3 + \ldots\ldots$$

If $\frac{\Delta\phi}{\phi_t}$ is small, the higher order terms may be dropped and

$$\delta = \frac{\Delta\phi}{\phi_t} \qquad 30a$$

Thus the logarithmic decrement is approximately equal to the fractional decrease (or increase in case increment) in amplitude during one cycle of the oscillation; with better approximation:

$$\delta = \frac{2\Delta\phi}{\phi_t + \phi_t + 2\pi} \qquad 30b$$

According to Eq.15 the total energy of the system, in one of

its extreme positions with zero angular velocity:-

$$E_{T_1} = \tfrac{1}{2}K\phi_t^2$$

One cycle later this energy will be:

$$E_{T_2} = \tfrac{1}{2}K(\phi_t - \Delta\phi)^2$$

Therefore energy loss per cycle is

$$\Delta E_T = E_{T_1} - E_{T_2} = \tfrac{1}{2}K\phi_t^2 - \tfrac{1}{2}K\phi_t + K\phi_t\Delta\phi - \tfrac{1}{2}(\Delta\phi)^2$$

This energy loss can be expressed as a fraction of the total energy of the system as follows:-

$$\frac{\Delta E_T}{E_T} = 2\,\frac{\Delta\phi}{\phi_t} - \left(\frac{\Delta\phi}{\phi_t}\right)^2$$

If the damping is small the square term can be dropped. Hence:-

$$\frac{\Delta E_T}{E_T} \simeq 2\left(\frac{\Delta\phi}{\phi_t}\right) \simeq 2\delta \qquad 30c$$

Thus for small damping the fraction of energy lost per cycle is approximately equal to twice the logarithmic decrement.

Introducing logarithmic decrement into Eq.23 yields:

$$\phi = \phi_o e^{-(\delta/2\pi)\omega_o t}\cos\omega_d t \qquad 31$$

If we assume that the ratio of the two consecutive peaks of amplitude of a rolling yacht is

$$\frac{\phi_t}{\phi_{t+T_d}} = 2,0$$

i.e. the yacht reduces the rolling amplitude in a round swing by two, then:

$$\delta = \ln 2,0 = 0.693$$

Therefore the damping ratio

$$\xi = \frac{\delta}{2\pi} \simeq \frac{0,693}{2\pi} \simeq 0.11$$

and

$$\frac{\phi_{t+T_d}}{\phi_t} = e^{-2\pi\xi} = e^{-0.693} = 0.5$$

The effect of damping on frequency and period is given by the following equations:

$$\omega_d = \frac{\omega_o}{\sqrt{1 + (\frac{\delta}{2\pi})^2}} \qquad 32$$

$$T_d = T_o \sqrt{1 + (\frac{\delta}{2\pi})^2} \qquad 33$$

For the case given above (δ = 0,693) the relevant values

of ω_d and T_d are:

$$\omega_d = \frac{\omega_o}{\sqrt{1.012}} = \frac{\omega_o}{1.006} = 0.994\omega_o$$

and

$$T_d = 1{,}006T_o$$

Since the magnitudes of ω_d and T_d differ from ω_o, T_o less than 1 per cent, the influence of a moderate amount of damping on the frequency and period of oscillation can be neglected in rolling investigation.

A.3. Excited Oscillation

The oscillation considered in §A1 and A2 can be defined as being "free", i.e. controlled only by the moments arising from inertia, stability and damping incorporated internally in the system. If such a free or "natural" oscillation is interfered with forces or moments external to the system, the resultant oscillations are usually defined to be "excited" or "forced".

In the simplest case, the exciting moments are independent of the natural behaviour of the system, and are functions of time alone. By adding a forcing non-homogeneous moment to the homogeneous Eq.16 the equation of motion becomes:

$$I\ddot{\phi} + b\dot{\phi} + c\phi = M(t) \qquad 34$$

An external moment does not prevent the system from oscillating in its own natural way, but gives the system supplementary

displacement represented by an independent additive term in the solution to the Eq.34.

The complete solution ϕ is thus made up of term ϕ_h which represents the solution of the homogeneous part of Eq.34 and of a term ϕ_p - the <u>particular solution</u> which supplements ϕ_h in such a way that

$$\phi = \phi_h + \phi_p$$

satisfies completely Eq.34, i.e. with the non-homogeneous part present. If the forcing function M(t) is harmonic in character, of type $M\cos\omega_f t$, where ω_f is forcing frequency, the complete solution to Eq.34 can be written as:
(transient part) + (permanent part)

$$\phi = \phi_h + \phi_p = e^{-\sigma t}\phi_o \cos\omega_d t + \Phi_{max}\cos(\omega_f t + \lambda) \qquad 35$$

where Φ_{max} is the maximum amplitude of forcing function and λ is the phase angle in an exciting term.

$$\lambda = \tan^{-1}\left(\frac{b\omega_f}{K - I\omega_f^2}\right) \qquad 36a$$

Or, since $\frac{K}{I} = \omega_o^2$ and $(b/K)\omega_f = 2(b/b_c)\left(\frac{\omega_f}{\omega_o}\right)$

then

$$\lambda = \tan^{-1}\left[\frac{2b/b_c \,\frac{\omega_f}{\omega_o}}{1 - \left(\frac{\omega_f}{\omega_o}\right)^2}\right] \qquad 36b$$

Introducing shorthand notation

$$\xi = {}^{b}/_{b_c} \qquad \text{and} \qquad \Omega = \frac{\omega_f}{\omega_o}$$

$$\lambda = \tan^{-1} \frac{2\xi\Omega}{1 - \Omega^2} \qquad 36c$$

Of the two parts ϕ_h and ϕ_p that make ϕ, the first, representing homogeneous part of oscillation with frequency ω_d, fades out with time on account of the damping term $e^{-\sigma t}$. This part is therefore called transient. The second part ϕ_p represents a simple harmonic motion in the rhythm of excitation. This part of the motion may continue indefinitely without change and is accordingly called permanent.

In the case when the time dependent driving function M(t) of Eq.34 is not simple harmonic but periodic, it can be expressed in the form of Fourier's series of period $T = {}^{2\pi}/_{\omega}$

$$M(t) = M_o + M_1 \sin(\omega t + \lambda_1) + M_2 \sin(2\omega t + \lambda_2) + \ldots$$

$$= M_o + \Sigma_1^{\infty} M_n \sin(n\omega t + \lambda_n) \qquad 37$$

The frequency ω is called the fundamental and the frequencies 2ω, 3ω, ...$n\omega$ are harmonics.

Due to the superimposition the combine motion, as indicated by Eq.35, has a complicated and irregular character, particularly before the transient part died out. The amplitude of oscillation will increase when the displacements brought about by the "free" and "forced" oscillations have the same sign and decrease when their signs are opposite. In other words, on account of the difference between circular frequencies ω_d and ω_f, the two oscillations pass

through cycles of getting into the same phase and getting out of the phase, thus alternatingly adding to each other or subtracting from each other. The periodic swellings and subsidences through which the resultant oscillation passes are known as beats.

The frequency of beats f_{beat} is the frequency of one wave with respect to the other, or

$$\pm \frac{\omega_f - \omega_d}{2\pi} = \frac{\Delta\omega}{2\pi} \text{ beats per sec} \qquad 38$$

the proper sign being chosen to obtain always the positive beat frequency. The relevant period of beats

$$T_{beat} = \frac{2\pi}{\Delta\omega} \qquad 39$$

The smaller the difference $\Delta\omega$ between the frequencies ω_d and ω_f of the two components of motion, the longer will be the time interval in beats.

Fig.9A represents the beat phenomenon in the forced oscillation starting from 'out of phase' condition for undamped (a) and damped (b) systems.

When damping is present the total amplitude peaks are never quite as high as in the absence of damping, and as the time goes on the peaks fall and the valleys rise on the envelope curve towards the amplitude level governed by the permanent motion ϕ_p. This is shown in Eq.35 and Fig.9A(b).

One may say that the function ϕ_h is, in a sense, a kind of cushion that carries ϕ through its transition from starting conditions to the ultimate steady state corresponding to ϕ_p. The initial response of a system to an excitation is a mixture of an oscillation in the natural rhythm of the system and of an oscillation in the rhythm of the forcing function.

A.4. Non-linear oscillation. Van der Pol equation with non-linear damping

The Eq.41 derived in §6.2 and rewritten below:

$$I_x \cdot \ddot{\phi} - (b_o - b_A'' \phi^2)\dot{\phi} + K\phi = 0 \quad \text{(rewritten)} \quad 41$$

can be simplified by reducing the number of coefficients. There are four, I_x, b_o, b_A'' and k at the moment.

Dividing Eq.41 by I_x and introducing the notation $k/I_x = \omega_o^2$ yields:

$$\ddot{\phi} - \left(\frac{b_o}{I_x} - \frac{b_A''}{I_x}\phi^2\right)\dot{\phi} + k\phi = 0 \qquad 42$$

Remaining three coefficients can be reduced to two by making the variable time t relative to which the differentiation is performed, i.e. $\frac{d\phi}{dt}$ and $\frac{d^2\phi}{dt^2}$, dimensionless. It can be done by measuring the time in terms of a unit inherent in the system, for example $T/2\pi$. Denoting the new time by t' and the old time by t, one can write

$$t' = \frac{t}{T/2\pi} = \omega_o t \qquad 43$$

The new differential coefficients can be expressed as follows:

$$\left.\begin{aligned} \frac{d^2\phi}{dt^2} &= \frac{d^2\phi}{dt'^2} \cdot \frac{t'^2}{t^2} = \omega_o^2 \ddot{\phi} \\ \frac{d\phi}{dt} &= \omega_o \dot{\phi} \end{aligned}\right\} \qquad 44$$

Substituting Eqs.43 and 44 into Eq.42 and dividing the resulting

equation by ω_o^2 yields

$$\ddot{\phi} - \frac{b_o}{I_x \omega_o}\left(1 - \frac{b_A''}{b_o}\phi^2\right)\dot{\phi} + \phi = 0 \qquad 45$$

where the dots now signify the differentiation with respect to the non-dimensional time t'.

In a similar way the amplitude ϕ can be made non-dimensional if it is measured in a unit inherent in the equation. Such a convenient unit is indicated in §6.2. Fig.37, namely the amplitude $\phi_{cr} = \sqrt{b_o/b_A''}$ for which the positive and negative damping moments balance each other.

Denoting the new non-dimensional amplitude by

$$y = \frac{\phi}{\sqrt{b_o/b_A''}} \qquad 46$$

and substitute it into Eq.45, the well known Van der Pol equation is derived:-

$$\ddot{y} - \varepsilon(1 - y^2)\dot{y} + y = 0 \qquad 47$$

where the single parameter $\varepsilon = b_o/I_x\omega_o$, is in fact the ratio between the maximum negative damping moment and the maximum stability moment, i.e.

$$\varepsilon = \frac{b_o}{I_x \omega_o} = \frac{\text{negative damping moment}}{\text{stability moment}} \qquad 48$$

This ratio has an important physical significance and can be

derived as follows,

assuming that $\phi = \phi_o \sin\omega_o t$ and $\dot{\phi} = \phi_o \omega_o \cos\omega_o t$

one can find that the maximum negative damping moment which occurs at $\dot{\phi}_{max}$ ($\phi = 0$) is

$$b_o \dot{\phi}_{max} = b_o \phi_o \omega_o \qquad 49$$

The maximum stability moment can be expressed as

$$k\phi_{max} = k\phi_o = \frac{k\, I_x}{I_x} \phi_o = \omega_o{}^2 I_x \phi_o \qquad 50$$

Dividing Eq.49 by Eq.50 verifies Eq.48. The approximate solution to Eq.47 given by Van der Pol (38) may be written:

$$y = \frac{2\sin(t' + \eta)}{\sqrt{1 + e^{-\varepsilon(t' + c)}}} \qquad 51$$

where η and c are constant depending on starting conditions. It is assumed that $\varepsilon << 1.0$.

An inspection of the equation reveals that the amplitude of oscillation increases at first with time but finally reaches the steady value $y_o = 2$ (the denominator, after a certain time, approaches 1). This conclusion derived from Eq.51 can be confirmed by the energy consideration. When amplitudes are smaller than the final one, the damping moment, which equals $\varepsilon(1 - y^2)\dot{y}$, puts energy into the system. For amplitudes greater than the final one, the damping dissipated energy. Therefore, at the final amplitude, the energy input for a full cycle is zero i.e.

$$0 = \int_o^{2\pi} \varepsilon(1 - y^2)\dot{y}^2 dt \qquad 52$$

Since $y = y_o \sin\omega_o t = y_o \sin t'$ (see Eq.43)

Then

$$0 = \int_0^{2\pi} (1 - y_o^2 \sin^2 t') y_o^2 \cos^2 t' \, dt$$

or

$$y_o^2 = \frac{\int_0^{2\pi} \cos^2 t' \, dt'}{\int_0^{2\pi} \sin^2 t' \cos^2 t' \, dt'} = \frac{\pi}{\pi/4} = 4 \qquad 53$$

By converting the non-dimensional amplitude y into the dimensional one ϕ and introducing again the dimensional time t instead of t', one can modify the Eq.51 into

$$\phi = \frac{2\sqrt{b_o/b''_A} \cdot \sin(\omega_o t + \eta)}{\sqrt{1 + e^{-\varepsilon(\omega_o t + c)}}} \qquad 54$$

From this one may infer that the final stable amplitude is twice as large as the critical amplitude

$$\phi_{cr} = \sqrt{b_o/b''_A}$$

at which the damping moment just becomes zero.

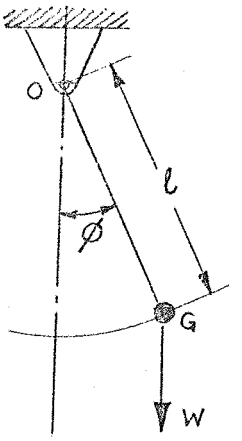

FIG. 1A.

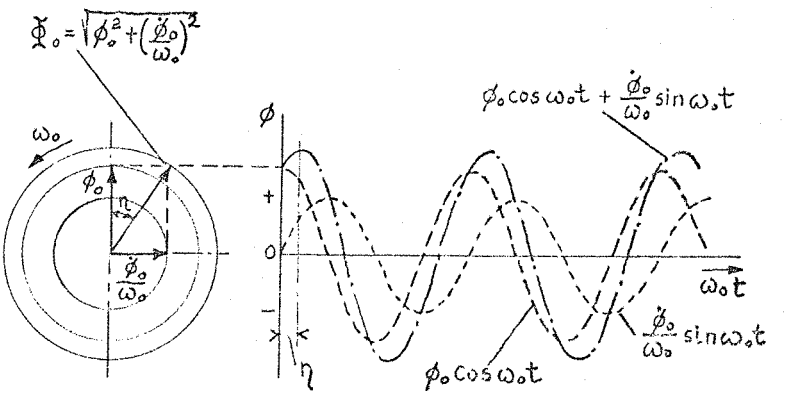

FIG. 2A.

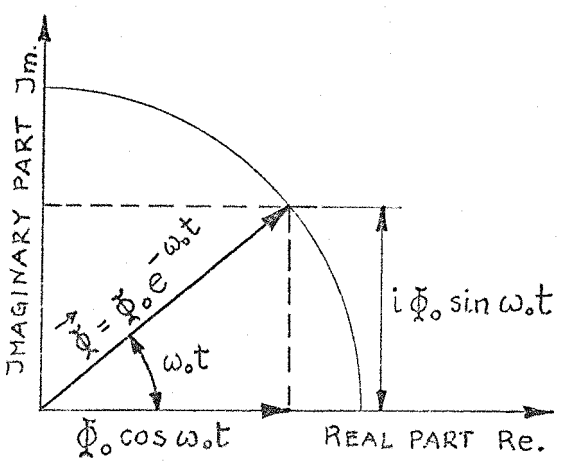

FIG. 3A.

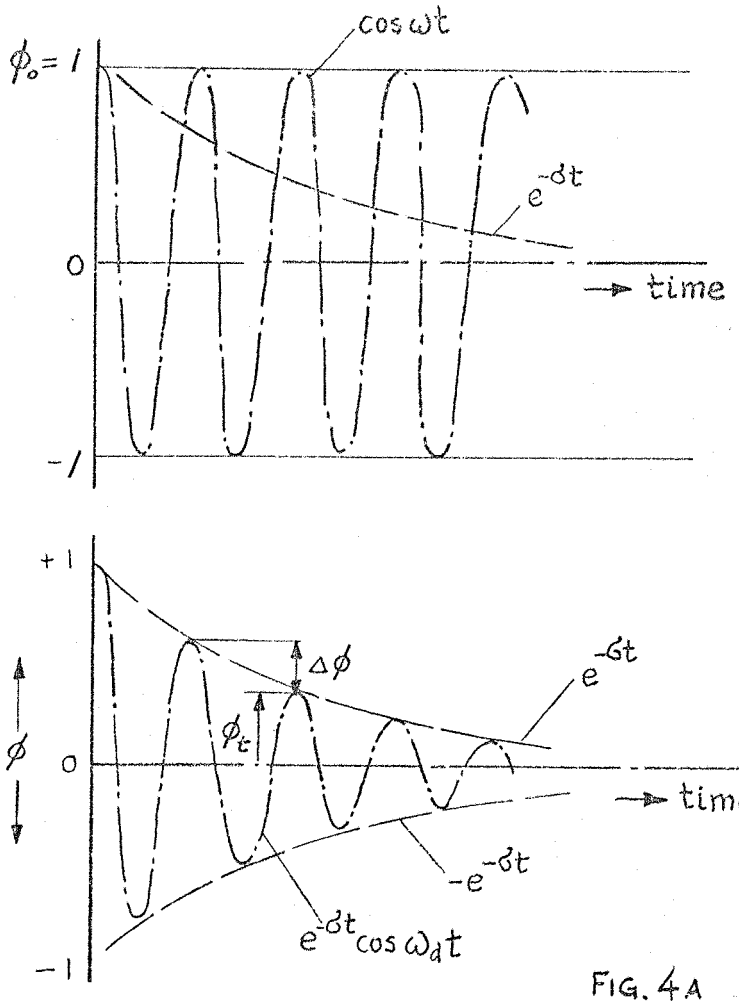

FIG. 4A

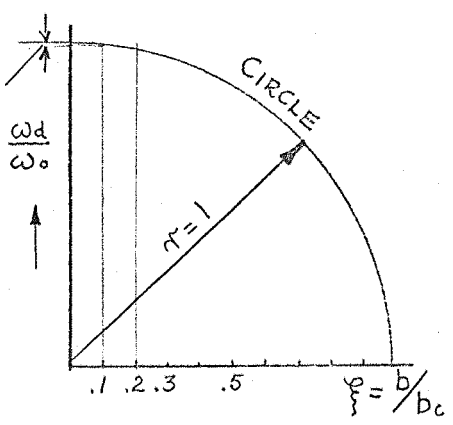

FIG. 5A.

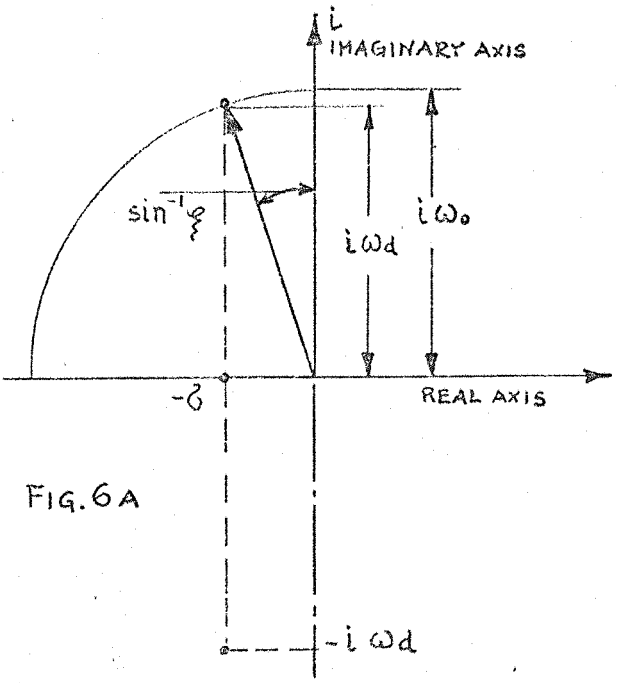

FIG. 6A

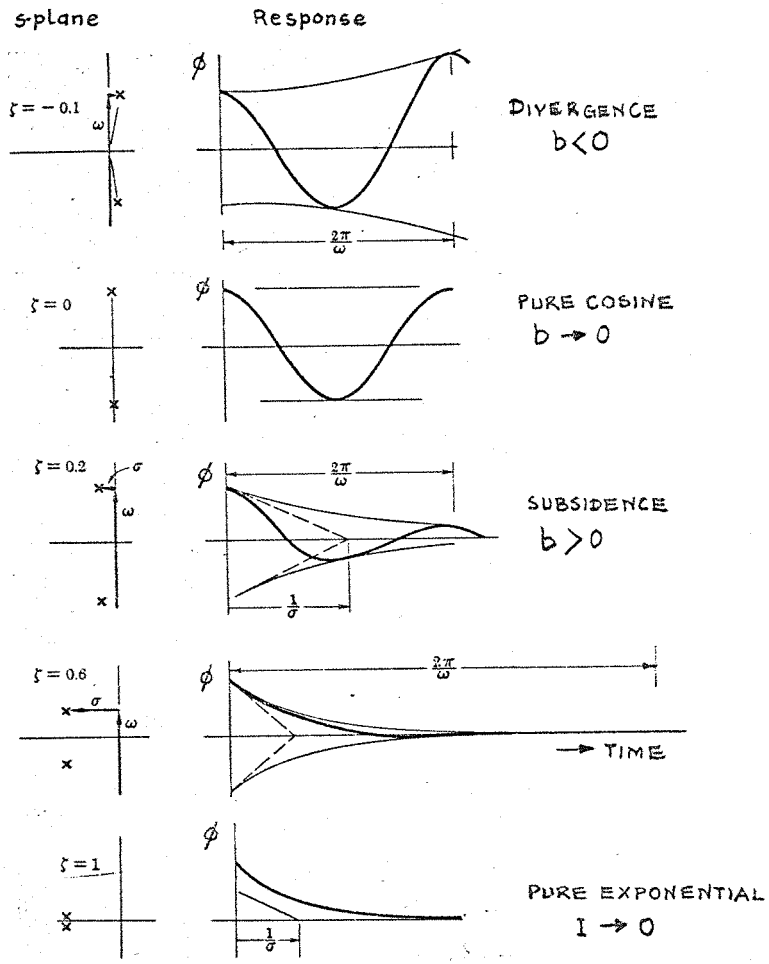

FIG. 7A. THE S PLANE AND TIME RESPONSE

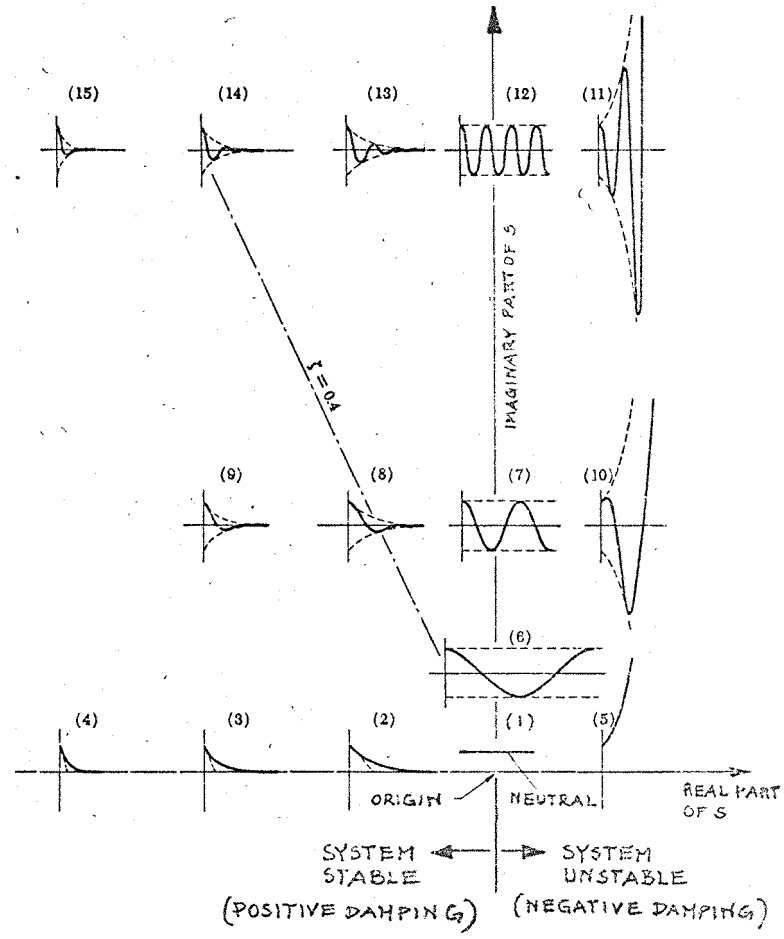

FIG. 8A. NATURAL RESPONSE VERSUS S-PLANE POSITION.

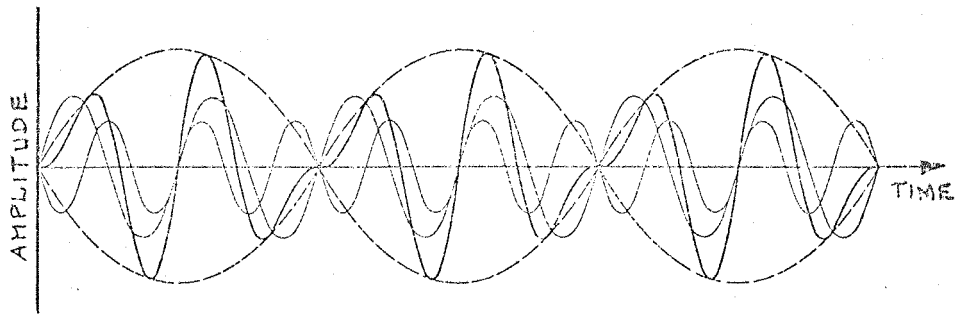

a. UNDAMPED SYSTEM (CONSERVATIVE).

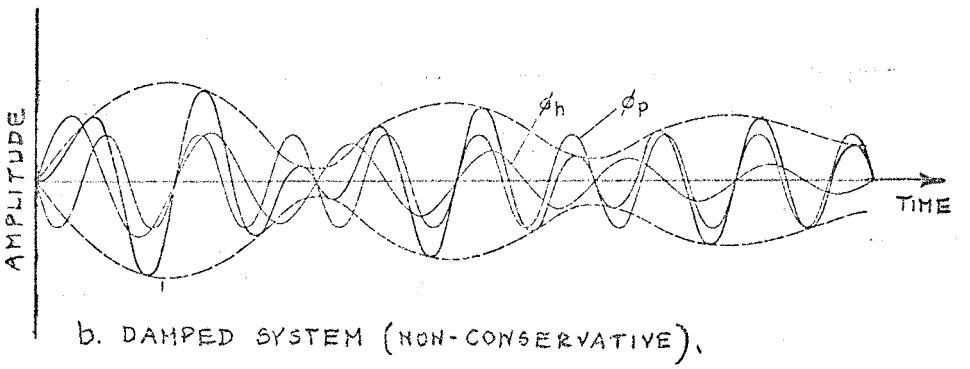

b. DAMPED SYSTEM (NON-CONSERVATIVE).

FIG. 9A THE TIME RESPONSE OF UNDAMPED AND DAMPED SYSTEM